

Electric Current Fluctuations in Mesoscopic Systems

by

Hyunwoo Lee

B.A. Physics

Korea Advanced Institute of Science and Technology, 1990

Submitted to the Department of Physics
in partial fulfillment of the requirements for the degree of

Doctor of Philosophy

at the

MASSACHUSETTS INSTITUTE OF TECHNOLOGY

June 1996

© 1996 Massachusetts Institute of Technology. All rights reserved.

Author

Department of Physics
April 25, 1996

Certified by

.....
Leonid S. Levitov
Assistant Professor of Physics
Thesis Supervisor

Accepted by

.....
George F. Koster
Professor of Physics
Chairman of Graduate Committee

MASSACHUSETTS INSTITUTE
OF TECHNOLOGY

JUN 05 1996

LIBRARIES

Science

Electric Current Fluctuations in Mesoscopic Systems

by

Hyunwoo Lee

Submitted to the Department of Physics
on April 25, 1996, in partial fulfillment of the
requirements for the degree of
Doctor of Philosophy

Abstract

The thesis consists of three parts. In the first part, electric current fluctuations in phase-coherent mesoscopic conductors are considered. For a dc transport, electron counting statistics shows that the fluctuations are reduced due to Fermi statistics. Fermi correlations lead to regularity of electron flow, and to binomial counting statistics. For a time-dependent voltage, the phase-coherence of electron transport results in non-trivial behavior of current fluctuations. Current fluctuations due to a pulse of voltage depend on detailed shape of the pulse and the mean square fluctuations diverge if the flux contained in the pulse is not an integer, as a result of Anderson orthogonality catastrophe.

In the the second part, current fluctuations in an ultra-small single tunnel junction are considered. Due to the Coulomb interaction, the charging energy tends to suppress the fluctuations whereas quantum fluctuations of charge induced by an electromagnetic environment tend to wipe out the charging energy effect. The interplay of the two effects makes current fluctuations depend on the part of the circuit in which they are measured, and also on the impedance of the environment. For several environments, the current fluctuations are calculated and for each environment, their sensitivity to the measurement scheme is discussed.

In the third part, the excitations induced by switching are discussed. Two kinds of perturbations are considered, an on-off operation and a switching-off perturbation. Firstly, the excitations induced by an on-off perturbation depend on the duration time τ of the perturbation. High frequency modes with inverse frequencies smaller than τ are significantly affected by the perturbation while low frequency modes are not excited. Secondly, the energy spectrum of the excitations induced by a switching-off perturbation resembles thermal equilibrium spectrum. However unlike thermal excitations, they are coherent which is manifest in the non-vanishing off-diagonal correlation functions.

Thesis Supervisor: Leonid S. Levitov
Title: Assistant Professor of Physics

Acknowledgements

It is a great pleasure to finally have the opportunity to thank the people who made all of this possible. I would like to express my deepest gratitude to my advisor, Leonid Levitov. Leonid has brought my attention to recent developments in mesoscopics, and provided me with many interesting and tractable problems. He was always willing to take time to explain even the most basic facts in condensed matter physics, and shared with me many of his deep physical insights.

Most of my understanding and knowledge in the condensed matter physics has been acquired through excellent lectures by professors at MIT and Harvard. I would like to take this opportunity to thank John Joannopolous, Mehran Kardar, Leonid Levitov, and Bertrand Halperin.

During my research works presented in this thesis, I have enjoyed working with my collaborators, Alexi Yakovets, Andrei Shytov, and Michael Reznikov. They have supplied valuable comments and suggested ways to resolve difficulties that caused me to stumble. Also I have benefited from numerous discussions with other graduate students and postdocs including Dongsu Bak, Yong Baek Kim, Don Kim, Ickjin Park, and Kyeongjae Cho. They have exposed me to many interesting developments in their research areas and helped me broaden my interest. In addition, I would like to thank my former and present officemates, Bruce Normand, Menke Ubbens, Mitya Chklovskii, and Dmitri Ivanov.

At various stages of my stay at MIT, I have had a good fortune of having generous mentors. Especially I would like to thank Manfred Sigrist and Peggy Berkovitz. They have given me pieces of invaluable advice when I was at a loss, and helped me enjoy pleasant days. I would also like to thank all my friends including, but not limited to, Young-Gyu Park, Jae Sang Kim, Seungheon Song, and Sukyoung Chey.

Finally I would like to thank my parents, Kwangja and Chongho Lee, and my fiancée, Ji-Kyung Choi, for all the supports and love they have given me. Without them this thesis could not have been written.

Biographical Note

Hyunwoo Lee was born in Seoul, Korea in 1969 and grew up there. From 1987 to 1990, he attended the Korea Institute of Technology (presently undergraduate course of Korea Advanced Institute of Science and Technology), where he graduated with a bachelor degree in physics. From 1990 to 1996, he attended graduate school at MIT and studied theoretical condensed matter physics under professor Leonid S. Levitov. In the fall of 1996, he will take a post-doctoral position at the Center for Theoretical Physics at Seoul National University in Seoul, Korea.

Publications

- [1] Hyunwoo Lee, L. S. Levitov, and A. V. Shytov, Excitations Induced by Switching Perturbations in Quantum Wires, in preparation.
- [2] Hyunwoo Lee and L. S. Levitov, Flux Lattices in Layered Superconductors, in preparation.
- [3] Leonid S. Levitov, Hyunwoo Lee and Gordey B. Lesovik, Electron Counting Statistics and Coherent States of Electric Current, preprint, submitted to J. Math. Phys.
- [4] Hyunwoo Lee and L. S. Levitov, Universality in Phyllotaxis: a Mechanical Theory, to be published in *Symmetry in Plants* (Cambridge University, Cambridge, 1996).
- [5] D. A. Ivanov, H.-W. Lee, and L. S. Levitov, Coherent States of Alternating Current, to be published in Phys. Rev. B.
- [6] Hyunwoo Lee and L. S. Levitov, Current Fluctuations in a Single Tunnel Junction, Phys. Rev. B **53**, 7383 (1996).
- [7] Hyunwoo Lee, L. S. Levitov, and A. Yu. Yakovets, Universal Statistics of Transport in Disordered Conductors, Phys. Rev. B **51**, 4079 (1995).
- [8] Hyunwoo Lee and L. S. Levitov, Estimate of Minimal Noise in a Quantum Conductor, unpublished (cond-mat/9507011).
- [9] Hyunwoo Lee and L. S. Levitov, Orthogonality Catastrophe in a Mesoscopic Conductor due to a Time-dependent flux, unpublished (cond-mat/9312013).

Contents

1	Introduction	13
1.1	Transport properties of mesoscopic devices	13
1.2	Single charge tunneling in nanostructures	16
1.3	Current fluctuations in macroscopic systems	19
2	Electron Counting Statistics	25
2.1	Introduction	25
2.2	Measuring electric current	26
2.3	Spin 1/2 as a galvanometer	29
2.4	Single-channel conductor. General formalism	32
2.5	Equilibrium fluctuations	35
2.6	Statistics of a dc current: quantum shot noise	37
2.7	Universal statistics of transport in disordered conductors	38
2.8	Conclusion	48
3	Coherent States of Electric Current	49
3.1	Introduction	49
3.2	Noise due to a voltage pulse: Orthogonality catastrophe	50
3.3	Coherent states of current	56
3.4	Conclusion	62
4	Current Fluctuations in a Single Tunnel Junction	65
4.1	Introduction	65

4.2	Formulation	67
4.3	Tunneling current and relaxed current	70
4.4	Noise spectrum of tunneling current	73
4.4.1	Noise spectrum of tunneling current	73
4.4.2	Low impedance limit	74
4.4.3	High impedance limit	75
4.4.4	Ohmic environment	78
4.4.5	Noise power	78
4.5	Noise spectrum of relaxed current	79
4.5.1	Noise spectrum of relaxed current	79
4.5.2	Low impedance limit	81
4.5.3	High impedance limit	85
4.5.4	Ohmic impedance environment	86
4.5.5	Experimental implications	87
4.5.6	Weak scattering limit	88
4.6	Conclusion	88
5	Excitations Induced by Switching in Quantum Wires	91
5.1	Introduction	91
5.2	Excitations generated by an on-off perturbation	93
5.3	Excitations generated by a switching-off perturbation	97
A	Larmor Clock Measurement of Tunneling Time	103
B	Asymptotic Expression for $\langle\langle Q^k \rangle\rangle$	109
C	Variance of $\langle\langle Q^k \rangle\rangle$	111
D	Correlation Function at Finite Temperature	113

List of Figures

1-1 Transport through a quantum dot. Two electrodes are separated by an insulating gap, and in the middle of the gap lies a metallic island. At low temperatures, the island induces the Coulomb blockade effect. 17

1-2 A single tunnel junction. Two electrodes are separated by an insulating gap. Unlike the quantum dot in Figure 1-1, a single tunnel junction does not contain an island. However it may still exhibit the Coulomb blockade effect if electron relaxation in the leads is slow. 18

4-1 (a) A schematic diagram of the circuit. The circuit contains a single tunnel junction, a voltage source, and external leads of impedance $Z(\omega)$. (b) The tunneling current and the relaxed current. The tunneling current represents the electron flow right at the potential barrier of a junction. On the other hand, the relaxed current represents the electron flow through the external leads. In the figure, an Ohmic environment with resistance R is shown. 69

4-2 The zero temperature current-voltage characteristics for three environments, $Z(\omega) = 0.01R_Q$ (solid line), $Z(\omega) = 100R_Q$ (dashed line), and $Z(\omega) = R_Q$ (dash-dotted line). 72

4-3 The zero temperature equilibrium noise spectra of the tunneling current $S_{I_T}(\omega)$ for $Z(\omega) = 0.01R_Q$ (solid line), $Z(\omega) = 100R_Q$ (dashed line), and $Z(\omega) = R_Q$ (dash-dotted line). 74

4-4	(a) The zero temperature excess noise spectra of the tunneling current $S_{I_T}^x(\omega)$ for $Z(\omega) = 0.01R_Q$ (solid line), $Z(\omega) = 100R_Q$ (dashed line) and $Z(\omega) = R_Q$ (dash-dotted line). Voltage bias of $eV = 0.5E_C$ is assumed. (b) Evolution of the zero temperature tunneling excess noise with voltage bias in the high impedance environment $Z(\omega) = 100R_Q$. $eV = 0.5E_C$ (solid line), $eV = 1.5E_C$ (dashed line), and $eV = 2.5E_C$ (dash-dotted line).	76
4-5	The excess noise spectrum of the relaxed current $S_{I_R}^x(\omega)$ (solid line) vs. the excess noise spectrum of the tunneling current $S_{I_T}^x(\omega)$ (dashed line) at zero temperature. The dash-dotted line shows $1/(1+\omega^2 R^2 C^2)S_{I_T}^x(\omega)$ for comparison. (a) $Z(\omega) = 0.01R_Q$, $eV = 200E_C$. The dash-dotted line is not visible because it overlaps with the solid line. (b) $Z(\omega) = 100R_Q$, $eV = 0.5E_C$. The solid line and the dash-dotted line are scaled up by a factor of 10^4 to magnify their features. Note that $S_{I_R}^x(\omega)$ is negative around $\hbar\omega \approx \pm E_C$	83
5-1	Wave reflection. The evolution of the field $\hat{\phi}(x, t)$ can be obtained from the analogy to the classical wave reflection problem.	95
5-2	The conformal transformations used to simplify the boundary conditions.	99

Chapter 1

Introduction

This thesis consists of three parts. In the first part, we discuss current fluctuations in phase-coherent mesoscopic conductors. In the second part, we discuss the effects of the Coulomb interaction on the current fluctuations in single tunnel junctions. In the third part, we discuss excitations induced by switching perturbations in quantum wires. The bulk of the work presented in this thesis has been presented in seven research papers [1, 2, 3, 4, 5, 6, 7], which form the bodies of Chap. 2-5.

1.1 Transport properties of mesoscopic devices

In the last decade, there has been rapid progress in nano-fabrication technology. Nowadays, it has become a rather routine task to build systems with controlled structure in sub-micron scale. In addition, it is now possible to reach temperatures in the milikelvin range. At such low temperatures, many interesting phenomena occur in small devices. In this section we discuss the effects of the quantum-mechanical wave nature of electrons on transport properties of small devices.

In the conventional Boltzmann transport theory, it is assumed that electrons possess well defined positions and momenta. The basic quantity in the theory is the electron distribution function $f(\mathbf{r}, \mathbf{p}, t)$, describing the density of electrons at point \mathbf{r} with momentum \mathbf{p} . The Boltzmann equation determines the evolution of the function $f(\mathbf{r}, \mathbf{p}, t)$, and all transport properties result from $f(\mathbf{r}, \mathbf{p}, t)$.

The classical kinetic theory, however, ignores the wave nature of electrons. At room temperature, electrons undergo many inelastic scatterings and loose phase coherence. In this situation, ignoring quantum mechanics is justified, and the Boltzmann equation is a good approximation. On the other hand, at very low temperature the inelastic scattering rates become very small, and electrons maintain their phase coherence up to some relatively large length scale, called the phase coherence length L_ϕ . For very small systems, L_ϕ becomes comparable to system dimension and the quantum coherence becomes important. As a result, properties of such devices are different from those of macroscopic devices, and the name *mesoscopic* devices is used to emphasize this fact.

To take into account the quantum-mechanical coherence of electrons, it is useful to adopt a different point of view, and to treat electron conduction as a scattering problem, as first proposed by Landauer [8, 9, 10]. The Landauer's picture can be explained with the Feynman functional integral description. For example, the transmission probability $T(\mathbf{r}_1 \rightarrow \mathbf{r}_2)$ for an electron to go from \mathbf{r}_1 to \mathbf{r}_2 is given by a phase-coherent sum of amplitudes for all possible trajectories from \mathbf{r}_1 to \mathbf{r}_2 :

$$T(\mathbf{r}_1 \rightarrow \mathbf{r}_2) = \left| \sum_i t_i(\mathbf{r}_1 \rightarrow \mathbf{r}_2) \right|^2, \quad (1.1)$$

where $t_i(\mathbf{r}_1 \rightarrow \mathbf{r}_2)$ is the amplitude for a trajectory i .

The difference from the Boltzmann theory becomes evident if Eq. (1.1) is split into diagonal terms and interference terms,

$$T(\mathbf{r}_1 \rightarrow \mathbf{r}_2) = \sum_i |t_i(\mathbf{r}_1 \rightarrow \mathbf{r}_2)|^2 + \sum_{i \neq j} t_i^*(\mathbf{r}_1 \rightarrow \mathbf{r}_2) t_j(\mathbf{r}_1 \rightarrow \mathbf{r}_2). \quad (1.2)$$

While the interference terms tend to average out, and the diagonal terms are dominant in conventional macroscopic systems, in the mesoscopic systems the interference terms may give contributions comparable to the diagonal terms.

The Landauer's picture has been applied to various mesoscopic phenomena such as Aharonov-Bohm oscillations in multiply connected geometry, or weak localization

in disordered conductors, and it has been proven useful.

Recently, the Landauer's picture has been applied to the noise study of the current through a one-dimensional quantum wire [11, 12, 13]. For simply connected wires, the interference effects are negligible, and naive reasoning suggests that the wave coherence is also unimportant, and that transport in such wires exhibit classical shot noise. In the strong scattering limit, the noise power P is indeed found to be $P = 2eI$, in agreement with the classical shot noise theory. In the weak scattering limit, however, it has been found that the noise is suppressed below the classical noise level, $P \ll 2eI$.

To understand the suppressed noise, let us briefly review the classical shot noise theory. Electron conduction through a one-dimensional conductor can be viewed as successive attempts by electrons to pass through the conductor, with each attempt having two outcomes, either passing or getting reflected. In the classical shot noise theory, each attempt is assumed to be independent. As a result, there is no correlation between two successive attempts, and the electron transmission becomes a Poisson process. It is well known that the root mean square deviation of a Poisson process is given by \sqrt{pN} where N is the number of attempts and p is the transmission probability. Applied to the noise problem, this analysis leads to the full shot noise power, $P = 2eI$.

Then, following the classical shot noise theory, the full shot noise in the strong scattering limit can be interpreted as an absence of the correlation between electron tunneling events, whereas the suppressed shot noise in the weak scattering limit can be interpreted as a presence of some mechanism that regularizes transmission events.

One may expect that the Fermi statistics of electrons should induce such correlation. In fact, by incorporating the Fermi statistics into the conventional Boltzmann equation, a recent theoretical calculation [14] has demonstrated that the noise can be indeed suppressed due to the Fermi statistics.

In the first part of the thesis, we discuss electron transport in mesoscopic conductors. We concentrate on the nature of the correlation induced by the Fermi statistics, and the effects of the quantum coherence of electrons on the fluctuations.

In Chapter 2, we study the electron counting statistics. Specifically, we first de-

velop a measurement scheme that allows us to directly probe the number of transmitted electrons during a given time interval t . From the scheme, we derive a probability distribution of the number of transmitted electrons. Then, by examining the dependence of the probability distribution on the time t and the voltage V , we show that the electron transmission becomes correlated due to the Fermi statistics. We also show that the nature of the correlation can be quite accurately described by the binomial statistics: the time average interval between every successive attempts is $h/|eV|$, and the fluctuations about the average are negligible.

In Chapter 3, we probe deeper into the correlation by discussing the current fluctuations when a time-dependent voltage is applied. As a specific example, we calculate the fluctuations due to a pulse of voltage, and show that due to the transport coherence, Anderson orthogonality catastrophe [15] occurs. And as a result, we find that the mean square fluctuations diverge logarithmically if the Faraday's flux contained in the voltage pulse is not an integer.

1.2 Single charge tunneling in nanostructures

In the previous section, we have seen that quantum mechanics is important in mesoscopic systems. In this section, we discuss another important effect occurring in such systems, called *Coulomb blockade*.

Let us imagine that we have two electrodes separated by an insulating gap, and in the middle of the gap lies a metallic island (see Figure 1-1). Suppose a voltage bias is applied between the two electrodes. For current to flow, electrons in the source first have to tunnel on the island, and then to the drain. During this process, the number of electrons in the island changes from N to $N + 1$ and then from $N + 1$ to N . Normally there is a large number of electrons, $N \sim 10^{23}$, on the island, and the change by one is not important. However, in mesoscopic systems, this is not quite true. For example, in a metallic island of size $0.1 \mu\text{m} \times 0.1 \mu\text{m} \times 1 \text{nm}$, the number is around 10^3 . Though the number is still large, the effect of the additional electron is not negligible because of the Coulomb interaction.

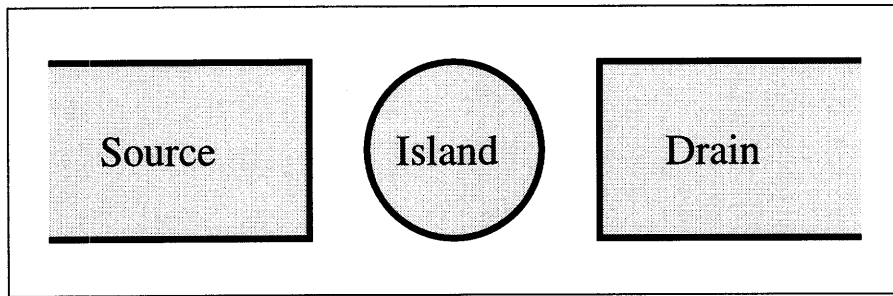


Figure 1-1: Transport through a quantum dot. Two electrodes are separated by an insulating gap, and in the middle of the gap lies a metallic island. At low temperatures, the island induces the Coulomb blockade effect.

Since electrons interact via the Coulomb potential, there is an energy cost associated with adding a new electron. For an island with capacitance C , the energy cost can be estimated by the charging energy $E_C = e^2/2C$. For the island mentioned above, the capacitance is about 1 fF (10^{-15} F) and it corresponds to the charging energy $E_C \sim 1$ K, which is rather high temperature in the cryogenics technology standard. Then at temperatures below E_C , thermal fluctuations cannot supply electrons with enough energy to overcome the energy barrier. As a result, at small voltage, the current does not flow. This phenomenon is the so called Coulomb blockade.

The Coulomb blockade is observed in many systems. For example, it occurs for a semiconducting island, and there the effect is usually stronger due to lower charge density than in a metallic island of comparable size. The effect occurs even in a superconducting island and in this case, the Cooper pairs are affected by the charging energy.

It is interesting that the Coulomb blockade may occur even without an island. In a recent experiment [16] it was found that transport through a single tunnel junction shown in Figure 1-2 can also be affected by the Coulomb blockade.

To understand the Coulomb blockade effect in a single tunnel junction is a bit less simpler than the previous example. Let us assume that the time for an electron wave-packet to tunnel from the source to the drain is τ (for a discussion on the tunneling time, see Refs. [17, 18, 19]). Since electrons travel at a finite speed v_F , the size of the wave-packet right after the tunneling is about $v_F\tau$, and at the terminal of the drain

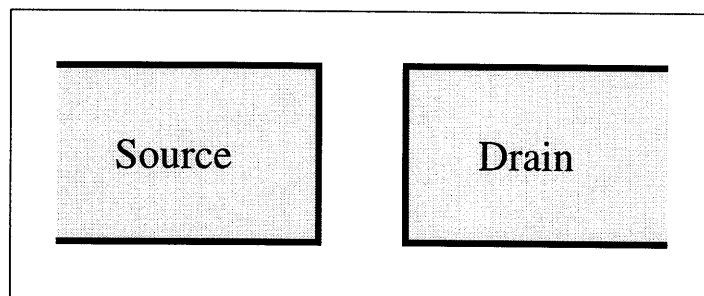


Figure 1-2: A single tunnel junction. Two electrodes are separated by an insulating gap. Unlike the quantum dot in Figure 1-1, a single tunnel junction does not contain an island. However it may still exhibit the Coulomb blockade effect if electron relaxation in the leads is slow.

there appears charge-unbalanced region of this size. Then, other electrons respond to the injection of the extra charge, and the Coulomb blockade effect should occur.

However, this analysis captures only a part of the relevant physics. Let us compare the single tunnel junction with the Coulomb island. The metallic island in the previous example is surrounded by insulators and so the charge on the island is a good quantum number. In contrast, there is no region in single tunnel junctions where electrons can be confined for a long time, and thus charge is not a good quantum number. Then one should examine the quantum fluctuations of charge, and the analysis in the previous paragraph is not valid if the mean square fluctuations of charge are larger than e^2 .

Recently Devoret *et al.* [20] and Girvin *et al.* [21] have developed a theory of single tunnel junctions that includes both the Coulomb blockade effect and the quantum fluctuations of charge. The theory shows that the strength of the quantum fluctuations of charge is determined by the electromagnetic environment of a junction, and thus transport properties depend on the impedance of the environment.

In Chapter 4, we consider current fluctuations in a single tunnel junction. While the charging energy tends to suppress the fluctuations, the quantum fluctuations of charge tend to wipe out the charging effect. We find that the interplay of the two effects makes the current fluctuations depend on the part of the circuit in which they are measured. For illustration, we calculate the fluctuations of the tunneling current,

which is measured at the insulator between the source and the drain, and of the relaxed current, which is measured deep in the drain, far from the tunneling junction. For a low impedance environment, the charging effect is suppressed by quantum fluctuations of charge. Hence the tunneling current exhibits Ohmic fluctuations while the relaxed current shows fluctuations due to a shunt resistor. For a high impedance environment, the charging energy effect survives and thus the fluctuations of the tunneling current are strongly suppressed. Also the quantum fluctuations of charge become correlated with electron tunnelings, and consequently the relaxed current shows negative excess noise. The results are compared with recent experiments [22, 23], and good agreement is found.

1.3 Current fluctuations in macroscopic systems

Before we finish this chapter, it is useful to review the topic of current fluctuations in macroscopic systems. Due to intrinsic stochasticity, the representation of fluctuating quantities in terms of exact time evolution is not useful. Instead, such quantities are usually characterized by averages and correlation functions. For the current, these are $\langle I(t) \rangle$ and $\langle I(t_1)I(t_2) \rangle$. For the current fluctuations, it is useful to define $\delta I(t) = I(t) - \langle I(t) \rangle$. Then the relevant correlation function is $K(t_1, t_2) = \langle \delta I(t_1)\delta I(t_2) \rangle$. For stationary current flow, the correlation function is invariant under time-translation and thus depends only on the difference $\tau = t_2 - t_1$: $K(t_1, t_2) = K(\tau) = \langle \delta I(0)\delta I(t) \rangle$.

Due to time-translation symmetry, it is useful to analyze the correlation in the frequency space:

$$K(t) = \int \frac{d\omega}{2} e^{-i\omega t} S_I(\omega) , \quad (1.3)$$

where the Fourier component $S_I(\omega)$ is called spectral density. The spectral density possesses the following properties:

$$\begin{aligned} \text{(i)} \quad & S_I(\omega) = S_I^*(\omega) \\ \text{(ii)} \quad & S_I(\omega) = S_I(-\omega) \end{aligned} \quad (1.4)$$

$$(iii) \quad S_I(\omega) \geq 0 .$$

In other words, it is a real positive number. From that, $S_I(\omega)$ can be interpreted as an intensity of the current harmonic with the frequency ω : $\langle \delta I(\omega_1) \delta I(\omega_2) \rangle = 2\pi^2 \delta(\omega_1 + \omega_2) S_I(\omega_1)$.

White noise: Let us consider a resistor R at temperature T . Without external voltage bias, there is no net current and the current correlation function $K(t)$ becomes $\langle I(0)I(t) \rangle$. It should be expected that $K(t)$ vanishes for large t . In fact, $K(t)$ has a peak at $t = 0$ whose width is given by some microscopic time scale, and vanishes rapidly away from the peak. Therefore, as long as we are not interested in the microscopic times, the correlation function can be approximated by a delta function: $K(t) = K_0 \delta(t)$. Here the magnitude K_0 depends on R and T . Since the current fluctuations are induced by thermal fluctuations, the magnitude K_0 is proportional to T . Also one can expect that K_0 is inversely proportional to R since larger resistance suppresses electron flow stronger. In fact, using the fluctuation-dissipation theorem one can show that $K_0 = k_B T / 2R$ [24]

Then by taking a Fourier transform, one obtains

$$S_I(\omega) = \frac{k_B T}{2\pi R} , \tag{1.5}$$

the so called Nyquist theorem [25]. Note that $S_I(\omega)$ is independent of frequency. For that reason, this result is often referred as *white noise*, with the word “white” used in analogy to visible light which is a mixture of harmonics with broad spectrum.

Johnson-Nyquist noise: The white noise spectrum (1.5) predicts no fluctuations at zero temperature. However, even at zero temperature, the fluctuations do not vanish since the uncertainty principle requires residual zero point motion of electrons. Hence Eq. (1.5) is valid only at high temperatures where zero-point fluctuations can be ignored compared to thermal fluctuations.

To generalize to lower temperature, we should formulate the problem quantum-mechanically. The current $I(t)$ should be replaced by a current operator $\hat{I}(t)$ and

the ensemble average $\langle \dots \rangle$ should be interpreted as $\text{Tr}\{\rho \dots\}$ where ρ is a density matrix. Also, the correlation function $K(t)$ should be interpreted as the average of the current-current anticommutator [26],

$$K(t) = \frac{1}{2} \langle \{ \hat{I}(0), \hat{I}(t) \} \rangle - \langle \hat{I}(0) \rangle \langle \hat{I}(t) \rangle , \quad (1.6)$$

since two current operators at different times do not commute.

Callen and Welton [27] performed a quantum-mechanical calculation and obtained

$$S_I(\omega) = \frac{1}{\pi R} \hbar \omega \coth \frac{\beta \hbar \omega}{2} , \quad (1.7)$$

which is usually referred as Johnson-Nyquist noise. For high temperature, $k_B T \gg \hbar \omega$, it is reduced to the white noise. However, for low temperature, $k_B T \ll \hbar \omega$, it becomes $\hbar |\omega| / \pi R$. Notice that the crossover from high to low temperature regime depends on the frequency.

To understand the factor $\hbar \omega$ in the low temperature spectral density, let us recall the approach to dissipative systems proposed by Caldeira and Leggett [28, 29]. A resistor absorbs energy from all harmonics of the current. Quantum-mechanically, one can imitate energy absorption at a particular frequency ω by introducing a harmonic oscillator with the same natural frequency ω which is linearly coupled to the current. In the Caldeira-Leggett approach, a resistor can be described by infinite number of harmonic oscillators with natural frequencies ranging from zero to infinity.

In this approach, it can be easily shown that a harmonic oscillator with natural frequency ω is responsible for the spectral density $S_I(\omega)$ at the same frequency. The average energy of thermal fluctuations in this harmonic oscillator at high temperature, $k_B T \gg \hbar \omega$, is of the order of $k_B T$, which corresponds to the white noise. At low temperature, $k_B T \ll \hbar \omega$, the energy in the harmonic oscillator is only due to its zero point motion, that is, it is equal to $\hbar \omega / 2$. Then, since this energy is responsible for the spectral density, one can roughly expect that $k_B T$ in the white noise spectrum (1.5) is replaced by $\hbar \omega$ at low temperatures, which agrees with the low temperature behavior of Eq. (1.7) up to a numerical factor. So, the low temperature behavior of the Johnson-

Nyquist noise can be understood in terms of the zero-point fluctuations.

Quantum shot noise: So far we have considered thermal equilibrium. Now, let us generalize to nonequilibrium situation when voltage bias is applied. Dahm *et al.* [30] calculated the spectral density in Ohmic junctions and obtained

$$S_i(\omega) = \frac{1}{2\pi R} \sum_{\pm} (\hbar\omega \pm eV) \coth \frac{\beta(\hbar \pm eV)}{2}. \quad (1.8)$$

For simplicity, let us consider the zero temperature limit. The spectrum shows two kinds of behavior depending on the ratio between the frequency and the voltage. For high frequency, $\hbar|\omega| > |eV|$, Eq. (1.8) reduces to $\hbar|\omega|/\pi R$, which is identical to the Johnson-Nyquist noise at low temperatures. So, the voltage bias does not affect high frequency spectral density. For low frequency, $\hbar|\omega| < |eV|$, Eq. (1.8) gives $|eV|/\pi R = eI/\pi$. Here we see that the voltage bias affects only low frequency spectral density.

Note that the low frequency spectral density is proportional to the electron charge e , which implies that this noise would be absent if the electron charge has infinitesimal value. In fact, this noise is related with the finiteness of electron charge. Each electron carries finite charge and it generates a short pulse of current when it passes a cross-section in which the current is measured. Overall current can be viewed as a train of such pulses rather than a steady flow of charge fluid. Because of that, this noise is often called “shot noise”.

To gain some understanding of underlying dynamics, let us focus on the noise power defined as $P = 2\pi S_I(\omega = 0)$. For an Ohmic junction, one obtains

$$P = 2eI. \quad (1.9)$$

The noise power has a simple physical meaning in terms of electron counting statistics. Let us consider a net charge $\hat{Q} = \int_0^t dt' \hat{I}(t')$ that has transmitted through an Ohmic junction in a time interval t . For a dc transport, one obtains $\langle \hat{Q} \rangle = \langle \hat{I} \rangle t$. Next let us

consider fluctuations of \hat{Q} . For its variance, one obtains

$$\langle \delta \hat{Q}^2(t) \rangle = \int_0^t dt_1 \int_0^t dt_2 \left\langle \frac{1}{2} \{ \delta \hat{I}(t_1), \delta \hat{I}(t_2) \} \right\rangle , \quad (1.10)$$

which reduces to $\pi S_I(\omega = 0)t$ for the times much longer than microscopic correlation time. Then one finds an interesting relation between the noise power and the variance:

$$P = 2 \frac{\langle \delta \hat{Q}^2 \rangle}{t} . \quad (1.11)$$

This relation allows one to interpret P as variance of the number of transmitted electrons per unit time.

By comparing the two equations, (1.9) and (1.11), one finds that $\langle \delta \hat{Q}^2 \rangle / e^2$ for an Ohmic junction is equal to $\langle \hat{Q} \rangle / e$, that is, the average number of electron tunneling is the same as its variance. Obviously, in the absence of correlation between electron attempts to tunnel through a tunneling barrier, the probability distribution $P(n)$ of having n successful attempts becomes Poissonian, and by definition, the variance of the Poisson distribution is equal to the average. Thus, the result (1.9) implies the absence of correlations. It is plausible to expect that if there is any correlation that regulates electron tunneling, the noise power will become smaller. In this sense, the result (1.9) is referred as a “full” shot noise.

Chapter 2

Electron Counting Statistics

2.1 Introduction

Quantum transport in nanostructures has been a subject of many recent studies [31]. Transport properties like Ohmic conductivity can be understood in terms of the quantum scattering problem in the conductor, which provides a theory of quantum coherence of transport [8, 10, 9]. Fluctuations of electric current due to the discreteness of electric charge are intrinsic to quantum transport [11, 12, 13, 32]. It has been found that current fluctuations have interesting properties reflecting profound aspects of underlying quantum dynamics [33, 34, 35, 36]. For example, the quantum noise caused by a dc current is reduced below classical shot noise level [11, 12, 13, 32, 33, 34, 35, 36]. This suppression has been understood as an effect of enhanced regularity of transmission events due to Fermi statistics [37]. Besides theoretical interest, such phenomena may lead to applications. Given the development of nano-technologies, the transmission of signals by single- or few-electron pulses will become common, and then one will see the quantum statistics of current working.

In this chapter we present the theory of quantum measurement of electric current [38]. Our goal is a complete description of charge fluctuations, rather than developing measurement theory (see Secs. 2.2, 2.3). We shall derive a microscopic formula for electron counting distribution (see Sec. 2.3, Eq. (2.10), and Sec. 2.4, Eq. (2.25)) that can be used for any system, e.g., with an interaction or with a time-

dependent potential [39]. As an application, we test the method on the statistics in a single channel ideal conductor for non-equilibrium and equilibrium noise at finite temperature, and for zero-point equilibrium fluctuations (Secs. 2.4, 2.5). In particular, the fluctuations of a dc current at zero temperature are found to be binomial (Sec. 2.6) with the probabilities of outcomes related with transmission coefficients of elastic scattering in the system, and with the number of attempts $N = eVt/h$, where V is applied voltage, and t is the time of measurement.

2.2 Measuring electric current

Instantaneous measurement is described in quantum mechanics by wave-packet reduction that involves projecting on eigenstates of an observable. A different kind of measurement, extended in the time domain, is realized in detectors and other counting devices. It is known that in such cases a certain revision of the measurement description is necessary. A famous example is the theory of photon detectors [40, 41, 42] in quantum optics. Due to Bose statistics, photons entering a photo-counter are correlated in time, and this makes the theory of photon detection a problem of many-particle statistics. For a single normal mode of radiation field the probability P_m to count m photons over time t is given by

$$P_m = \frac{(\eta t)^m}{m!} \langle : (a^+ a)^m e^{-\eta t a^+ a} : \rangle , \quad (2.1)$$

where a^+ and a are Bose operators of the mode, η is “efficiency” of the counter, $\langle \dots \rangle$ stands for the average over a quantum state. The normal ordering $: \dots :$ is important — physically, it means that, after having been detected, each photon is destroyed, e.g., it is absorbed in the detector. Instead of the probabilities, it is more convenient to deal with the generating function

$$\chi(\lambda) = \sum_m P_m e^{i\lambda m} . \quad (2.2)$$

For the single normal mode Eq. (2.1) leads to

$$\chi(\lambda) = \langle : \exp \eta t (e^{i\lambda} - 1) a^\dagger a : \rangle . \quad (2.3)$$

Eqs. (2.1,2.2,2.3) account very well for numerous experimental situations [43, 44]. Particularly interesting is the case of a coherent state $|z\rangle$, $a|z\rangle = z|z\rangle$, where z is a complex number. It corresponds to the radiation field of an ideal laser, and with Eq. (2.3) one easily gets Poisson counting distribution,

$$P_m = \frac{(Jt)^m}{m!} e^{-Jt}, \quad J = \eta|z|^2, \quad (2.4)$$

which describes a minimally bunched light source.

Similar to the photon detection, electric measurement is performed on a system containing an enormous number of particles — in this case fermions — and thus one expects the effects of Fermi statistics to be important. Also, the duration of electric measurement is typically much longer than the time it takes the system to transmit one electron by microscopic tunneling, scattering or diffusion. Apart from these similarities, there is, however, a crucial difference from the photon counting: the number of electrons is not changed by current measurement, since electric charge is conserved. This has to be contrasted with absorption of photons in photo-counters. Related to this, there is another important difference: at every detection of a photon, its energy $\hbar\omega$ is taken from the radiation field, which makes plain photodetectors insensitive to zero-point fluctuations of electromagnetic field. On the contrary, the measurement of current fluctuation is usually performed without changing energy of the system, which makes the zero-point noise an unavoidable component of any electric measurement [45]. (Let us emphasize that the difference has nothing to do with the type of quantum statistics, Fermi or Bose. Rather it is the difference between the two kinds of measurement, e.g., see [46], where counting of fermions was discussed using an optical-like counter that has to capture an electron in order to detect it.)

In the classical picture, the measurement gives the charge $Q(t) = \int_0^t j(t') dt'$ transmitted during the measurement time t . The probabilities P_m of counting m electrons

can then be obtained by averaging $\delta(Q(t) - me)$ over the state of the system. In a quantum problem electric current is an operator, and since currents at different moments do not commute, the operator of transmitted charge $\hat{Q}(t) = \int_0^t \hat{j}(t') dt'$ generally does not make any sense. Instead, since we are interested in higher-order statistics of current fluctuations, beyond $\langle \hat{j}(t) \rangle$ and $\langle\langle j(t_1)j(t_2) \rangle\rangle_+$, in order to compute electron counting distribution, we have to include the measuring system in the quantum Hamiltonian. Our approach is motivated by the example of the quantum mechanical systems with strong coupling to macroscopic environment, introduced by Leggett, that can be treated consistently only by adding the “measuring environment” to the quantum problem [47].

For that we introduce a model quantum galvanometer, a spin 1/2 that precesses in the magnetic field B of the current. For a classical system, the rate of precession is proportional to $B(t)$, and $B(t)$ is proportional to the current $I(t)$: $B(t) = \text{const } I(t)$. Therefore, the precession angle of the spin directly measures transmitted charge $\delta Q = \int_0^t I(t') dt'$. We adopt the same measurement procedure for the quantum circuit, i.e., we include in the electron Hamiltonian the vector potential due to the spin:

$$\vec{A}(r) = -\mu \vec{\sigma} \times \vec{\nabla} \frac{1}{|r|}, \quad (2.5)$$

where $\vec{\sigma} = (\sigma_x, \sigma_y, \sigma_z)$ are Pauli matrices. Thus we obtain a Hamiltonian describing motion of electrons, the measuring spin, and their coupling. Now, according to what has been said, we have to solve dynamics of the spin in the presence of the fluctuating current, find the distribution of precession angles, and then interpret it as a distribution of transmitted charge. Of course, a question remains about the back effect of the spin on the system, as in any other problem of quantum measurement. However, as we find below in (2.17) and (2.18), only the phase of an electron state is affected by the presence of the spin, not the amplitude. Moreover, the phase will change only for the transmitted, but not for the reflected wave. As a result, the probabilities we obtain do not depend on the coupling constant of the spin. This justifies the assumption that the spin measures charge transfer in a non-invasive way.

It is worth remarking that our scheme resembles the “Larmor clock” approach [17, 18, 19] to the problem of traversal time for motion through a classically forbidden region. In this problem one is interested, e.g., in the time spent by a particle tunneling through a barrier. The Larmor clock approach involves an auxiliary constant magnetic field B added in the classically forbidden region, and a spin $1/2$ carried by the particle that interacts with the field: $\mathcal{H}_{int} = -\hat{\sigma}_z B$. The precession angle of the spin measures traversal time. Comparing the two approaches is very tutorial: see Appendix A, where the Larmor clock is reviewed.

2.3 Spin 1/2 as a galvanometer

Having clarified our motivation, we proceed semiphenomenologically and choose a new vector potential in the spin-current interaction $-\frac{1}{c}\vec{j}\vec{A}$. We replace the Ampère’s long-range form (2.5) by a model vector potential

$$\hat{A}_i(r) = \frac{\lambda\Phi_0}{4\pi} \hat{\sigma}_z \nabla_i \theta(f(r) - f_0) \quad (2.6)$$

concentrated on some surface S defined by the equation $f(r) = f_0$. Here $\Phi_0 = hc/e$, λ is a coupling constant, $f(r)$ is an arbitrary function, and, as usual, the step-function $\theta(x) = 1$ for $x > 0$, 0 for $x < 0$. The surface S defines a section of the conductor on which the interaction is localized:

$$\mathcal{H}_{int} = \int -\frac{1}{c} \vec{j} \vec{A} d^3r = -\frac{\lambda\hbar}{2e} \hat{\sigma}_z \hat{I}_S, \quad (2.7)$$

where $\hat{I}_S = \int_S \vec{j} d\vec{s}$, i.e., the spin now is coupled to the total current through the section S . With the choice (2.6) of the vector potential one can study current fluctuations in an arbitrary section of the conductor. Another advantage of the phenomenological Eq. (2.6) is that it involves only one Pauli matrix, which makes the spin dynamics essentially trivial. The choice of the quantization axis of the spin is arbitrary since (2.6) will be the only spin-dependent part of the Hamiltonian. Finally, by switching from the smooth function (2.5) to the singular form (2.6) we enforce integer values

of counted charge. To understand this, let us note that in the “fuzzy” case (2.5) the measurement can start at the moment when one of the electrons is located somewhere in the middle of the volume where $A \neq 0$, and then a fractional part of electron charge will be counted. On the contrary, in the “sharp” case (2.6), the spin reacts to the presence of an electron only when it crosses the section S . We shall see below in a microscopic calculation, that integer values of charge follow automatically from gauge invariance, since the form (2.6) is a gradient of a scalar.

Thus we come to the Hamiltonian

$$\hat{\mathcal{H}}_\sigma = \hat{\mathcal{H}}(\tilde{p}, r), \quad \tilde{p}_i = p_i - \frac{e}{c} \hat{A}_i, \quad (2.8)$$

where the spin-dependent \vec{A} is taken in the form (2.6). An essential feature of our approach is that we treat the constant λ of coupling between the spin and the current as a variable, i.e., we consider the spin precession as a function of the parameter λ . The reason is that, unlike the photon counting problem, our measurement scheme directly generates the function $\chi(\lambda)$, and then the counting probabilities P_m are obtained by reading Eq. (2.2) backwards.

At this point we are able to formulate our main result. Let us define a new Hamiltonian

$$\hat{\mathcal{H}}_\lambda = \hat{\mathcal{H}}(\tilde{p}, r), \quad \tilde{p}_i = p_i - \frac{1}{2} \lambda \hbar \nabla_i \theta(f(r) - f_0), \quad (2.9)$$

simply by suppressing $\hat{\sigma}_z$ in Eq. (2.6). The Hamiltonian $\hat{\mathcal{H}}_\lambda$ involves only quantities of the electron subsystem. Below we show that by measuring precession of the spin coupled to the current, one obtains the quantity

$$\chi(\lambda) = \langle e^{i\hat{\mathcal{H}}_{-\lambda}t} e^{-i\hat{\mathcal{H}}_\lambda t} \rangle. \quad (2.10)$$

Here the brackets $\langle \dots \rangle$ stand for averaging over initial state of electrons. Note that $\chi(\lambda)$ is written in terms of a purely electron problem, not involving spin variables. We shall find that the function $\chi(\lambda)$ defines the result of any measurement of the spin polarization at the time t when the spin-current coupling is switched off. Moreover, we

shall see that the function (2.10) has the meaning of a generating function of electron counting distribution, i.e., Fourier transform of $\chi(\lambda)$ gives counting probabilities, entirely analogous to (2.2).

Our goal now will be to express evolution of the spin in terms of quantities corresponding to the electron system. The interaction is given by Eqs. (2.6),(2.8). Suppose that the measurement starts at the moment 0 and lasts until time t , i.e., the spin-current interaction is switched on during the time interval $0 < \tau < t$. Let us evaluate the density matrix $\hat{\rho}_s(t)$ of the spin, right after it is disconnected from the circuit. We have

$$\hat{\rho}_s(t) = \text{tr}_e(e^{-i\hat{\mathcal{H}}_\sigma t} \hat{\rho} e^{i\hat{\mathcal{H}}_\sigma t}) , \quad (2.11)$$

where $\hat{\rho}$ is initial density matrix $\hat{\rho}_e \otimes \hat{\rho}_s$ at $t = 0$, $\hat{\rho}_e$ is initial density matrix of electrons, and $\text{tr}_e(\dots)$ means partial trace taken over electron indices, the spin indices left free. In terms of the spin variables, the operator $e^{-i\hat{\mathcal{H}}_\sigma t}$ is a function only of $\hat{\sigma}_z$, and hence it is diagonal in spin: $\langle \uparrow | e^{-i\hat{\mathcal{H}}_\sigma t} | \downarrow \rangle = \langle \downarrow | e^{-i\hat{\mathcal{H}}_\sigma t} | \uparrow \rangle = 0$. In other words, if initially the spin is in a pure state, up or down, it will not precess. For $\hat{\rho}_s(t)$ this remark yields:

$$\hat{\rho}_s(t) = \begin{bmatrix} \rho_{\uparrow\uparrow}(0) & \chi(\lambda)\rho_{\uparrow\downarrow}(0) \\ \chi(-\lambda)\rho_{\downarrow\uparrow}(0) & \rho_{\downarrow\downarrow}(0) \end{bmatrix}. \quad (2.12)$$

Here $\chi(\lambda) = \text{tr}_e(e^{-i\hat{\mathcal{H}}_\lambda t} \hat{\rho}_e e^{i\hat{\mathcal{H}}_\lambda t})$, where $e^{-i\hat{\mathcal{H}}_\lambda t}$ is the evolution operator for the problem (2.9). Now, after the spin degrees of freedom are taken care of by (2.12), we are left with a purely electron problem, that involves only electron degrees of freedom but not the spin. By using cyclic property of the trace one can show that $\chi(\lambda)$ in Eq. (2.12) is identical to (2.10).

In principle, any entry of a density matrix can be measured, hence the quantity $\chi(\lambda)$ is also measurable. In order to make clear the relation of $\chi(\lambda)$ with the distribution of precession angles, let us recall the transformation rule for the spin 1/2 density matrix under rotation by an angle θ around the z -axis:

$$\mathcal{R}_\theta(\hat{\rho}) = \begin{bmatrix} \rho_{\uparrow\uparrow} & e^{-i\theta} \rho_{\uparrow\downarrow} \\ e^{i\theta} \rho_{\downarrow\uparrow} & \rho_{\downarrow\downarrow} \end{bmatrix}. \quad (2.13)$$

By combining this with Eq. (2.2) we write $\hat{\rho}_s(t)$ as

$$\hat{\rho}_s(t) = \sum_m P_m \mathcal{R}_{\theta=m\lambda}(\hat{\rho}), \quad (2.14)$$

which assigns to P_m the meaning of the probability to observe precession angle $m\lambda$. Let us finally note that such interpretation of P_m is consistent with what one expects on classical grounds, because for a *classical* magnetic moment $\vec{\sigma}$ interacting with the current according to (2.6) the angle $\theta = \lambda$ corresponds to the precession due to a current pulse carrying the charge of one electron.

2.4 Single-channel conductor. General formalism

In order to see Eq. (2.10) working, let us consider an ideal single channel conductor, i.e., the Schrödinger equation

$$i\frac{\partial\psi}{\partial t} = \left[\frac{1}{2} \left(-i\frac{\partial}{\partial x} - \frac{\lambda}{2}\delta(x) \right)^2 + U(x) \right] \psi \quad (2.15)$$

in one dimension, where the potential $U(x)$ represents scattering region and the vector potential is inserted according to (2.6) at the $x = 0$ section. In order to describe transport, we shall use scattering states, left and right. Their population $n_{L(R)}(E)$ are equilibrium Fermi functions with temperature T and chemical potentials shifted by eV , $\mu_L - \mu_R = eV$, representing a dc voltage.

For the problem (2.15) one can write the time dependent scattering states as

$$\begin{aligned} \psi_{L,k}(x,t) &= e^{-iE_k t} \begin{cases} e^{ikx} + B_L e^{-ikx}, & x < -a/2 \\ e^{i\lambda/2} A_L e^{ikx}, & x > a/2 \end{cases} \\ \psi_{R,k}(x,t) &= e^{-iE_k t} \begin{cases} e^{-i\lambda/2} A_R e^{-ikx}, & x < -a/2 \\ e^{-ikx} + B_R e^{ikx}, & x > a/2 \end{cases} \end{aligned} \quad (2.16)$$

where a is the width of the barrier, and $A_{L,R}$ and $B_{L,R}$ are the transmission and reflection amplitudes in the absence of the spin vector potential. To make expressions

less heavy, we suppress electron spin. The phase factors $e^{\pm i\lambda/2}$ in (2.16) are found immediately by observing that the vector potential in the Schrödinger equation can be eliminated by the gauge transformation $\psi(x) \rightarrow \exp(i\lambda/2 \theta(x))\psi(x)$. Scattering amplitudes form a unitary matrix:

$$\hat{S}_\lambda = \begin{bmatrix} e^{i\lambda/2} A_L & B_R \\ B_L & e^{-i\lambda/2} A_R \end{bmatrix} \quad (2.17)$$

We will study the range of small $T, eV \ll E_F$, when only the states close to the Fermi level are important. In this case there is additional simplification because the states near Fermi energy have almost linear dispersion law, and thus all wave-packets travel with the speed v_F without changing shape. Then, following Landauer and Martin [35], instead of the usual scattering states (2.16), it is convenient to use their Fourier transform. By ignoring the energy-dependence of $A_{L,R}$ and $B_{L,R}$, which is equivalent to saying that the scattering time is negligible, and assuming that the dispersion is strictly linear, one obtains the representation of scattering in terms of time-dependent scattering wave packets

$$\begin{aligned} \psi_{L,\tau}(x,t) &= \begin{cases} \delta(x_-), & t < \tau \\ e^{i\lambda/2} A_L \delta(x_-) + B_L \delta(x_+), & t > \tau \end{cases} \\ \psi_{R,\tau}(x,t) &= \begin{cases} \delta(x_+), & t < \tau \\ e^{-i\lambda/2} A_R \delta(x_+) + B_R \delta(x_-), & t > \tau \end{cases} \end{aligned} \quad (2.18)$$

where $x_\pm = x \pm v_F(t - \tau)$. Here τ is the moment of scattering of a packet, which in this representation is a label in the continuum of states, like k in (2.16). The assumption that the scattering amplitudes are energy-independent (and that scattering takes no time) is equivalent to replacing the barrier $U(x)$ of finite width by $U_0\delta(x)$ and is consistent with the closeness to E_F .

Second-quantized, electron states (2.18) lead to $\hat{\psi}(x,t) = \hat{\psi}_L(x,t) + \hat{\psi}_R(x,t)$ with

$$\hat{\psi}_{L(R)}(x,t) = \sum_\tau \psi_{L(R),\tau}(x,t) \hat{c}_{1(2),\tau}, \quad (2.19)$$

where $c_{1,\tau}$ and $c_{2,\tau}$ are canonical Fermi operators corresponding to the states (2.18), the left and the right respectively. One checks that fermionic commutation relations for $c_{1(2),\tau}$,

$$c_{i,\tau}^+ c_{j,\tau'} + c_{j,\tau'} c_{i,\tau}^+ = \delta_{ij} \delta(\tau - \tau') \quad (2.20)$$

$$c_{i,\tau} c_{j,\tau'} + c_{j,\tau'} c_{i,\tau} = 0 \quad , \quad c_{i,\tau}^+ c_{j,\tau'}^+ + c_{j,\tau'}^+ c_{i,\tau}^+ = 0 \quad , \quad (2.21)$$

yield the usual commutation relations for $\psi_{L(R)}(x, t)$. From that one finds the meaning of the summation in (2.19): $\sum_{\tau} \dots = \int_{-\infty}^{\infty} \dots d\tau$. Mathematically, in this paragraph we defined second-quantized $\psi(x)$ in (2.15).

The advantage of introducing the basis of the wave-packets (2.18),(2.19) is that now it is straightforward to write the many-particle evolution operator through the single-particle scattering matrix \hat{S}_{λ} :

$$e^{-i\hat{\mathcal{H}}_{\lambda}t} = \exp \int_0^t d\tau \sum_{ij} \ln[\hat{S}_{\lambda}]_{ij} c_{i,\tau}^+ c_{j,\tau} \quad , \quad (2.22)$$

To verify (2.22) let us note that in the wave-packet representation (2.18) Fermi correlations occur only for the pairs of left and right states that scatter at the same instant of time. For each of such pairs the evolution operator $e^{-i\hat{\mathcal{H}}_{\lambda}t}$ is $\hat{1}$ if both states are occupied or both are empty, otherwise it is given by the single-particle scattering matrix (2.17).

Using similar arguments, we compute

$$e^{i\hat{\mathcal{H}}_{-\lambda}t} e^{-i\hat{\mathcal{H}}_{\lambda}t} = \exp \int_0^t d\tau \sum_{ij} \hat{W}_{ij} c_{i,\tau}^+ c_{j,\tau} \quad , \quad (2.23)$$

where $e^{\hat{W}} = \hat{S}_{-\lambda}^{-1} \hat{S}_{\lambda}$ is readily obtained from (2.17):

$$e^{\hat{W}} = \begin{bmatrix} e^{i\lambda} |A_L|^2 + |B_L|^2 & 2i \sin \lambda \bar{A}_L B_R \\ 2i \sin \lambda \bar{B}_R A_L & e^{-i\lambda} |A_R|^2 + |B_R|^2 \end{bmatrix} \quad (2.24)$$

Using unitarity of $e^{\hat{W}}$ and commutation rules for $c_{\alpha,\tau}$ one can rewrite (2.23) in terms

of normal ordering:

$$e^{i\hat{H}_{-\lambda}t}e^{-i\hat{H}_{\lambda}t} = : \exp \int_0^t d\tau \sum_{ij} [e^{\hat{W}} - 1]_{ij} c_{i,\tau}^+ c_{j,\tau} : \quad (2.25)$$

This form is ready to be plugged into Eq. (2.10) and averaged over the initial state. Let us note the striking similarity of the two formulas obtained by different means: the fermionic Eq. (2.25) and the bosonic Eq. (2.3).

Also, let us mention that the periodicity of the matrix (2.24) in λ ensures periodicity of $\chi(\lambda)$, and thus guarantees integer values of charge.

2.5 Equilibrium fluctuations

Let us start with a simple example of a single particle in the state $c_{1,\tau}^+|\text{vac}\rangle$ that corresponds to scattering at the moment τ . In this case, from (2.25) and (2.10) one gets $\chi(\lambda) = e^{i\lambda}|A|^2 + |B|^2$ for $0 < \tau < t$, 1 otherwise. ($|A| = |A_L| = |A_R|$, $|B| = |B_L| = |B_R|$) Evidently, according to Eq. (2.2), this simply means that for the scattering occurring during operation of the detector, the counting probabilities are identical to the one-particle scattering probabilities, as it should be expected.

Now, let us consider current fluctuations in an equilibrium Fermi gas. Assume perfect transmission: $B_{L(R)} = 0$. Then Eq. (2.24) gives $\hat{W} = i\lambda\sigma_z$, and thus Eq. (2.23) becomes

$$e^{i\hat{H}_{-\lambda}t}e^{-i\hat{H}_{\lambda}t} = \exp i\lambda \int_0^t (c_{1,\tau}^+ c_{1,\tau} - c_{2,\tau}^+ c_{2,\tau}) d\tau , \quad (2.26)$$

i.e., the right and the left states separate. We observe that the averaging of (2.26) over the Fermi ground state is identical to that performed in the orthogonality catastrophe calculation [48]. Thus, averaging of (2.26) can be done using the bosonization method [49] that replaces the fermionic Hamiltonian by a bosonic one:

$$\hat{\mathcal{H}}_{\text{Bose}} = \frac{\hbar v_F}{4\pi} \int : (\nabla\theta_L)^2 : + : (\nabla\theta_R)^2 : dx , \quad (2.27)$$

where $\theta_{L(R)}(x)$ are Bose operators,

$$[\nabla\theta_{L(R)}(x), \theta_{L(R)}(y)] = \pm 2\pi i \delta(x - y) . \quad (2.28)$$

The density of the left- and right-moving electrons is written in terms of $\theta_{L(R)}(x)$ as $\rho_{L(R)}(x) = \frac{1}{2\pi} \nabla\theta_{L(R)}(x)$. Therefore, the average of (2.26) is equal to the average

$$\langle \exp \frac{i\lambda}{2\pi} (\theta_L(t) - \theta_L(0) - \theta_R(t) + \theta_R(0)) \rangle \quad (2.29)$$

taken over the ground state of the Hamiltonian (2.27). Performing this gaussian average one gets

$$\chi(\lambda) = e^{-\tilde{\lambda}^2 f(t, T)} , \quad (2.30)$$

where $\tilde{\lambda}/2\pi + 1/2 = [\lambda/2\pi + 1/2]$, with $[...]$ being the fractional part. The function

$$f(t, T) = \left\langle \left\langle \left(\int_0^t c_{1,\tau}^+ c_{1,\tau} d\tau \right)^2 \right\rangle \right\rangle \quad (2.31)$$

$$= \begin{cases} \frac{1}{2\pi^2} \ln E_F t & , \quad \hbar/E_F \ll t \ll \hbar/T \\ Tt/h & , \quad t \gg \hbar/T \end{cases} . \quad (2.32)$$

At long times, according to (2.2), this leads to gaussian counting statistics.

Let us remark that, incidentally, Eq. (2.30) also gives a solution to another problem: the statistics of the number of fermions inside a segment of fixed length in one dimension. The relation is immediately obvious after one assigns to τ in Eq. (2.26), the meaning of a coordinate on a line. Thus, in this problem the statistics are gaussian as well.

Now, it turns out that the general case $B \neq 0$ can be reduced to (2.26) by a canonical transformation of $c_{\alpha,\tau}$ that makes the quadratic form in (2.23) diagonal. The transformation is related in the usual way with the eigenvectors of the matrix \hat{W} . Thus, we come to Eqs. (2.26),(2.30) with λ replaced by λ_* :

$$\sin \frac{\lambda_*}{2} = |A| \sin \frac{\lambda}{2} . \quad (2.33)$$

The counting statistics in this case are non-gaussian:

$$\chi(\lambda) = e^{-\lambda^2 f(t, T)} . \quad (2.34)$$

One checks that the second moment of the distribution

$$\langle\langle m^2 \rangle\rangle = - \left. \frac{\partial^2 \chi(\lambda)}{\partial \lambda^2} \right|_{\lambda=0} = 2|A|^2 f(t, T) \quad (2.35)$$

agrees with the Johnson-Nyquist formula for the equilibrium noise.

2.6 Statistics of a dc current: quantum shot noise

Let us consider non-equilibrium noise. In this case, due to the asymmetry in the population, $n_{L(R)}(E) = (\exp(E \pm \frac{1}{2}eV)/T + 1)^{-1}$, generally one cannot uncouple the two channels by a canonical transformation. We calculate the statistics within an approximation that ignores the effect of switching at $\tau = 0$ and $\tau = t$. Let us close the axis τ into a circle of length t , which amounts to restricting on periodic states:

$$\psi(\tau) = \psi(\tau \pm t) . \quad (2.36)$$

For the t -periodic problem, by going to the Fourier space, one has

$$\chi(\lambda) = \prod_{k \in \mathbb{Z}} \left[1 + |A|^2 (e^{-i\lambda} - 1) n_L(E_k) (1 - n_R(E_k)) + |A|^2 (e^{i\lambda} - 1) n_R(E_k) (1 - n_L(E_k)) \right] , \quad (2.37)$$

where $E_k = 2\pi\hbar k/t$, k is an integer. For large t , $t \gg \hbar/T$ or $t \gg \hbar/eV$, the product is converted to an integral:

$$\ln(\chi(\lambda)) = \frac{t}{2\pi\hbar} \int_{-\infty}^{+\infty} dE \ln \left(1 + |A|^2 (e^{-i\lambda} - 1) \times n_L(1 - n_R) + |A|^2 (e^{i\lambda} - 1) n_R(1 - n_L) \right) . \quad (2.38)$$

We evaluate it analytically, and get

$$\chi(\lambda) = \exp(-tTu_+u_-/h) , \quad (2.39)$$

where

$$u_{\pm} = v \pm \cosh^{-1}(|A|^2 \cosh(v + i\lambda) + |B|^2 \cosh v) , \quad (2.40)$$

$v = eV/2T$. The answer simplifies in the two limits: $T \gg eV$ and $eV \gg T$. In the first case we return to the equilibrium result (2.34). In the second case, corresponding to the recently discussed quantum shot noise [11, 12, 13, 32], we have

$$\chi(\lambda) = (e^{i\epsilon\lambda}|A|^2 + |B|^2)^{e|V|t/h}, \quad \epsilon = \text{sgn}V , \quad (2.41)$$

Analyzed according to Eq. (2.2), this $\chi(\lambda)$ leads to the binomial distribution

$$P_N(m) = p^m q^{N-m} C_N^m ,$$

$p = |A|^2$, $q = |B|^2$, $N = e|V|t/h$. One checks that the moments $\langle m \rangle = pN$ and $\langle\langle m^2 \rangle\rangle = pqN$ correspond directly to the Landauer formula and to the formula for the intensity of the quantum shot noise [11, 12, 13, 32]. The correction to the statistics due to the switching effects is insignificant [37].

2.7 Universal statistics of transport in disordered conductors

The physics of current fluctuations at low temperature presents an interesting quantum mechanical problem. Classical Johnson-Nyquist noise formula [25, 50] gives a good description of current fluctuations due to thermal fluctuations. However, at low temperature thermal fluctuations are small and a new type of noise becomes important. At low temperature, the quantum nature of the current and the discreteness of electron charge is the main source of current fluctuations and due to these reasons,

this noise is called “quantum shot noise”.

Lots of the low temperature current fluctuation studies deal with a disordered conductor because it has a simple and well established mathematical description based on Landauer’s approach [8]. Lesovik [11] and Yurke and Kochanski [12] studied the quantum shot noise in a two-terminal conductor using this approach and found an expression for noise power which is a factor $1-T$ off the classical shot noise, where T is a transmission coefficient. This analysis was generalized to a multiterminal conductor by Büttiker [13], and he also found the reduction of the noise. Physically, the noise reduction is due to the Fermi statistics that leads to correlation of transmission events.

In Landauer’s approach, details of current transport are determined by transmission coefficients and there have been many works on the distribution of the coefficients. In the past decade, pioneered by Dorokhov [51], the random matrix theory of disordered conductors was developed [52], motivated by theoretical discovery and experimental observation of the universal conductance fluctuations. The theory succeeded in providing a complete characterization of the distribution and it also succeeded in providing the insight on the origin of the universal conductance fluctuations. One of the fundamental results in the random matrix theory is the universality of the distribution in the metallic regime and the universality provides a link between the microscopically calculated transmission coefficients and the macroscopically measurable conductance.

Application of the universal distribution to current fluctuations also provides insights on the current fluctuations of a disordered conductor. Recently Beenakker and Büttiker [34] calculated the sample averaged noise power using the universal distribution and found that it depends only on the conductance and that it is one-third of the classical value.

Noise power is a useful characteristic of fluctuations that reveals the reduction of noise due to Fermi correlation. However, compared to Johnson-Nyquist noise, our understanding of the quantum shot noise is limited because not many things are known besides the noise magnitude. Our goal in this paper is to explore the physics of low temperature current fluctuations beyond the noise power. For that purpose,

it is useful to look at the behavior of current fluctuations in the time domain, which brings one to the notion of counting statistics of charge transmitted in a conductor over fixed time. A previous study of the counting statistics for a single channel conductor revealed that the attempts to transmit electrons are highly correlated and almost periodic in time, which leads to binomial statistics [37].

In the time domain picture, the charge $Q(t)$ (measured in the units of e) transmitted over a time interval t is the quantity of interest and the probability distribution $P(Q(t))$ tells everything about the current fluctuations. Even at zero temperature, $P(Q(t))$ has finite peak width due to the quantum nature of current. To study $P(Q(t))$, it is useful to introduce the characteristic function $\chi(\lambda)$,

$$\chi(\lambda) = \sum_{\text{integer } Q} e^{iQ\lambda} P(Q) \quad \text{for } -\pi < \lambda < \pi, \quad (2.42)$$

because in many cases, $\chi(\lambda)$ is easier to calculate than $P(Q(t))$ itself. The function $\chi(\lambda)$ is a Fourier transform of $P(Q(t))$ and so once $\chi(\lambda)$ is known, we can either take inverse Fourier transform to get an explicit expression for $P(Q(t))$, or expand its logarithm to get all cumulants of the distribution:

$$\log \chi(\lambda) = \sum_{k=1}^{\infty} \frac{(i\lambda)^k}{k!} \langle\langle Q^k \rangle\rangle. \quad (2.43)$$

In the linear transport regime, we derive a general expression for $\chi(\lambda)$ in terms of transmission coefficients and by combining it with the transmission coefficients distribution for quasi one dimensional conductors, we derive

$$\overline{\log \chi(\lambda)} = \frac{GVt}{e} \operatorname{arcsinh}^2 \sqrt{e^{i\lambda} - 1}, \quad (2.44)$$

where V is the dc voltage, $G = g(e^2/h) = (Nl/L)(e^2/h)$ is the average conductance, and the bar on the left hand side represents the sample average. Cumulant expansion of Eq. (2.44) implies that on average, for $GVt/e \gg 1$, $P(Q(t))$ has a Gaussian peak at GVt/e with $\langle\langle Q^2(t) \rangle\rangle = GVt/3e$. It also implies that even though the peak is Gaussian, the tails show deviation from both Gaussian and Poisson distributions.

We estimate sample to sample variations of $P(Q(t))$ by studying variances of various quantities and find that for $GVt/e \gg 1$ sample to sample variations of $P(Q(t))$ appear only in the tails of $P(Q(t))$ and that around the peak, $P(Q(t))$ is universal.

Before we present the derivation of the above result, let us stress that there are two kinds of averages involved. To avoid confusion, we will use a bar($\overline{\dots}$) for an ensemble average, or an average over samples, and a bracket($\langle \dots \rangle$) for a quantum average, or a quantum expectation value. Also we reserve a double bracket($\langle\langle \dots \rangle\rangle$) for a cumulant of a quantum expectation value and “var”(var(\dots)) for $\overline{\dots^2} - \overline{\dots}^2$.

Now, let us derive Eq. (2.44). Following the Landauer’s approach [8], we consider a conductor sandwiched between two perfect leads. In the linear transport regime, scattering properties of a conductor are described by a unitary scattering matrix \hat{S} that relates incoming and outgoing amplitudes, $I_{L(R)}$ and $O_{L(R)}$:

$$\hat{S} \begin{pmatrix} I_L \\ I_R \end{pmatrix} = \begin{pmatrix} O_L \\ O_R \end{pmatrix}, \quad (2.45)$$

where the subscripts L and R stand for the left and the right leads.

The unitarity of \hat{S} is due to the current conservation, and it allows a system to be decomposed into independent channels [53]. Then the decomposition motivates one to study single channel transport first, where a transmission coefficient T determines the transport. Recently, the counting statistics of the single channel transport was studied [37]. In the low temperature limit ($k_B T \ll eV$), the characteristic function $\chi_1(\lambda)$ of a single channel system becomes

$$\chi_1(\lambda) = (pe^{i\lambda} + q)^M, \quad (2.46)$$

where $p = T$, $q = 1 - T$, $M = eVt/h^1$ and $M \gg 1$ is assumed. The inverse Fourier transform of Eq. (2.46) gives the binomial distribution, which implies that

¹The spin degeneracy is ignored. To include the degeneracy, M has to be multiplied by 2. Also the positivity of M is assumed. If M is negative, Eq. (2.46) has to be complex conjugated with M replaced by its absolute value.

the intervals between subsequent attempts to transmit electrons are quite regular. This regularity is due to Pauli exclusion principle.

Having the characteristic function of a single channel, we write the total characteristic function $\chi(\lambda)$ as a product,

$$\chi(\lambda) = \prod_j (T_j e^{i\lambda} + 1 - T_j)^M, \quad (2.47)$$

where T_j is a transmission coefficient of channel j . The product form Eq. (2.47) follows from the mutual independence of channels. By taking logarithm of Eq. (2.47), we get

$$\log \chi(\lambda) = M \sum_j \log \left(T_j e^{i\lambda} + 1 - T_j \right), \quad (2.48)$$

and by expanding Eq. (2.48) in terms of λ , we find

$$\langle\langle Q^k(t) \rangle\rangle = M \sum_j \left(T(1-T) \frac{d}{dT} \right)^{k-1} T|_{T=T_j}. \quad (2.49)$$

We note that both $\log \chi(\lambda)$ and $\langle\langle Q^k(t) \rangle\rangle$ are linear statistics of T_j 's.

Current fluctuations are determined by distribution of transmission coefficients and the distribution varies from sample to sample even though samples have the same macroscopic parameters. Therefore in principle each sample exhibits distinctive current fluctuations. However according to the random matrix theory of disordered conductors, in the metallic regime ($1 \ll g \ll N$) where N is the number of channels, the distribution approaches a universal one [52]. This result provides a motivation to approximate the sample-dependent distribution by the universal one. To exploit the universal distribution, we introduce new variables ν_j 's and the density function $D(\nu)$ defined by $T_j = 1/\cosh^2 \nu_j$ and $D(\nu)d\nu = D(T)dT$, where $D(T)$ is the density function of T_j 's. According to Ref. [52], $D(\nu)$ is uniform over a wide range of ν ,

$$D(\nu) = g \text{ for } \nu < \nu_c. \quad (2.50)$$

We combine Eq. (2.48) with the universal distribution to obtain

$$\overline{\log \chi(\lambda)} = Q_0 \int_0^\infty d\nu \log \left(\frac{e^{i\lambda} - 1}{\cosh^2 \nu} + 1 \right), \quad (2.51)$$

where $Q_0 = gM$. In Eq. (2.51) the upper limit ν_c is replaced by infinity, which is valid in the metallic regime because for large ν , the integrand is exponentially small. The evaluation of the integral then leads to Eq. (2.44). We note that because $\log \chi(\lambda)$ is a linear statistic, the universal distribution approximation is equivalent to taking an average over samples.

Cumulants are useful in understanding features of the probability distribution. By using the formula Eq. (2.43), we obtain sample averaged cumulants

$$\begin{aligned} \overline{\langle\langle Q(t) \rangle\rangle} &= Q_0, & \overline{\langle\langle Q^2(t) \rangle\rangle} &= \frac{1}{3} Q_0, \\ \overline{\langle\langle Q^3(t) \rangle\rangle} &= \frac{1}{15} Q_0, & \overline{\langle\langle Q^4(t) \rangle\rangle} &= -\frac{1}{105} Q_0, \\ \overline{\langle\langle Q^5(t) \rangle\rangle} &= -\frac{1}{105} Q_0, & \overline{\langle\langle Q^6(t) \rangle\rangle} &= \frac{1}{231} Q_0, \\ \overline{\langle\langle Q^7(t) \rangle\rangle} &= \frac{27}{5005} Q_0, & \overline{\langle\langle Q^8(t) \rangle\rangle} &= -\frac{3}{715} Q_0, \\ \overline{\langle\langle Q^9(t) \rangle\rangle} &= -\frac{233}{36465} Q_0, & \overline{\langle\langle Q^{10}(t) \rangle\rangle} &= \frac{6823}{969969} Q_0, \dots \end{aligned} \quad (2.52)$$

The first cumulant is trivial. It is just a definition of G and it shows where the peak of $P(Q(t))$ is. The second cumulant measures the width square of the peak. It is also directly related to the noise power $P = \int dt \langle\langle I(0)I(t) \rangle\rangle$, a widely used measure of noise magnitude, by $\langle\langle Q^2(t) \rangle\rangle = tP$ for large t , and its ensemble average is one-third of the classical value Q_0 , as first pointed out by Beenakker and Büttiker [34]. The third and the fourth cumulants are measures of skewness and sharpness of the peak, respectively and they are related to 3 and 4-point current current correlation functions by similar relations. We note that all cumulants are proportional to Q_0 and that for $Q_0 \gg 1$, $\overline{\langle\langle Q(t) \rangle\rangle}^k \gg \overline{\langle\langle Q^k(t) \rangle\rangle}$. Therefore the peak of the distribution $P(Q(t))$ is Gaussian for large conductance limit or long time limit. This result is quite expected from the central limit theorem. Now, to see the structure of the tails of $P(Q(t))$, let us study higher order cumulants. From Eq. (2.51), we obtain a general formula for

the ensemble averaged k -th order cumulants

$$\overline{\langle\langle Q^k(t)\rangle\rangle} = -i^k \frac{Q_0}{4} \int_{-\infty}^{\infty} dx \frac{1}{\sqrt{1+e^{-x}}} \int_{-\infty}^{\infty} dq e^{-iqx} \frac{q^{k-1}}{\sinh(\pi q - i0^+)}, \quad (2.53)$$

and by using the steepest descent method twice (see Appendix B), we obtain the asymptotics for large k ,

$$\overline{\langle\langle Q^k(t)\rangle\rangle} \sim \frac{Q_0}{(2\pi)^{k-1}} \frac{(k-1)!}{\sqrt{k}} \begin{cases} (-1)^{\frac{k+2}{2}} & \text{for even } k, \\ (-1)^{\frac{k+1}{2}} & \text{for odd } k. \end{cases} \quad (2.54)$$

The high order cumulants diverge factorially, which suggests that at the tails, $P(Q(t))$ is different from both Gaussian distribution and Poisson distribution which describes the classical current fluctuations. In comparison, $\overline{\langle\langle Q^k(t)\rangle\rangle} = 0$ for $k \geq 2$ for Gaussian distribution and $\overline{\langle\langle Q^k(t)\rangle\rangle} = Q_0$ for $k \geq 1$ for Poisson distribution.

It is known that in the presence of time reversal symmetry, there are of the order of M corrections to $\overline{\langle\langle Q(t)\rangle\rangle}$ and $\overline{\langle\langle Q^2(t)\rangle\rangle}$ due to weak localization [36], and it is natural to expect the same kind of corrections to higher order cumulants. However, because we are interested in the metallic regime, these corrections are small by a factor g and we will ignore them.

A proper next step is to estimate the magnitude of sample to sample variations of $P(Q(t))$. Here instead of $\log \chi(\lambda)$, we examine variance of $\langle\langle Q^k(t)\rangle\rangle$ to see the variations of $P(Q(t))$. $\langle\langle Q^k(t)\rangle\rangle$ is a linear statistic and the general formula for the variance of a linear statistic $A = \sum_j a(T_j)$ is obtained recently by Beenakker and Rejaei [54], and Chalker and Mecêdo [55],

$$\text{var}(A) = \frac{1}{\beta\pi^2} \int_0^\infty dk \frac{k\tilde{a}^2(k)}{1 + \coth(\frac{1}{2}\pi k)}, \quad (2.55)$$

$$\tilde{a}(k) = 2 \int_0^\infty d\nu a\left(\frac{1}{\cosh^2 \nu}\right) \cos k\nu, \quad (2.56)$$

where β is a symmetry constant, 1, 2, or 4 depending on the symmetry. We use this

formula to obtain

$$\begin{aligned} \text{var} (\langle\langle Q(t) \rangle\rangle) &= \frac{2}{15\beta} M^2, \\ \text{var} (\langle\langle Q^2(t) \rangle\rangle) &= \frac{46}{2835\beta} M^2, \end{aligned} \tag{2.57}$$

$$\text{var} (\langle\langle Q^3(t) \rangle\rangle) = \frac{11366}{1447875\beta} M^2. \tag{2.58}$$

We note that for low order cumulants, $\overline{\langle\langle Q^k(t) \rangle\rangle}^2$ is larger than $\text{var} (\langle\langle Q^k(t) \rangle\rangle)$ by at least a factor of g^2 , which is large in the metallic regime. Low order cumulants decide the shape of $P(Q(t))$ around the peak and therefore the small variance of low order cumulants implies that the peak shape shows little sample to sample variations, that is, it is almost universal.

To see the behavior of higher order cumulants, we obtain an asymptotic form of the variance (Appendix C) from an approximate variance formula in Ref. [56],

$$\text{var} (\langle\langle Q^k(t) \rangle\rangle) \sim \frac{4(2k-1)!}{(2\pi)^{2k}\beta} M^2. \tag{2.59}$$

According to Eq. (2.59), for high order cumulants, $\text{var} (\langle\langle Q^k(t) \rangle\rangle)$ becomes larger than $\overline{\langle\langle Q^k(t) \rangle\rangle}^2$ due to its rapidly growing factorial factor, which suggests that the tails of $P(Q(t))$ show large sample to sample variations. We argue that this rapid growth of $\text{var} (\langle\langle Q^k(t) \rangle\rangle)$ is not an artifact of the approximate variance formula used above because it assumes stronger spectral rigidity than the formula Eq. (2.55,2.56) and it has a tendency to slightly underestimate variances. Therefore large sample to sample variations at the tails of $P(Q(t))$ obtained above is not an artifact of the approximation.

In the above, we derived the shape of $P(Q(t))$ by examining $\overline{\log \chi(\lambda)}$ and its cumulant expansion instead of $\log \overline{\chi(\lambda)}$, which might be an intuitively more appropriate ensemble average because it is directly related to $\overline{P(Q(t))}$. However we argue that in contrast to the intuition, $\overline{\log \chi(\lambda)}$ is an appropriate ensemble average for the study of current fluctuations. One reason is that as we remarked earlier, a k -point current current correlation function is linearly related to $\langle\langle Q^k(t) \rangle\rangle$, whose ensemble average

can be obtained from $\overline{\log \chi(\lambda)}$ by a simple expansion. Another reason is that as we show later, $\log \overline{\chi(\lambda)}$ either becomes identical to $\overline{\log \chi(\lambda)}$ at short time limit, or is dominated by the conductance fluctuations instead of the current fluctuations.

Calculation of $\overline{\chi(\lambda)}$ is not simple because $\chi(\lambda)$ is not a linear statistic. Muttalib and Chen [57] did this calculation recently by large N limit continuum approximation and showed that in the long time limit, $\log \overline{\chi(\lambda)}$ becomes quite different from $\overline{\log \chi(\lambda)}$. Here we present improved calculation by a perturbation method and we believe that our calculation clarifies the reason why two averages become so different at large t .

Because $\chi(\lambda)$ is not a linear statistic, we need joint probability distribution of transmission coefficients to average it over ensembles. After standard variable change, $T = 1/(1+x)$, the joint probability distribution $P(\{x\})$ is

$$P(\{x\}) = \exp \left(\beta \sum_{a < b} V(x_a, x_b) + \beta \sum_a U(x_a) \right). \quad (2.60)$$

We choose $V(x, y) = (1/2) \log(x-y) + (1/2) \log(\operatorname{arcsinh}^2 \sqrt{x} - \operatorname{arcsinh}^2 \sqrt{y})$ and $U(x) = g \operatorname{arcsinh}^2(\sqrt{x})$ based on the exact calculation of the joint probability distribution function for $\beta = 2$ by Beenakker and Rejaei [54]. Then,

$$\overline{\chi(\lambda)} = \frac{Z_M}{Z_0}, \quad (2.61)$$

$$Z_M = \int \prod_a dx_a \exp \left(\beta \sum_{a < b} V(x_a, x_b) + \beta \sum_a U(x_a) + \sum_a M \log \frac{x_a + e^{i\lambda}}{x_a + 1} \right),$$

$$Z_0 = \int \prod_a dx_a \exp \left(\beta \sum_{a < b} V(x_a, x_b) + \beta \sum_a U(x_a) \right).$$

By expanding $\log \overline{\chi(\lambda)}$ in terms of M , we find

$$\log \overline{\chi(\lambda)} = \overline{\log \chi(\lambda)} + \operatorname{var}(\log \chi(\lambda)) + O(M^3), \quad (2.62)$$

and from the formula Eq. (2.55,2.56), we obtain

$$\log \overline{\chi(\lambda)} = g M \operatorname{arcsinh}^2 \sqrt{e^{i\lambda} - 1} \quad (2.63)$$

$$-\frac{M^2}{\beta} \left(3 \log \frac{\operatorname{arcsinh} \sqrt{e^{i\lambda} - 1}}{\sqrt{e^{i\lambda} - 1}} + \frac{1}{2} i\lambda \right) + O(M^3) .$$

Note that for $M \ll g$ (short time limit), $\log \overline{\chi(\lambda)}$ reduces to $\overline{\log \chi(\lambda)}$. We expand $\log \overline{\chi(\lambda)}$ in terms of λ to see features of $\overline{P(Q(t))}$:

$$\begin{aligned} \log \overline{\chi(\lambda)} &= gM(i\lambda) + \left(\frac{g}{3}M + \frac{2}{15\beta}M^2 \right) \frac{(i\lambda)^2}{2!} \\ &+ \left(\frac{g}{15}M + \frac{2}{315\beta}M^2 + O(M^3) \right) \frac{(i\lambda)^3}{3!} + \dots . \end{aligned} \quad (2.64)$$

The first expansion coefficient shows that $\overline{\langle Q(t) \rangle} = Q_0 = gM$, which is trivial. The second expansion coefficient, $\overline{\langle Q^2(t) \rangle} - \overline{\langle Q(t) \rangle}^2 = \overline{\langle \langle Q^2(t) \rangle \rangle} + \operatorname{var}(\langle \langle Q(t) \rangle \rangle) = Q_0/3 + (2/15\beta)M^2$ indicates that the peak width of $\overline{P(Q(t))}$ has two contributions. The first contribution is related to the noise power, and the second one to the universal conductance fluctuations because $\operatorname{var}(\langle \langle Q(t) \rangle \rangle)$ is proportional to the variance of the conductance. (The factor $2/15\beta$ is precisely the variance of the dimensionless conductance.) Note that as $t \rightarrow \infty$, the second contribution becomes dominant over the first one. It can be shown that the k -th order expansion coefficient contains k different contributions and in the long time limit, the most dominant contribution, which is proportional to M^k , is related to the k -th cumulant of the conductance fluctuations. From this analysis we see that the behavior of $\overline{\chi(\lambda)}$ for large t is governed by the conductance fluctuations instead of the current fluctuations.

As a short remark, we report that the continuum approximation calculation of $\log \overline{\chi(\lambda)}$, as suggested by Muttalib and Chen [57], produces the same result as Eq. (2.63) up to M^2 order. In Ref. [57], however, they adopted linear confining potential for $U(x)$ and obtained a result which is quite different from Eq. (2.63) even in the short time limit. We believe that this difference comes from their choice of the confining potential which is a good approximation only for very small x .

In summary, we examine the counting statistics of charge to study current fluctuations at low temperature. By calculating the characteristic function of the probability distribution $P(Q(t))$, we find that $P(Q(t))$ has a Gaussian peak at Q_0 with

$\langle\langle Q(t) \rangle\rangle = Q_0/3$ and we also find that the tails of $P(Q(t))$ are much more intense than the tails of Gaussian and classical Poisson distribution. By studying the variances of the cumulants, we establish that even though the peak location of $P(Q(t))$ varies from sample to sample due to universal conductance fluctuations, the peak shape of $P(Q(t))$ is universal in the metallic regime, and that the sample to sample variations show up only at the tails of $P(Q(t))$.

2.8 Conclusion

We introduced a quantum-mechanical scheme that gives complete statistical description of electron transport. It involves a spin 1/2 coupled to the current so that the spin precession measures transmitted charge. The off-diagonal part of the spin density matrix, taken as a function of the coupling constant, gives the generating function for the electron counting statistics. We find the statistics in a single-channel ideal conductor for arbitrary relation between temperature and voltage. In equilibrium, the counting statistics are gaussian, both for zero-point fluctuations and at finite temperature. At constant voltage and low temperature the statistics are Bernoullian and the distribution is binomial.

Chapter 3

Coherent States of Electric Current

3.1 Introduction

Another property of quantum noise that does not have classical analog is its phase sensitivity [1, 58]. For the current correlator $\langle\langle j(t_1)j(t_2) \rangle\rangle_+$ it results in a periodic sinusoidal dependence on Faraday's flux due to applied voltage, $\Phi = c \int_{t_1}^{t_2} V(t)dt$, with the period $\Phi_0 = hc/e$. The phase sensitivity manifests in singularities of the low frequency noise power in a junction driven by ac and dc signals together [59].

Even more remarkable is the behavior of current fluctuations due to a pulse of voltage [1, 5]. Total charge that flows through the conductor due to a voltage pulse fluctuates in such a way that the mean square fluctuation diverges whenever the flux of the pulse is not an integer: $\varphi = \frac{e}{\hbar} \int_{-\infty}^{\infty} V(t)dt \neq 2\pi n$. However, for integer φ the fluctuation of the transmitted charge is finite (Sec. 3.2). This result has simple interpretation in terms of the Anderson orthogonality catastrophe theory, since the flux φ enters the time dependent scattering matrix of the conductor through the forward scattering amplitude.

With this, one is led to address the issue of current states that minimize the current fluctuations at fixed mean transmitted charge [2, 5]. It is found in Sec. 3.3

that such states are produced by time-dependent voltage of the form

$$V(t) = \pm \frac{\hbar}{\pi e} \sum_{k=1}^n \frac{\tau_k}{(t - t_k)^2 + \tau_k^2}, \tau_k > 0, \quad (3.1)$$

a sum of Lorentzian pulses of unit flux each. It is remarkable that the minimal noise due to such sequence of pulses is independent of the pulse positions t_k and widths τ_k , which leads to obvious parallels with solitons. The noise minimizing current states can be compared to the coherent states that minimize the quantum-mechanical uncertainty. Apart from obvious similarity, there is a difference: the coherent current states are many-body time-dependent scattering states. Their role in transport is an interesting subject of future work.

3.2 Noise due to a voltage pulse: Orthogonality catastrophe

Here we consider the fluctuations of current in a single-channel conductor induced by a voltage pulse. The result will be that the dependence of the fluctuations on Faraday's flux $\Phi = -c \int V(t) dt$ contains a logarithmically divergent term periodic in Φ with the period $\Phi_0 = hc/e$. The fluctuation is smallest near $\Phi = n\Phi_0$. The divergence is explained by a comparison with the orthogonality catastrophe problem. The Φ_0 -periodicity is related with the discreteness of "attempts" in the binomial statistics picture of charge fluctuations presented above.

Historically, the orthogonality catastrophe problem emerged from the observation that the ground state of a Fermi system with a localized perturbation is orthogonal to the non-perturbed ground state, no matter how weak the perturbation [60]. Originally, the discussion was focused on the purely static effect of Fermi correlations on the ground state that leads to the orthogonality, but then it shifted to dynamical effects. When a sudden localized perturbation is switched on in a Fermi gas, the number of excited particle-hole pairs detected over a large time interval t diverges as $\ln t/\tau$, where τ is the time of switching of the perturbation. This effect leads to power

law singularities in transition rates involving collective response of fermions, such as X-ray absorption in metals [15, 61]. In this section we present an application of the orthogonality catastrophe picture to the electric current noise.

Let us consider a single channel conductor in an external field described by the one-dimensional Schrödinger equation

$$i\dot{\psi}(x, t) = \hat{\mathcal{H}}\psi(x, t) ,$$

$$\hat{\mathcal{H}} = \frac{1}{2} \left(-i\frac{\partial}{\partial x} - \frac{e}{c}A(x, t) \right)^2 + U(x) , \quad (3.2)$$

where the potential $U(x)$ represents the scattering region and $A(x, t)$ is the vector potential corresponding to the applied pulse of electric field. Since the pulse duration τ is assumed to be much longer than the time of scattering, one can treat the vector potential as static and apply a gauge transformation in order to accumulate the flux $\varphi(t) = e/\hbar \int_{-\infty}^t V(t')dt'$ in the phases of the transmission amplitudes, thus making them time dependent. By going through the argument presented in Sec. 2.4, one obtains the scattering states (2.16) and (2.18) with time-dependent forward scattering amplitudes:

$$A_{L(R)} \rightarrow A_{L(R)} e^{\pm i\varphi(t_r)} , \quad (3.3)$$

where the time $t_r = t - |x|/v_F$ is taken retarded to account for the finite speed of motion after scattering. As before, here we assume that scattering by the potential and traversing the region where the voltage is applied takes negligible time compared to the duration of the voltage pulse. In this approximation the amplitudes of backward scattering $B_{L(R)}$ are time-independent constants.

To draw a relation with the orthogonality catastrophe problem, let us study the effect of the voltage pulse on the scattering phases δ_1, δ_2 . They can be found by diagonalizing the scattering matrix

$$\hat{\mathcal{S}}(t) = \begin{bmatrix} A_L e^{i\varphi(t)+i\lambda/2} & B_R \\ B_L & A_R e^{-i\varphi(t)-i\lambda/2} \end{bmatrix} \quad (3.4)$$

that has eigenvalues $e^{i\delta_1}, e^{i\delta_2}$. The relation between the phases $\delta_{1,2}$ before and after the pulse is written conveniently through $\delta_{\pm} = (\delta_1 \pm \delta_2)/2$. The phase δ_+ does not change at any time, and the phase δ_- changes according to

$$\begin{aligned} \cos^2 \delta_-(t') + \cos^2 \delta_-(t) - 2 \cos \delta_-(t') \cos \delta_-(t) \\ \times \cos \Delta\varphi = |A_L|^2 \sin^2 \Delta\varphi \quad , \end{aligned} \quad (3.5)$$

where $\Delta\varphi = \varphi(t') - \varphi(t)$. Now, let us compare to the orthogonality catastrophe in the Fermi system subjected to a time-dependent perturbation (3.4). Change of the flux induces the shift of the phases $\delta_{\pm} \rightarrow \delta'_{\pm}$ and makes the new ground state orthogonal to the old one:

$$\langle 0'|0 \rangle = \exp \left(-2 \frac{\delta_*^2}{\pi^2} \ln \frac{L}{\lambda_F} \right) , \quad (3.6)$$

where L is the system size, λ_F is Fermi wavelength, and $e^{i\delta_*}$ is an eigenvalue of the matrix $\hat{\mathcal{S}}^{-1}(t = \infty)\hat{\mathcal{S}}(t = -\infty)$:

$$\sin \frac{\delta_*}{2} = |A_L| \sin \frac{\Delta\varphi}{2} . \quad (3.7)$$

In terms of dynamics this implies that the old ground state is shaken up so that infinitely many particle-hole pairs are excited [15]. It should lead to a logarithmically diverging contribution to noise, since for each of the particle-hole pairs there is a finite probability (equal to $|A_L B_R|^2$) that the particle and the hole will go to different terminals of the conductor, thus resulting in a current fluctuation. The periodicity in Faraday's flux $\Phi = -c \int V(t) dt$ follows from the gauge invariance and is explicit in Eqs. (3.5,3.7) for δ'_{\pm} . The logarithmic divergence vanishes at $\Phi = n\Phi_0$, as expected, since at integer Φ there is no long-term change of the scattering.

Let us calculate the mean square fluctuation of the charge $\langle\langle Q^2 \rangle\rangle$ transmitted through the system due to the pulse. For that, one can use the formula (2.25) with the time-dependent scattering matrix (3.4). To get the second cumulant $\langle\langle Q^2 \rangle\rangle$ one expands the exponent (2.25) up to second order terms in λ , and takes an irreducible

average using Wick theorem. The averages of $c_{i,\tau}$ have the usual form:

$$\begin{aligned}\langle c_{i,\tau}^+ c_{j,\tau'} \rangle &= \delta_{ij} \int n(E) e^{-iE(\tau-\tau')} \frac{dE}{2\pi}, \\ \langle c_{i,\tau} c_{j,\tau'}^+ \rangle &= \delta_{ij} \int (1-n(E)) e^{-iE(\tau-\tau')} \frac{dE}{2\pi},\end{aligned}\quad (3.8)$$

where $n(E) = (e^{E/T} + 1)^{-1}$ is the Fermi distribution. The result reads

$$\langle\langle Q^2 \rangle\rangle = \frac{ge^2}{2\pi} \int \left(|A|^4 \left| \int_0^t e^{i\omega t'} dt' \right|^2 + |AB|^2 \left| \int_0^t e^{i\varphi(t') + i\omega t'} dt' \right|^2 \right) \omega \coth \frac{\hbar\omega}{2T} \frac{d\omega}{2\pi}. \quad (3.9)$$

The first term in (3.9) is a part of equilibrium noise since it does not depend on φ . To analyze the second term, let us take a step-like time dependence of φ resulting from an abrupt voltage pulse applied at the time t_0 , $0 < t_0 < t$, the pulse duration τ being much shorter than t . Taking the integral and keeping only the terms diverging at $t \rightarrow \infty$, we find

$$\begin{aligned}& \frac{ge^2}{2\pi} \int \left| \frac{e^{i\omega t_0} - 1}{i\omega} + e^{2\pi i\Phi/\Phi_0} \frac{e^{i\omega t} - e^{i\omega t_0}}{i\omega} \right|^2 |\omega| \frac{d\omega}{2\pi} \\ &= \frac{ge^2}{\pi^2} \left(\ln \frac{tE_F}{\hbar} + 2 \sin^2 \frac{\pi\Phi}{\Phi_0} \ln \frac{t}{\tau} \right),\end{aligned}\quad (3.10)$$

where the ultraviolet-divergent integrals are cut at frequency $\sim E_F/\hbar$. By subtracting the result for $\Phi = 0$ as corresponding to equilibrium one obtains a logarithmic contribution to the non-equilibrium noise:

$$\langle\langle Q^2 \rangle\rangle = ge^2 |AB|^2 \left[\frac{2}{\pi^2} \sin^2 \frac{\pi\Phi}{\Phi_0} \ln \frac{t_0}{\tau} + \frac{\Phi}{\Phi_0} \right] + \dots, \quad (3.11)$$

The origin of the non-diverging second term in Eq. (3.11) will be discussed below. The dots in Eq. (3.11) represent corrections higher order in Φ_0/Φ and the equilibrium noise

$$\langle\langle Q^2 \rangle\rangle_{eq} = \frac{e^2 G}{\pi^2} \ln \frac{tE_F}{\hbar}, \quad G = g \frac{e^2}{\hbar} |A|^2, \quad (3.12)$$

that can be obtained in the same way at $\Phi = 0$. The expression (3.12) agrees with

the Nyquist formula

$$\langle\langle j_\omega j_{-\omega} \rangle\rangle = e^2 G \omega \coth \frac{\omega}{2T} \quad (3.13)$$

taken at $T = 0$, Fourier transformed, and combined with the relation $Q = \int_0^t j(t') dt'$.

The term in Eq. (3.11) proportional to Φ/Φ_0 is obtained by rewriting the integral in the second term of (3.9) as

$$\int \int \int \frac{d\omega}{2\pi} |\omega| dt_1 dt_2 e^{i(\varphi(t_1) - \varphi(t_2) + \omega(t_1 - t_2))}, \quad (3.14)$$

and extracting the contribution of almost coinciding times t_1 and t_2 by going to new variables $t = (t_1 + t_2)/2$, $t' = t_1 - t_2$ and changing the order of integration:

$$\int dt \int \frac{d\omega}{2\pi} |\omega| \int dt' e^{i\varphi(t_1) - i\varphi(t_2) + i\omega t'} = \int |\dot{\varphi}| dt, \quad (3.15)$$

where we replaced $\varphi(t_1) - \varphi(t_2) = \varphi(t + t'/2) - \varphi(t - t'/2)$ by $\dot{\varphi} t'$. The result (3.15) is approximate: it does not give the log-term because the transformation (3.15) properly takes care of the integral (3.14) only in the domain $t_1 \simeq t_2$, under the restriction that $\Phi(t)$ is varying sufficiently smoothly. When $\Phi(t)$ is a monotonous function, $\dot{\varphi} > 0$, the integral in the r.h.s. of (3.15) equals $2\pi\Phi/\Phi_0$ and thus produces the second term of Eq. (3.11).

It is clear from the derivation that the two terms of Eq. (3.11) arise from different integration domains in the t_1 - t_2 space: the first term corresponds to $|t_{1,2}| \geq \tau$, $t_1 t_2 < 0$, while the second one is due to almost coinciding moments, $|t_1 - t_2| \ll \tau$. Since the domains are almost non-overlapping, the two contributions to the noise (3.11) do not interfere (cross terms are small).

In order to estimate the correction to the result (3.11), let us derive it by another method that allows to trace out the higher order terms. For that, let us take the flux in the form $\varphi(t) = N\lambda(t)$, where $\lambda(t)$ is a smooth monotonous function, $\lambda(-\infty) = 0$, $\lambda(\infty) = 2\pi$. For integer $N \gg 1$ the Fourier component of $e^{iN\lambda(t)}$ entering Eq. (3.15)

in the stationary phase approximation is given by

$$\int_{-\infty}^{\infty} e^{iN\lambda(t)+i\omega t} dt = \sum_k \sqrt{\frac{2\pi i}{N\ddot{\lambda}(t_k)}} e^{iN\lambda(t_k)+i\omega t_k} + \dots \quad (3.16)$$

where the dots indicate terms $\sim O(N^{-3/2})$, and t_k 's are real solutions of the equation $N\dot{\lambda}(t) + \omega = 0$. Then we can write

$$\left| \int_{-\infty}^{\infty} e^{iN\lambda(t)+i\omega t} dt \right|^2 = \sum_k \frac{2\pi}{N\ddot{\lambda}(t_k)} + O(N^{-2}), \quad (3.17)$$

and thus obtain

$$\langle\langle Q^2 \rangle\rangle = A \int_{-\infty}^{\infty} \sum_k \frac{|\omega| d\omega}{N\ddot{\lambda}(t_k)} + \dots, \quad (3.18)$$

where the dots represent higher order terms. By differentiating both sides of the equation $N\dot{\lambda}(t) = -\omega$ one finds the relation $d\omega = -N\ddot{\lambda}(t_k) dt_k$, which means that $|\omega| d\omega / \ddot{\lambda}(t_k) = -|\dot{\lambda}(t_k)| dt_k$, and therefore the integral in Eq. (3.18) equals $N \int_{-\infty}^{\infty} d\lambda = 2\pi N$. Since $|\omega| d\omega$ scales as N^2 , the correction to Eq. (3.18) can be evaluated as $O(1)$, i.e., it is of the order of one for any N . This means that relative accuracy of Eq. (3.37) is $O(1/N)$.

The second term in (3.11) is interesting in connection with the picture of binomial statistics presented in Sec. 2.6. In the dc bias case, the distribution of charge for a single channel situation was found to be binomial with frequency of attempts equal to eV/h and the probabilities of outcomes $p = |A|^2$, $q = |B|^2$. Taken literally, this means that the attempts to transfer charge are repeated regularly in time, almost periodic with the period h/eV , with each attempt having two outcomes – transmission or reflection – occurring with the probabilities p and q . However, the regularity of the attempts does not lead to an ac component in the current, rather it appears just as a part of statistical description of charge fluctuations. Still, the presence of a non-zero frequency in a non-interacting system requires interpretation.

Let us suppose that the flux varies linearly with time, $\Phi(t) = -cVt$. Since the e.m.f. = $-\partial\Phi/c\partial t$, the linear dependence of $\Phi(t)$ is equivalent in its effect on the

noise to constant voltage V . In accordance with one's expectation, second term of Eq. (3.11) for a single channel is $\langle\langle Q^2 \rangle\rangle = ge^2|AB|^2\Phi/\Phi_0$, i.e., it is precisely of the form arising from the binomial distribution with probabilities of outcomes p and q , and the number of attempts $N = \Phi/\Phi_0$. (Let us recall that the second moment of the binomial distribution equals pqN .) Taking into account that the time during which the flux changes by Φ_0 is h/eV , we can interpret the number of attempts in the statistical picture as the number of flux quanta by which the flux is changed. Such a conclusion suggests an interesting generalization of the picture of binomial statistics by attributing the meaning of the number of attempts to the flux change measured in the units of Φ_0 , regardless of the linear or non-linear character of the flux dependence on time.

It is appealing to put the special role of integer fluxes in connection with the binomial statistics of current, where the flux quanta are naturally interpreted as discrete attempts to transmit charge. Although this picture is yet to be confirmed by analytic treatment, it receives some support from the property of the Φ_0 -periodic term in (3.11) to vanish at every integer Φ . One may conjecture that the statistics are close to binomial only when the flux change is an integer, and have diverging logarithmic corrections otherwise. The distinction that Eq. (3.11) makes between integer and non-integer values of the flux and the relation of integer flux change to the number of attempts in the binomial distribution, gives another perspective to the statistical picture of a current pulse.

To summarize, the fluctuations caused by a voltage pulse, in contrast to the average transmitted charge, distinguish between integer and non-integer flux change. As a result, the dependence of noise on the flux is non-monotonous and has minima near integer values.

3.3 Coherent states of current

The question we address in this section is about optimal way of changing flux that minimizes induced noise. It is clear from what has been said that to achieve minimum

of the noise one should change the flux by an integer amount,

$$\Delta\varphi = \varphi(t = \infty) - \varphi(t = -\infty) = 2\pi n, \quad (3.19)$$

in order to suppress the logarithmically divergent term. However, since for a given $\Delta\varphi$ the noise depends on the actual function $\varphi(t)$, not just on $\Delta\varphi$, we have a variational problem to solve for the noise as a functional of the time dependence of the flux. This functional was derived in Sec. 3.2. At zero temperature it is given by

$$\langle\langle Q^2 \rangle\rangle = \frac{ge^2}{2\pi} |AB|^2 \int \left| \int e^{i\varphi(t)+i\omega t} dt \right|^2 |\omega| \frac{d\omega}{2\pi}, \quad (3.20)$$

where A and B are transmission and reflection amplitudes, and g is spin degeneracy. We shall study the variational problem (3.10) with the boundary condition (3.19) and show that its general solution has the form of a sum of soliton-like functions:

$$\Phi(t) = \pm \frac{\Phi_0}{\pi} \sum_{k=1}^n \tan^{-1} \left(\frac{t - t_k}{\tau_k} \right), \quad \tau_k > 0, \quad (3.21)$$

where t_k and τ_k are arbitrary constants. Under condition (3.19) any time dependence of the form (3.21) gives absolute minimum to the noise:

$$\min[\langle\langle Q^2 \rangle\rangle] = ge^2 |AB|^2 |n|. \quad (3.22)$$

For an optimal time dependence of the voltage $V = -\partial\Phi/c\partial t$ therefore one has a sum of Lorentzian peaks:

$$V(t) = \mp \frac{\Phi_0}{c\pi} \sum_{k=1}^n \frac{\tau_k}{(t - t_k)^2 + \tau_k^2}. \quad (3.23)$$

In order to compare quantum noise with conductance, let us mention that average transmitted charge

$$\langle\langle Q \rangle\rangle = ge|A|^2 \frac{\Delta\varphi}{2\pi} = g \frac{e^2}{h} |A|^2 \int V(t) dt \quad (3.24)$$

is in accordance with the Ohm's law, i.e., there is no particular dependence on the way the flux change $\Delta\varphi$ is realized.

The result (3.21),(3.22) has a simple interpretation in terms of the binomial statistics picture of charge fluctuations. For the binomial distribution with probabilities of outcomes p and q , $p + q = 1$, and with the number of attempts N , second moment is known to be equal to pqN . The comparison with Eq. (3.22) suggests to attribute to $n = \Delta\Phi/\Phi_0$ the meaning of the number of attempts. This interpretation is supported by the structure of the function (3.21) consisting of n terms, each corresponding to unit change of flux. A remarkable property of the function (3.21) is its separability, manifest both in the form of the terms and in the way the parameters t_k, τ_k enter the expression. Let us note that by making some of the t_k 's close to each other one can have an overlap in time of the "attempts". The overlap, however, does not change the fluctuations (3.22). The situation reminds the one with solitons in integrable non-linear systems, or with non-interacting instantons in integrable field theories. Also, the absence of interference is interesting in the context of coherent nature of transport in this system: after all, we simply have scattering by a time-dependent potential. Perhaps, proper interpretation of this effect should be sought in establishing relation with the theory of coherent states, known to eliminate to some extent the quantum mechanical interference.

Let us now turn to the variational problem. It is convenient to do the integral over ω first and to rewrite (3.10) as

$$\langle\langle Q^2 \rangle\rangle = -\frac{D}{\pi} \int \int \frac{e^{i\varphi(t)-i\varphi(t')}}{(t-t')^2} dt dt' , \quad (3.25)$$

where $D = \frac{ge^2}{2\pi}|AB|^2$. In order to avoid divergence at $t = t'$ the denominator in (3.25) should be understood as

$$\frac{1}{2} \left[\frac{1}{(t-t'+i\delta)^2} + \frac{1}{(t-t'-i\delta)^2} \right] , \delta \rightarrow 0 , \quad (3.26)$$

the condition that one obtains by introducing regularization in (3.10): $|\omega| \rightarrow |\omega|e^{-|\omega|\delta}$.

By considering variation of the functional (3.25) we have the equation for an extremum:

$$\text{Im}\left[e^{i\varphi(t)} \int \frac{e^{-i\varphi(t')}}{(t-t')^2} dt'\right] = 0 . \quad (3.27)$$

By using Cauchy formula one checks that the functions

$$e^{i\varphi(t)} = \prod_{k=1}^n \frac{t - \lambda_k}{t - \bar{\lambda}_k} , \quad \lambda_k = t_k + i\tau_k , \quad (3.28)$$

satisfy (3.27) provided all τ_k are of same sign. Obviously, the functions (3.28) are just another form of (3.21).

It remains to be shown that the functional reaches its minimum on the solutions (3.28). To prove it we proceed in the following steps. Let us write $e^{i\varphi(t)}$ as

$$e^{i\varphi(t)} = f_+(t) + f_-(t) , \quad (3.29)$$

where $f_+(t)$ and $f_-(t)$ are bounded analytic functions of complex t in the upper and lower half plane, respectively. Representation (3.29) exists for any non-singular function and defines the functions f_+ and f_- up to a constant. Then we substitute Eq. (3.29) in (3.25) and apply Cauchy formula for the derivative,

$$\dot{f}_{\pm}(t) = \pm \frac{i}{2\pi} \oint \frac{f_{\pm}(t') dt'}{(t-t' \pm i0)^2} , \quad (3.30)$$

where the contour of integration is chosen in the half-plane of analyticity of f_+ or f_- , respectively. Thus one gets

$$\langle\langle Q^2 \rangle\rangle = -iD \int (\bar{f}_+ \dot{f}_+ - \bar{f}_- \dot{f}_-) dt . \quad (3.31)$$

On the other hand,

$$\begin{aligned} n &= \frac{1}{2\pi i} \int e^{-i\varphi(t)} \frac{d}{dt} e^{i\varphi(t)} dt \\ &= -\frac{i}{2\pi} \int (\bar{f}_+ \dot{f}_+ + \bar{f}_- \dot{f}_-) dt , \end{aligned} \quad (3.32)$$

where the last equality is a result of substituting (3.29) and using $\int \bar{f}_+ \dot{f}_- = \int \bar{f}_- \dot{f}_+ = 0$ that follows from Cauchy theorem. Now, Eq. (3.31) can be rewritten through Fourier components of f_+ and f_- as

$$\langle\langle Q^2 \rangle\rangle = D \int_0^\infty (|f_+(\omega)|^2 + |f_-(-\omega)|^2) \omega \frac{d\omega}{2\pi}, \quad (3.33)$$

thus demonstrating positivity of both terms in (3.31). (It is used that $f_+(\omega) = f_-(-\omega) = 0$ for $\omega < 0$.) With this, by comparing (3.31) and (3.32) we obtain

$$\langle\langle Q^2 \rangle\rangle \geq 2\pi D |n|. \quad (3.34)$$

Equality in (3.34) is reached only when either $f_+(t)$ or $f_-(t)$ vanishes. Therefore, to obtain the minimum one has to take the functions $e^{i\varphi(t)}$ that are regular in one of the half-planes. This remark is sufficient to see that the functions (3.28) form a complete family of solutions.

It is worth mentioning that the method used to derive (3.34) copies almost entirely the procedure of derivation of the duality condition in the theory of instantons. Like in other situations where the duality condition holds our “solitons” do not interact: $\langle\langle Q^2 \rangle\rangle$ shows no dependence on the parameters λ_k of the solution (3.28). Among numerous field theories that allow for exact solution of the instanton problem the one most similar to our case is the theory of classical Heisenberg ferromagnet in two dimensions. For this problem the instantons were found by mapping the order parameter space (i.e., the unit sphere) on the complex plane [62, 63]. Duality condition was shown to take the form of the constraint of analyticity or anti-analyticity of the mapped order parameter function (compare with the above derived condition $f_+ = 0$ or $f_- = 0$). Multi-instanton solutions were given as products of single instanton solutions (cf. Eq. (3.28)). This analogy obviously deserves more attention.

At this point let us examine an interesting non-optimal time dependence of the

flux, the sum of two solitons with opposite charge:

$$\varphi(t) = 2 \left[\tan^{-1} \left(\frac{t - t_1}{\tau_1} \right) - \tan^{-1} \left(\frac{t - t_2}{\tau_2} \right) \right] , \quad (3.35)$$

$\tau_{1,2} > 0$. This function corresponds to $e^{i\varphi(t)}$ of the form (3.28) but with the poles in both half planes. In this case $\Delta\varphi = 0$ and thus $\langle\langle Q \rangle\rangle = 0$, so $\min[\langle\langle Q^2 \rangle\rangle] = 0$. With the function (3.35), however, one finds

$$\langle\langle Q^2 \rangle\rangle = 4\pi D \left| \frac{\lambda_1 - \lambda_2}{\lambda_1 - \bar{\lambda}_2} \right|^2 , \quad (3.36)$$

where $\lambda_{1,2} = t_{1,2} + i\tau_{1,2}$. For different values of the parameters $t_{1,2}$, $\tau_{1,2}$ Eq. (3.36) interpolates between two trivial limiting cases: (i) $\langle\langle Q^2 \rangle\rangle \rightarrow 0$ when the two flux steps in (3.35) have nearly the same duration and almost overlap; (ii) $\langle\langle Q^2 \rangle\rangle \rightarrow 4\pi A$, when the flux steps either differ strongly in their duration or do not overlap. In the case (ii) the noise is two times bigger than the noise due to a single step, as it should be.

We see that when $\Delta\varphi/2\pi$ is of the order of one a non-optimal time dependence $\varphi(t)$ can considerably enhance the noise. It is not the case, however, for $\Delta\varphi/2\pi \gg 1$. This limit was studied in Sec. 3.2, where it was found that when $\varphi(t)$ is a monotonous function the result

$$\langle\langle Q^2 \rangle\rangle = g e^2 |AB|^2 |\Delta\varphi/2\pi| \quad (3.37)$$

is rather accurate [1].

A more intuitive way to understand the accuracy of Eq. (3.37) is to note that for a given n the number of parameters in the optimal flux dependence (3.14) is $2n$, which means that half of them are in some sense redundant. Because of that any smooth monotonous function with sufficiently large variation $\Delta\varphi$ can be rather accurately approximated by a function of the form (3.14), and therefore the noise exceeds the lower bound just slightly.

An implication of this result for the binomial statistics picture is as follows. As it was discussed above there is a (conjectured) correspondence of the terms of Eq. (3.21) and of the attempts. The deviation from the binomial distribution, that of course

should exist for a non-optimal flux function, will remain bounded in the case of a smooth $\varphi(t)$ as $\Delta\varphi$ increases taking integer values. More precisely, the distribution will be written as a mixture of binomial distributions with different numbers N of attempts, $P(m) = \sum_N \rho_N P_N(m)$, where $P_N(m) = p^m q^{N-m} C_N^m$. The estimated correction implies that the distribution of attempts ρ_N has finite variance in the limit $N = \Delta\varphi/2\pi \rightarrow \infty$.

Before closing let us mention that in order to apply the results of Secs. 3.2, 3.3 to transport in a mesoscopic metallic conductor with disorder, described by many conducting channels with transmission constants T_n , one just needs to replace $|AB|^2$ by $\sum_n T_n(1 - T_n)$, since different scattering channels contribute to the noise independently. The condition of validity of our treatment then is that the variation of the flux is sufficiently slow, so that $\min[\tau_k] \gg \hbar/E_c$, the time of diffusion across the sample. However, at non-zero temperature one also has to satisfy the condition $\tau_k \ll \hbar/T$, the time of phase breaking. So, the temperature interval where our estimate of the noise holds is $T \leq E_c$.

3.4 Conclusion

The theory leads to interesting conclusions applied to the current fluctuations produced by a voltage pulse. In this case, the noise has phase sensitivity: it oscillates as function of Faraday's flux, $c \int V(t) dt$, reaching minimum at integer fluxes. We studied the noise as function of the shape of the voltage pulse and found optimal time dependence that provides absolute minimum of the noise for given average transmitted charge. Solution displays interesting analogy with the problem of instantons in the field theories obeying duality symmetry. Optimal time dependence is a sum of Lorentzian peaks of voltage, each corresponding to a soliton of flux. The change of flux for a soliton is equal to the flux quantum Φ_0 . The solitons are interpreted in terms of the binomial statistics picture of charge fluctuations as attempts to transmit electrons, one electron per soliton.

Acknowledgements

We are grateful to Gordey Lesovik for the influence he had on this work.

Chapter 4

Current Fluctuations in a Single Tunnel Junction

4.1 Introduction

In small devices, at low temperature, electric current displays quantum effects, both due to the Fermi statistics of electrons, and due to the Coulomb interaction. This leads to interesting effects in current fluctuations that have recently drawn a lot of attention. For example, the noise power in disordered conductors is suppressed below the classical value [11, 12, 13] and the noise spectrum in the Luttinger liquid is modified by interaction in a non-trivial way [64, 65].

Also, there have been experimental studies of the noise (see, for example, [66, 67, 68]). However, it turns out that comparison of experimental data with theoretical predictions is not simple. Most theoretical works calculate current fluctuations at a specific point of a device of interest, for example, at a potential barrier or in the middle of a junction. In contrast, experiments do not directly measure the fluctuations within a device. Instead, the fluctuations are measured, for example, at a resistor connected to a device in series. Though the two fluctuations are certainly related, they are not identical, as it was pointed out by Landauer *et al.* [69].

The difference between the two fluctuations originates from the fact that the noise measuring part of the circuit, such as a series resistor, has its own intrinsic noise. To

compare experiments with theories, the effect of the intrinsic noise should be taken into account. In the analysis of experimental data, it is commonly assumed that the total spectral density of the measured noise is a linear sum of two spectral densities, one for the intrinsic noise, and the other for the noise within the device (for example, see Ref. [68]). To our knowledge, this assumption does not have a reserved name and for definiteness, we call it the *linear superposition assumption*.

In this paper, we question the validity of the assumption by working out a specific example. For that, we take a single tunnel junction connected to external leads. We incorporate the effect of the leads explicitly into a formulation, and calculate current fluctuations both in the middle of the junction and at the leads. The former represents the fluctuations which most theoretical works calculate, while the latter gives the fluctuations measured in a conventional experiment. We compare the two fluctuations, and find that the linear superposition assumption is not universally correct.

To summarize the results, it is found that the linear superposition assumption is valid only in the frequency range where

$$|Z(\omega)| \ll \frac{1}{|i\omega C|}. \quad (4.1)$$

Here $Z(\omega)$ is the impedance of the leads and C is effective capacitance of the junction. In particular, for Ohmic leads, Eq. (4.1) implies that the assumption is valid only in a low frequency regime. For low impedance leads ($Z(\omega) = R \ll R_Q = h/e^2$), the failure of the assumption in a high frequency regime is due to a finite relaxation time of the charge on the junction. For high impedance leads ($Z(\omega) = R \gg R_Q$), the failure is a combined effect of the finite relaxation time and the quantum dynamics of the leads.

In Sec. 4.2, a Hamiltonian of a single tunnel junction is presented which incorporates the charging energy and the external leads. In Sec. 4.3, we construct two current operators. One corresponds to the current at the potential barrier of the junction, which we call the *tunneling current*. The other corresponds to the current in the

leads, which we call the *relaxed current*. Expectation values of the two operators are evaluated in several situations. In Sec.4.4, the noise spectrum of the tunneling current is calculated. It is compared with existing theories, and an agreement is obtained in several limiting cases. In Sec.4.5, the noise spectrum of the relaxed current is calculated. It is compared to the noise spectrum of the tunneling current, and the difference is identified. We discuss the origin of the difference and compare the spectrum to results of recent experiments.

4.2 Formulation

In this paper, we use the formulation developed in Ref. [20] which incorporates the charging energy and the external leads. Below the formulation is sketched briefly and for more detailed discussion, we refer the readers to Ref. [20, 70].

In the weak tunneling limit, a single tunnel junction is almost identical to a capacitor. As a first step, one develops a description of a capacitor connected to external leads. To model the leads, one notices that the primary role of the external leads is to provide the capacitor with an electromagnetic environment. Then, since an electromagnetic environment is characterized by its impedance, it is reasonable to model the external leads as an impedance $Z(\omega)$. According to Caldeira and Leggett [28, 29], a general impedance can be treated in a Hamiltonian formulation by introducing a set of harmonic oscillators. Following Ref. [28, 29], one obtains a Hamiltonian H_{env} of a capacitor connected to an impedance $Z(\omega)$,

$$H_{env} = \frac{\tilde{Q}^2}{2C} + \sum_{n=1}^N \left[\frac{q_n^2}{2C_n} + \left(\frac{\hbar}{e} \right)^2 \frac{1}{2L_n} (\tilde{\varphi} - \varphi_n)^2 \right], \quad (4.2)$$

where \tilde{Q} is the capacitor charge fluctuations in the steady state, $\tilde{Q} = Q - CV$, and $\tilde{\varphi}$ is the phase fluctuations which is conjugate to \tilde{Q} ,

$$[\tilde{\varphi}, \tilde{Q}] = ie. \quad (4.3)$$

The canonical variables of harmonic oscillators, q_n and φ_n , satisfy similar commutation relations.

Next one develops a description of a single tunnel junction connected to external leads (Fig. 4-1(a)). The Hamiltonian (4.2) should be modified to account for quasi-particles and their tunneling. Quasi-particles can be described by the following second-quantized Hamiltonian,

$$H_{qp} = \sum_{k\sigma} (\epsilon_k + eV) c_{k\sigma}^\dagger c_{k\sigma} + \sum_{q\sigma} \epsilon_q c_{q\sigma}^\dagger c_{q\sigma}, \quad (4.4)$$

where k and q label the quasi-particle states in the left and the right electrodes, respectively, and σ represents the spin.

The tunneling of the quasi-particles is taken into account by the following tunneling Hamiltonian,

$$H_T = e^{-i\tilde{\varphi}} \sum_{kq\sigma} T_{kq} c_{q\sigma}^\dagger c_{k\sigma} + \text{H.c.}, \quad (4.5)$$

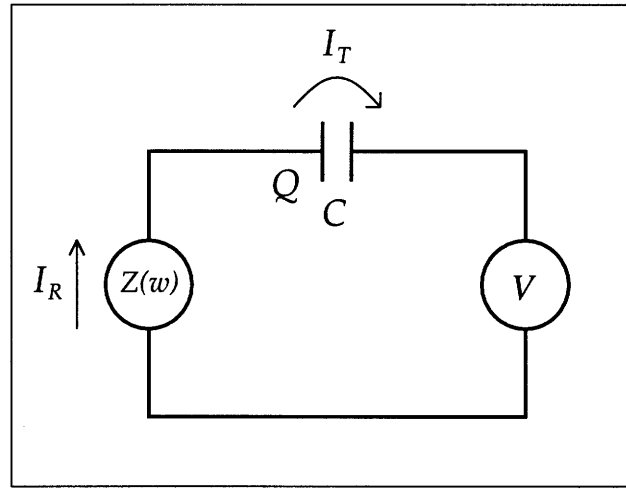
where T_{kq} is the tunneling matrix element. The operator $c_{q\sigma}^\dagger c_{k\sigma}$ (and its Hermitian conjugate) describes the tunneling of the quasi-particles and $e^{\pm i\tilde{\varphi}}$ accounts for the change of the junction charge accompanied by the quasi-particle tunneling, which is evident from the following relation,

$$e^{i\tilde{\varphi}} \tilde{Q} e^{-i\tilde{\varphi}} = \tilde{Q} - e. \quad (4.6)$$

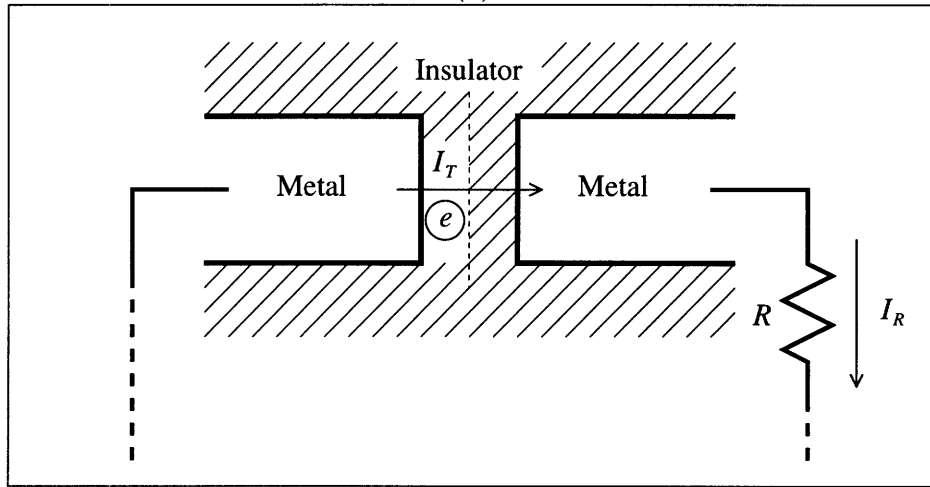
Note that, since the change of the junction charge is explicitly accounted for by $e^{\pm i\tilde{\varphi}}$, the macroscopic state operators of the junction, \tilde{Q} and $\tilde{\varphi}$ can be separated from its microscopic state operators,

$$[\tilde{Q}(\tilde{\varphi}), c_{k(q)\sigma}] = [\tilde{Q}(\tilde{\varphi}), c_{k(q)\sigma}^\dagger] = 0. \quad (4.7)$$

Now one obtains a Hamiltonian of a single tunnel junction by collecting the three



(a)



(b)

Figure 4-1: (a) A schematic diagram of the circuit. The circuit contains a single tunnel junction, a voltage source, and external leads of impedance $Z(\omega)$. (b) The tunneling current and the relaxed current. The tunneling current represents the electron flow right at the potential barrier of a junction. On the other hand, the relaxed current represents the electron flow through the external leads. In the figure, an Ohmic environment with resistance R is shown.

pieces (4.2),(4.4), and (4.5),

$$H = H_{qp} + H_{env} + H_T. \quad (4.8)$$

As a final remark, let us emphasize that the charging energy and the external leads are incorporated in the Hamiltonian (4.8) without introducing non-quadratic terms, and that the only non-quadratic terms come from the tunneling which is a small effect in the weak tunneling limit. This feature of the Hamiltonian (4.8) makes such a formulation useful, since simple perturbation calculation is possible.

4.3 Tunneling current and relaxed current

In order to calculate the current fluctuations, we first construct two current operators. One represents the flow of electrons through the insulating barrier in the middle of the junction, which we call the *tunneling current*. The other corresponds to the current flowing at the external leads, which we call the *relaxed current*. The tunneling current operator can be constructed from the following equation of motion,

$$\hat{I}_T = \frac{i}{\hbar} \left[H, e \sum_{q\sigma} c_{q\sigma}^\dagger c_{q\sigma} \right] = -\frac{e}{\hbar} \sum_{kq\sigma} \left(iT_{kq} c_{q\sigma}^\dagger c_{k\sigma} e^{-i\tilde{\varphi}} + \text{H.c.} \right), \quad (4.9)$$

and the relaxed current operator from its relation with the tunneling current operator (Fig. 4-1(a)),

$$\hat{I}_R = \frac{i}{\hbar} [H, \tilde{Q}] + \hat{I}_T = -\frac{\hbar}{e} \sum_n \frac{1}{L_n} (\tilde{\varphi} - \varphi_n). \quad (4.10)$$

The difference between the two current operators is illustrated in Figure 4-1(b).

The expectation values of the two operators are identical, and give the current-voltage characteristic. From a simple perturbation calculation, one obtains

$$I_T(V) = I_R(V) = \frac{2e}{\hbar^2} \text{Im} (X_{ret}(-eV/\hbar)), \quad (4.11)$$

where

$$X_{ret}(\omega) = -i \int_{-\infty}^{\infty} dt \Theta(t) e^{i\omega t} \left\langle [A(t) e^{-i\tilde{\varphi}(t)}, A^\dagger(0) e^{i\tilde{\varphi}(0)}] \right\rangle_0, \quad (4.12)$$

and $A(t) = \sum_{kq\sigma} T_{kq} c_{q\sigma}^\dagger(t) c_{k\sigma}(t)$. Notice that the reason why the two expectation values are the same is that the external leads (or environment) are connected to the junction in series. In the rest of the section, we drop the subscripts T and R . The expressions (4.11),(4.12) can be evaluated to obtain the current-voltage characteristic

$$I(V) = \frac{1}{eR_T} (1 - e^{-\beta eV}) \int_{-\infty}^{\infty} dE \frac{E}{1 - e^{-\beta E}} P(eV - E), \quad (4.13)$$

$$P(E) = \frac{1}{2\pi\hbar} \int_{-\infty}^{\infty} dt \exp(\langle [\tilde{\varphi}(t) - \tilde{\varphi}(0)] \tilde{\varphi}(0) \rangle_0 + iEt/\hbar), \quad (4.14)$$

$$\begin{aligned} \langle [\tilde{\varphi}(t) - \tilde{\varphi}(0)] \tilde{\varphi}(0) \rangle_0 &= 2 \int_0^\infty \frac{d\omega}{\omega} \frac{\text{Re } Z_t(\omega)}{R_Q} \\ &\times \left\{ \coth \frac{\beta\hbar\omega}{2} (\cos \omega t - 1) - i \sin \omega t \right\}, \end{aligned} \quad (4.15)$$

where $Z_t(\omega) = (Z^{-1}(\omega) - i\omega C)^{-1}$ and R_Q is the resistance quantum h/e^2 . The expressions (4.13),(4.14),(4.15) agree with Ref. [20] where the same expressions are obtained from the Fermi golden rule.

Next, let us review some predictions of the expressions (4.13),(4.14),(4.15) in the low temperature limit $k_B T \ll E_C = e^2/2C$, which later turns out to be related to the current fluctuations. For more discussions on the characteristic, see Ref. [20, 70, 21]. Firstly, in the low impedance limit $Z(\omega) = R \ll R_Q$, one obtains $P(E) = \delta(E)$ and the characteristic becomes Ohmic, $I(V) = V/R_T$. Secondly, in the high impedance limit $Z(\omega) = R \gg R_Q$, one obtains $P(E) = \delta(E - E_C)$ and the characteristic develops a gap of width $2E_C$. Finally, in the Ohmic environment $Z(\omega) = R$, the characteristic shows an intermediate behavior between the above two limiting cases. For small voltage bias $|eV| \ll E_C$, one finds

$$I(V) = \frac{\exp(-2\gamma R/R_Q)}{\Gamma(2 + 2R/R_Q)} \frac{V}{R_T} \left[\frac{\pi R |eV|}{R_Q E_C} \right]^{2R/R_Q}, \quad (4.16)$$

where $\gamma = 0.577\dots$ is the Euler constant. For large voltage bias $eV \gg E_C$, one finds

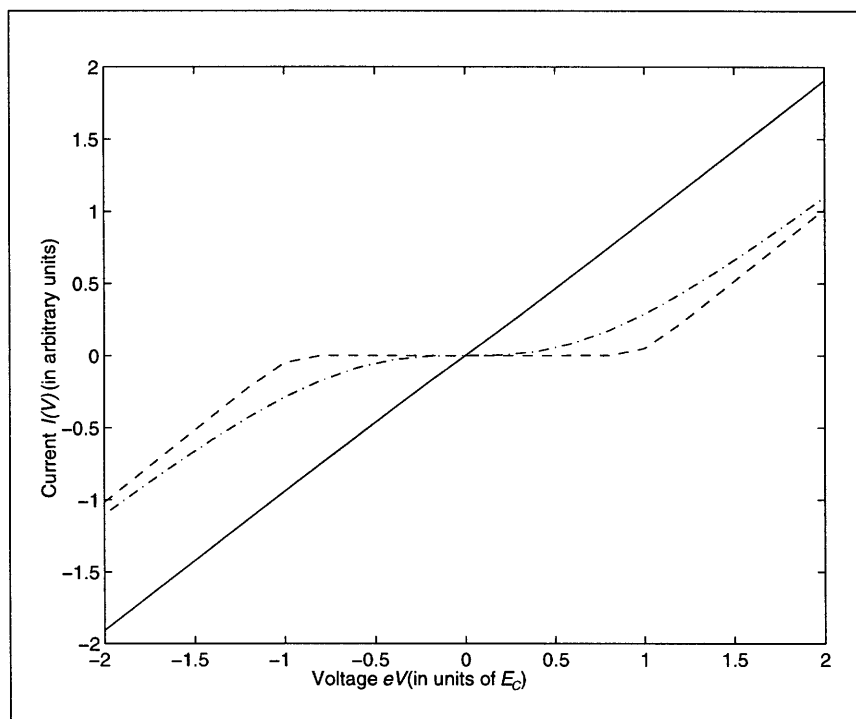


Figure 4-2: The zero temperature current-voltage characteristics for three environments, $Z(\omega) = 0.01R_Q$ (solid line), $Z(\omega) = 100R_Q$ (dashed line), and $Z(\omega) = R_Q$ (dash-dotted line).

that the characteristic asymptotically approaches the high impedance limit result,

$$I(V) = \frac{1}{eR_T} \left[eV - E_C + \frac{R_Q}{\pi^2 R} \frac{E_C^2}{eV} \right]. \quad (4.17)$$

The zero temperature current-voltage characteristics are presented in Figure 4-2. For the experimental measurement of the current-voltage characteristic, see Ref. [16].

4.4 Noise spectrum of tunneling current

4.4.1 Noise spectrum of tunneling current

The noise spectrum, or the noise spectral density of current, is defined as the Fourier transform of a current-current correlation function,

$$S_I(\omega) = \frac{1}{\pi} \int dt e^{i\omega t} \left(\frac{1}{2} \langle \{ \hat{I}(t), \hat{I}(0) \} \rangle - \langle \hat{I}(t) \rangle \langle \hat{I}(0) \rangle \right). \quad (4.18)$$

In this section, the subscripts T and R are restored since we later find that the tunneling current and the relaxed current have different spectra. Calculation of $S_{I_T}(\omega)$ is straightforward and one finds

$$S_{I_T}(\omega) = \frac{1}{2\pi R_T} \int dE \frac{E}{1 - e^{-\beta E}} \sum_{\pm} P(\hbar\omega \pm eV - E) \left(1 + e^{-\beta(\hbar\omega \pm eV)} \right). \quad (4.19)$$

Structure of Eq. (4.19) is similar to the expression (4.13) for the current-voltage characteristic and indeed, $S_{I_T}(\omega)$ can be related to $I(V)$,

$$S_{I_T}(\omega) = \frac{e}{2\pi} \sum_{\pm} \coth \frac{\beta(eV \pm \hbar\omega)}{2} I(V \pm \hbar\omega/e). \quad (4.20)$$

Eq. (4.20) enables one to obtain the noise spectrum of the tunneling current from the current-voltage characteristic. Let us mention that in the equilibrium, $V = 0$, Eq. (4.20) satisfies the fluctuation-dissipation theorem

$$S_{I_T}(\omega) = \hbar \coth \frac{\beta\hbar\omega}{2} \text{Im } \chi_T(\omega). \quad (4.21)$$

Here $\chi_T(\omega) = \langle \hat{I}_T(t) \rangle_{\omega} / f_T(\omega)$ is a response function to the force $f_T(t)$ which is conjugate to the tunneling current.

In the following, we take an Ohmic environment for illustration, and consider the equilibrium noise $S_{I_T}(\omega; V = 0)$ and the excess noise $S_{I_T}^x(\omega; V) = S_{I_T}(\omega; V) - S_{I_T}(\omega; V = 0)$ at zero temperature. The finite temperature noise will be discussed only when it allows a simple analytic expression.

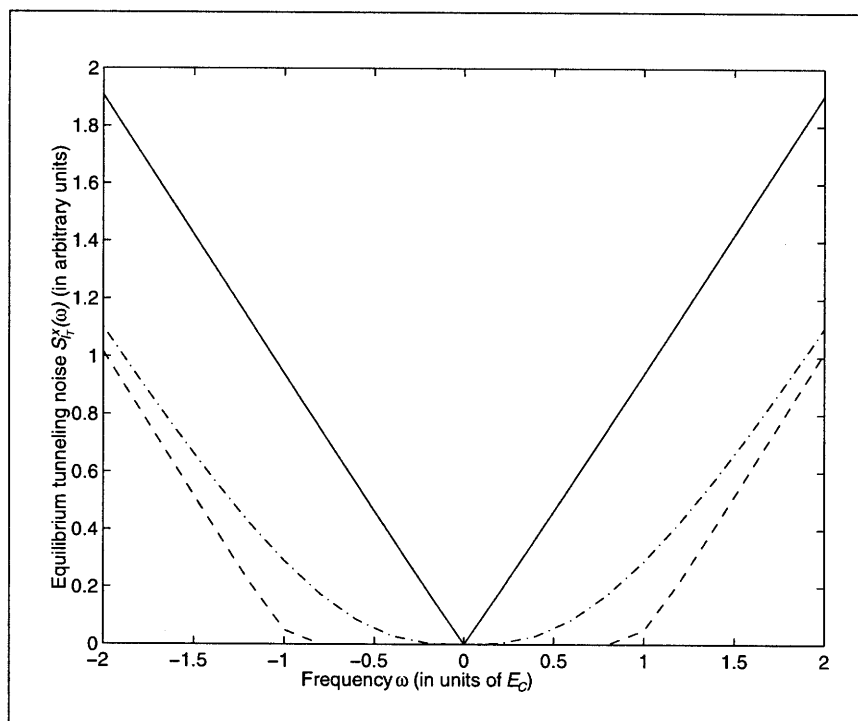


Figure 4-3: The zero temperature equilibrium noise spectra of the tunneling current $S_{I_T}(\omega)$ for $Z(\omega) = 0.01R_Q$ (solid line), $Z(\omega) = 100R_Q$ (dashed line), and $Z(\omega) = R_Q$ (dash-dotted line).

4.4.2 Low impedance limit

Let us first study the low impedance limit $Z(\omega) = R \ll R_Q$. In this limit, the current-voltage characteristic is found above to be Ohmic. Here one finds that the noise spectrum also shows Ohmic junction behavior. In equilibrium, Eq. (4.20) reduces to (see Figure 4-3)

$$S_{I_T}(\omega) = \frac{1}{\pi R_T} \hbar \omega \coth \frac{\beta \hbar \omega}{2}, \quad (4.22)$$

which is identical to the Johnson-Nyquist noise [27].

In non-equilibrium, the excess noise shows piecewise linear dependence on the frequency (Fig. 4-4(a)),

$$S_{I_T}^x(\omega; V) = \begin{cases} \frac{|eV| - |\hbar\omega|}{\pi R_T} & \text{for } |\hbar\omega| < |eV| \\ 0 & \text{for } |\hbar\omega| > |eV|, \end{cases} \quad (4.23)$$

which agrees with the excess noise of the Ohmic junction [30].

4.4.3 High impedance limit

In the high impedance limit $Z(\omega) = R \gg R_Q$, the equilibrium noise becomes

$$S_{I_T}(\omega) = \frac{1}{\pi R_T} (1 + e^{-\beta\hbar\omega}) \int_{-\infty}^{\infty} dE \frac{E}{1 - e^{-\beta E}} P(\hbar\omega - E), \quad (4.24)$$

where

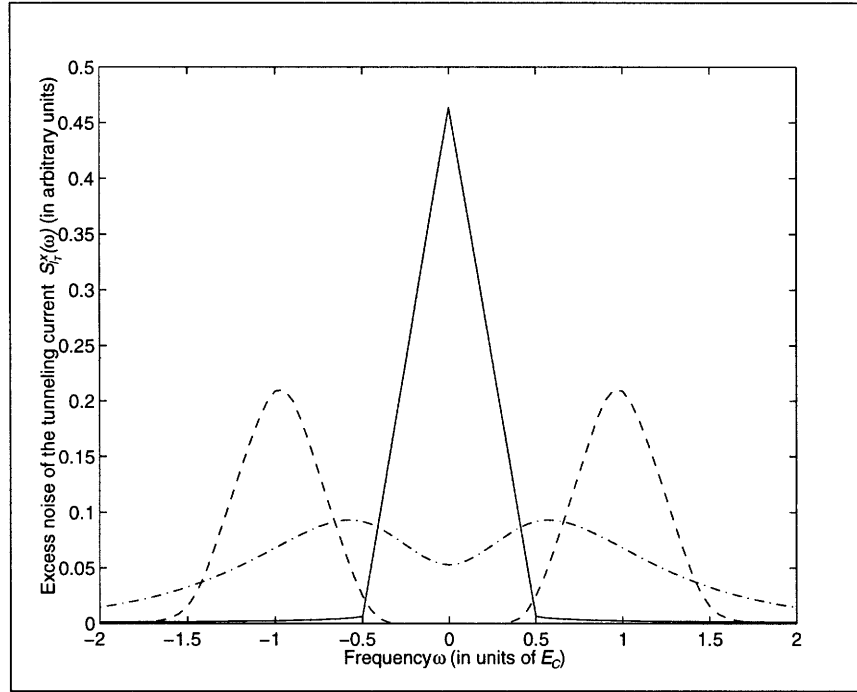
$$P(E) = \frac{1}{\sqrt{4\pi E_C k_B T}} \exp \left[-\frac{(E - E_C)^2}{4E_C k_B T} \right]. \quad (4.25)$$

Let us first study low frequency behavior of the equilibrium noise. At high temperature $k_B T \gg E_C$, $S_{I_T}(\omega)$ becomes $(2k_B T/\pi R_T)(1 - E_C/3k_B T + \mathcal{O}(E_C/k_B T)^2)$ for $\hbar\omega \ll E_C$. The first factor $2k_B T/\pi R_T$ corresponds to the white noise and the second factor represents the correction due to the charging energy. The effect of the charging energy is more evident at low temperature. At low temperature $k_B T \ll E_C$, $S_{I_T}(\omega)$ becomes $(2E_C/\pi R_T) \exp(-E_C/k_B T)$ for $\hbar\omega \ll k_B T$. The charging energy strongly suppresses the noise far below the white noise level (Fig. 4-3). Next, let us study the high frequency behavior. At high frequency, $S_{I_T}(\omega)$ is largely independent of the temperature and is given by

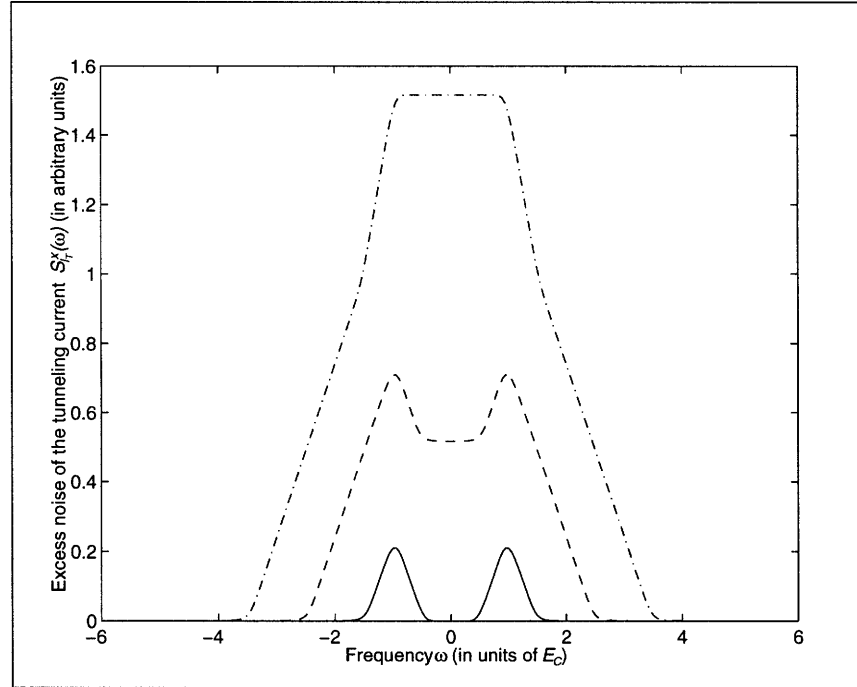
$$S_{I_T}(\omega) = \frac{|\hbar\omega| - E_C}{\pi R_T} \quad \text{for } |\hbar\omega| \gg k_B T, E_C. \quad (4.26)$$

Let us compare the equilibrium noise (4.24) with earlier calculation of Ben-Jacob *et al.* [71] where they calculated the equilibrium noise of an *open* tunnel junction which is not connected to external circuit. It is reasonable to expect that an open tunnel junction and a closed tunnel junction in a high impedance environment have similar equilibrium noise. Indeed, one finds that the two junctions share the same limiting behavior both in the high temperature limit and in the low temperature limit.

However, it turns out that there is delicate difference between the two junctions. The difference becomes evident by casting Ben-Jacob *et al.*'s result into the form of



(a)



(b)

Figure 4-4: (a) The zero temperature excess noise spectra of the tunneling current $S_{I_T}^x(\omega)$ for $Z(\omega) = 0.01R_Q$ (solid line), $Z(\omega) = 100R_Q$ (dashed line) and $Z(\omega) = R_Q$ (dash-dotted line). Voltage bias of $eV = 0.5E_C$ is assumed. (b) Evolution of the zero temperature tunneling excess noise with voltage bias in the high impedance environment $Z(\omega) = 100R_Q$. $eV = 0.5E_C$ (solid line), $eV = 1.5E_C$ (dashed line), and $eV = 2.5E_C$ (dash-dotted line).

Eq. (4.24). Then their result corresponds to Eq. (4.24) with $P(E)$ replaced by $P_{BJ}(E)$ where

$$P_{BJ}(E) = \left[\sum_{\text{integer } q} \exp\left(-\frac{q^2 E_C}{k_B T}\right) \right]^{-1} \sum_q \delta(E - E_C(2q + 1)) \exp\left(-\frac{q^2 E_C}{k_B T}\right). \quad (4.27)$$

Notice that $P_{BJ}(E)$ is a sum of equal-spaced delta functions and the envelope of the delta function is identical to $P(E)$. Hence $P_{BJ}(E)$ and $P(E)$ are discrete and continuous approximations of each other, respectively. In the high temperature limit $k_B T \gg E_C$, they are excellent approximations of each other and the two noise spectra become identical. However in the low temperature limit $k_B T \ll E_C$, they become distinct and the noise spectra agree only on their leading exponential terms presented above.

To study the origin of this difference, let us recall that $P(E)$ and $P_{BJ}(E)$ are probabilities for a quasi-particle to emit excitations of total energy E when it tunnels [70]. In the open junction, it is certain that the entire energy E goes to increase the charging energy $Q^2/2C$. Then, due to the charge quantization, the energy E should be quantized and $P_{BJ}(E)$ should have a discrete form. On the other hand, in the closed junction, the charging energy is coupled to the environment that has a continuous spectrum. Then, since the coupled system also has a continuous excitation spectrum, the energy is not quantized and $P(E)$ has a continuous form. Therefore one finds that the difference between Ben-Jacob *et al.* and the present calculation originates from the character of the environment.

Next, let us discuss the excess noise in non-equilibrium. At zero temperature, the excess noise shows piecewise linear dependence on the frequency. For small voltage bias $|eV| < E_C$, the excess noise becomes (see Fig. 4-4(a)),

$$S_{I_T}^x(\omega) = \begin{cases} \frac{|eV| - ||\hbar\omega| - E_C|}{2\pi R_T} & \text{for } E_C - |eV| < |\hbar\omega| < E_C + |eV| \\ 0 & \text{otherwise.} \end{cases} \quad (4.28)$$

Note that even though current does not flow when $|eV| < E_C$, the excess noise does

not vanish around $\hbar\omega = \pm E_C$. At higher voltage bias, a finite current flows and Fig. 4-4(b) shows the evolution of the excess noise with the voltage. The piecewise linear dependence in Fig. 4-4(b) originates from the narrow energy range of $P(E)$.

4.4.4 Ohmic environment

One can also obtain $S_{I_T}(\omega)$ in an Ohmic environment with arbitrary impedance $Z(\omega) = R$. At zero temperature, the equilibrium noise becomes

$$S_{I_T}(\omega) = \begin{cases} \frac{\exp(-2\gamma R/R_Q)}{\Gamma(2 + 2R/R_Q)} \frac{|\hbar\omega|}{\pi R_T} \left[\frac{\pi R}{R_Q} \frac{|\hbar\omega|}{E_C} \right]^{2R/R_Q} & \text{for } |\hbar\omega| \ll E_C \\ \frac{1}{\pi R_T} \left[|\hbar\omega| - E_C + \frac{R_Q}{\pi^2 R} \frac{E_C^2}{|\hbar\omega|} \right] & \text{for } |\hbar\omega| \gg E_C. \end{cases} \quad (4.29)$$

In the low frequency regime, the noise is suppressed by the charging energy and the suppression gets stronger as the impedance becomes higher. In the high frequency regime, the equilibrium noise eventually converges to the result of the high impedance limit and the convergence is faster with the higher impedance (Fig. 4-3).

Next, let us study the excess noise in non-equilibrium. With finite Ohmic impedance, the excess noise no longer exhibits piecewise linear dependence on the frequency because $P(E)$ allows a broad range of energy. Fig. 4-4(a) shows the excess noise in the Ohmic environment and at zero frequency, one finds

$$S_{I_T}^x(\omega = 0) = \frac{\exp(-2\gamma R/R_Q)}{\Gamma(2 + 2R/R_Q)} \frac{|eV|}{\pi R_T} \left[\frac{\pi R}{R_Q} \frac{|eV|}{E_C} \right]^{2R/R_Q}. \quad (4.30)$$

4.4.5 Noise power

In the presence of a finite current, the correlation between quasi-particle tunneling events can be estimated from the noise power P which is defined as $P = 2\pi S_I(\omega = 0)$. If there is no correlation between the tunneling events, the noise power retains its full Poisson value $P = 2eI$, and if there is any kind of correlation which regulates the tunneling, it suppresses the noise power below this level (for example, see Ref. [11, 12, 13]).

In a single tunnel junction, one finds from Eq. (4.20) that the noise power of the tunneling current has the full value independent of the environment,

$$P_T = 2eI(V), \quad (4.31)$$

where the subscript T is employed to denote that this is the noise power of the tunneling current. The origin of the Poisson-like noise power is that in the weak tunneling limit, the time interval between two consecutive tunneling events is large, and therefore, the Fermi statistics and the charging energy are not effective.

4.5 Noise spectrum of relaxed current

4.5.1 Noise spectrum of relaxed current

Usually, in a theoretical treatment of current fluctuations, the flow of electrons through a particular cross-section of the device is considered. However, as Landauer and Martin emphasize [69], conventional noise experiments do not directly measure the noise within the device. Instead, the noise is measured, for example, using a voltage across a small resistor connected in series to the device. To clarify the relation between conventional noise measurements and the noise spectrum calculated in various theoretical works [11, 12, 13, 30, 33, 71], it is necessary to take explicit account of the measuring part of the circuit. We assume that external leads connected to a single tunnel junction are used for the measurement, and therefore $S_{I_R}(\omega)$ corresponds to the spectral density of the current fluctuations obtained in conventional noise experiments.

Let us compare the relaxed noise $S_{I_R}(\omega)$ with $S_{I_T}(\omega)$ that corresponds to the noise spectra calculated in theoretical works. The no tunneling limit $R_T \rightarrow \infty$ (or $T_{kq} = 0$) illustrates the difference of $S_{I_R}(\omega)$ and $S_{I_T}(\omega)$. In this limit, the tunneling noise $S_{I_T}(\omega)$ vanishes since the tunneling current operator is proportional to the tunneling matrix elements. On the other hand, the relaxed current operator does not depend

on the tunneling matrix elements explicitly, and one finds $S_{I_R}(\omega) = S_{I_R}^{(0)}(\omega)$, where

$$S_{I_R}^{(0)}(\omega) = \frac{1}{\pi} \text{Re} \left(\frac{1}{Z(\omega) - (i\omega C)^{-1}} \right) \hbar\omega \coth \frac{\beta\hbar\omega}{2}. \quad (4.32)$$

Note that $S_{I_R}^{(0)}(\omega)$ is a generalization of the Johnson-Nyquist noise [27] $(1/\pi R)\hbar\omega \coth(\beta\hbar\omega/2)$. Then it is clear that the two noise spectra $S_{I_T}(\omega)$ and $S_{I_R}(\omega)$ are not identical even though the two currents $I_T(V)$ and $I_R(V)$ are the same.

The situation becomes more complicated if there is tunneling. In an analysis of experimental data (for example, see Ref. [68]), it is commonly assumed that the spectrum $S_{I_R}(\omega; V)$ is a sum of the equilibrium intrinsic noise $S_{I_R}(\omega; 0)$ and the excess tunneling noise $S_{I_T}^x(\omega; V)$. The linear superposition originates from the assumption that the two excess noises are identical, i.e., that $S_{I_T}^x(\omega; V) = S_{I_R}^x(\omega; V)$. In this section, we question the validity of the linear superposition by calculating $S_{I_R}(\omega)$.

Explicit calculation of $S_{I_R}(\omega)$ to the second order in the tunneling matrix gives

$$\begin{aligned} S_{I_R}(\omega) &= S_{I_R}^{(0)}(\omega) + S_{I_R}^{(2)}(\omega), \\ S_{I_R}^{(2)}(\omega) &= S_{I_R}^{(2A)}(\omega) + S_{I_R}^{(2B)}(\omega) + S_{I_R}^{(2C)}(\omega), \end{aligned} \quad (4.33)$$

where

$$\begin{aligned} S_{I_R}^{(2A)}(\omega) &= \frac{1}{|1 - i\omega CZ(\omega)|^2} S_{I_T}(\omega), \\ S_{I_R}^{(2B)}(\omega) &= -\frac{e}{\pi} \left\{ \text{Im} \frac{1}{1 - i\omega CZ(\omega)} \right\}^2 \sum_{\pm} \coth \frac{\pm\beta\hbar\omega}{2} I(V \pm \hbar\omega/e), \\ S_{I_R}^{(2C)}(\omega) &= \frac{e^2}{\pi\hbar^2} \text{Im} \left(\frac{1}{\{1 - i\omega CZ(\omega)\}^2} \right) \coth \frac{\beta\hbar\omega}{2} \\ &\quad \times \text{Re} \sum_{\pm} \{X_{ret}(-eV/\hbar \pm \omega) - X_{ret}(-eV/\hbar)\}. \end{aligned} \quad (4.34)$$

The superscript (2) in $S_{I_R}^{(2)}(\omega)$ denotes that this is the second order contribution in the perturbation calculation. Let us mention that in equilibrium, $V = 0$, Eq. (4.33)

satisfies the fluctuation-dissipation theorem

$$S_{I_R}(\omega) = \hbar \coth \frac{\beta \hbar \omega}{2} \text{Im } \chi_R(\omega). \quad (4.35)$$

Here $\chi_R(\omega) = \langle \hat{I}_R(t) \rangle_\omega / f_R(\omega)$ is a response function to a generalized force $f_R(t)$ conjugate to the relaxed current. It should be noticed that even though $S_{I_R}(\omega)$ is different from $S_{I_T}(\omega)$, it still obeys the fluctuation-dissipation theorem since it is related to the different response function.

Now we are ready to discuss the linear superposition. At zero frequency, Eq. (4.34) can be simply evaluated to give $S_{I_R}^{(2A)} = S_{I_T}(0)$ and $S_{I_R}^{(2B)}(0) = S_{I_R}^{(2C)}(0) = 0$. Hence the superposition holds for an arbitrary environment at zero frequency. At finite frequency, the situation becomes similar to the zero frequency case if

$$|Z(\omega)| \ll \frac{1}{|i\omega C|}. \quad (4.36)$$

One can use Eq. (4.36) as a criterion: the linear superposition holds only in the frequency range where the condition (4.36) is true. It is worth mentioning that since the assumption holds at zero frequency, the noise power of the relaxed current is always the same as the noise power of the tunneling current,

$$P_R = P_T = 2eI(V). \quad (4.37)$$

For illustration, we take the Ohmic environment in the following, and discuss the origin of the criterion (4.36).

4.5.2 Low impedance limit

Now, the real part of the retarded Green's function $X_{ret}(\omega)$ has to be evaluated. At zero temperature, with a constant tunneling density of states, one finds

$$\text{Re } \sum_{\pm} \{X_{ret}(-eV/\hbar \pm \omega) - X_{ret}(-eV/\hbar)\} \quad (4.38)$$

$$\begin{aligned}
&= \frac{\hbar^2}{2\pi e^2 R_T} \int dE (P(E) - P(-E)) \\
&\quad \times \sum_{\pm} \{ (eV - E \pm \hbar\omega) \ln |eV - E \pm \hbar\omega| - (eV - E) \ln |eV - E| \} .
\end{aligned}$$

In the low impedance limit $Z(\omega) = R \ll R_Q$, $S_{I_R}^{(2C)}(\omega)$ vanishes, and one finds the zero temperature equilibrium noise:

$$S_{I_R}(\omega) = S_{I_R}^{(0)}(\omega) + \frac{1}{\pi R_T} \text{Re} \left(\frac{1}{(1 - i\omega RC)^2} \right) |\hbar\omega|. \quad (4.39)$$

Note that Eq. (4.39) agrees, to the leading order in $1/R_T$, with the zero temperature equilibrium noise $S_I^{sh}(\omega)$ calculated from a shunt resistor model of a junction,

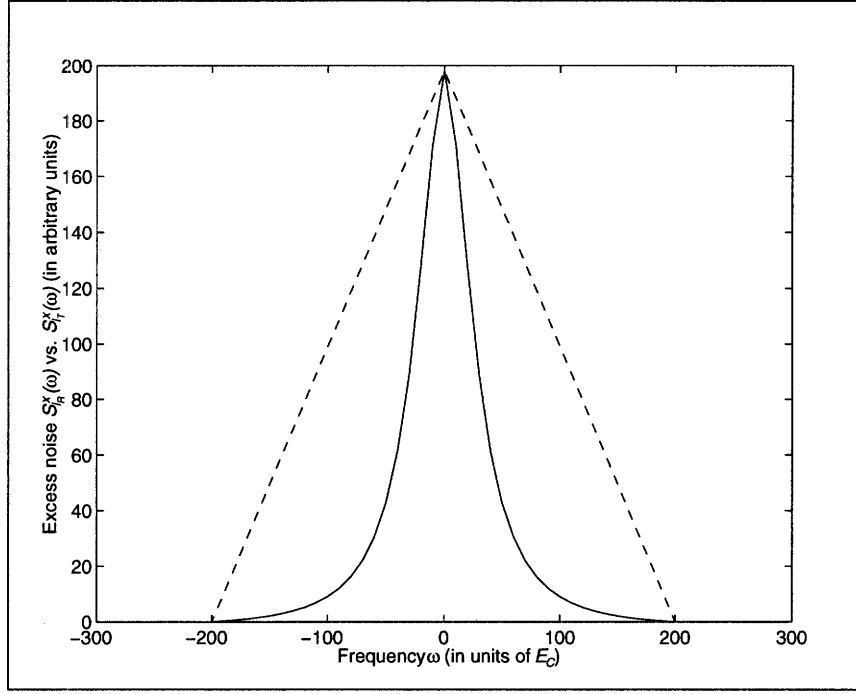
$$S_I^{sh}(\omega) = \frac{1}{\pi} \text{Re} \left(\frac{1}{R + (-i\omega C + 1/R_T)^{-1}} \right) |\hbar\omega|. \quad (4.40)$$

Next, let us calculate the excess noise. It is simple to verify that in the low impedance limit, only $S_{I_R}^{(2A)}(\omega)$ depends on the voltage bias and the zero temperature excess noise is given by

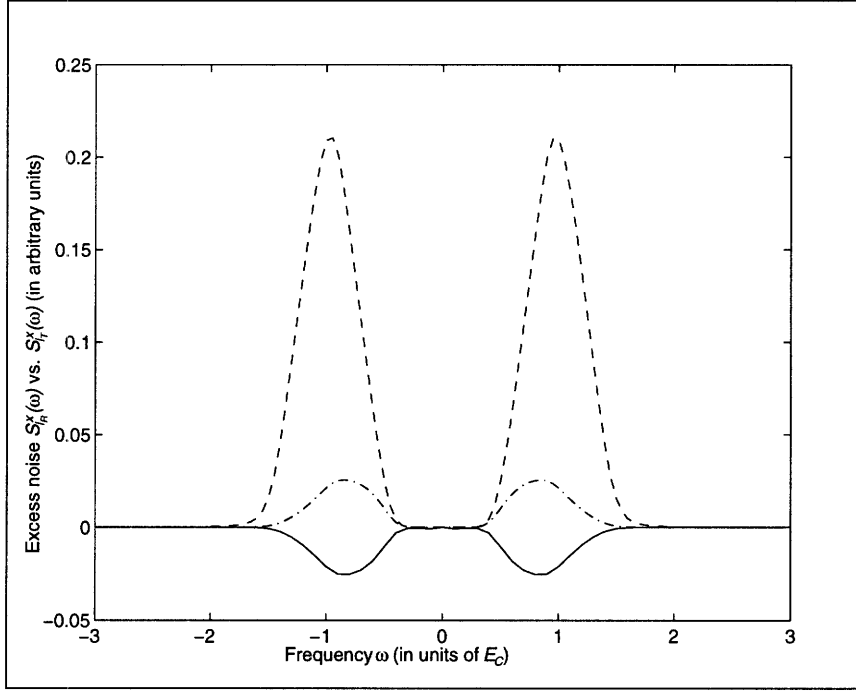
$$S_{I_R}^x(\omega) = \frac{1}{1 + \omega^2 R^2 C^2} S_{I_T}^x(\omega). \quad (4.41)$$

Recalling that the linear superposition assumption is equivalent to the statement $S_{I_R}^x(\omega) = S_{I_T}^x(\omega)$, one finds that the assumption is valid only in the low frequency regime $\omega \ll (RC)^{-1}$. Figure 4.5.2(a) shows the relaxed excess noise at zero temperature in comparison with the tunneling excess noise. Here it is assumed that $eV \gg \hbar/RC \gg E_C$. Note that while the relaxed excess noise (solid line) has the same magnitude as the tunneling excess noise (dashed line) at zero frequency, its peak width is given by \hbar/RC , making the decay of the relaxed excess noise faster than the tunneling excess noise.

To understand Eq. (4.41), one can argue in the following way. In the classical treatment of a tunnel junction, the junction is modeled as a capacitor, and the effect of the tunneling is just to add additional charge to the plates of the capacitor. This

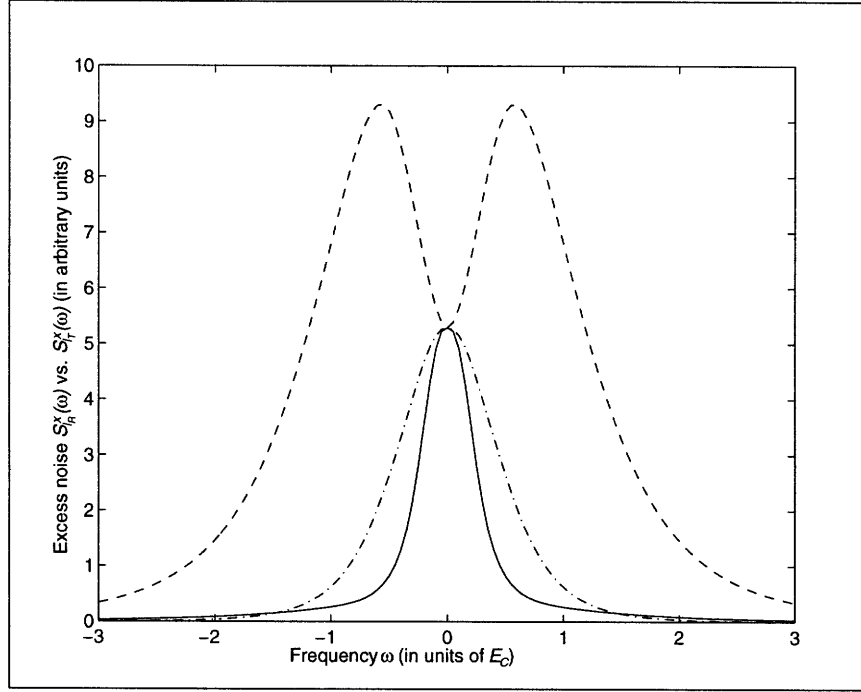


(a)

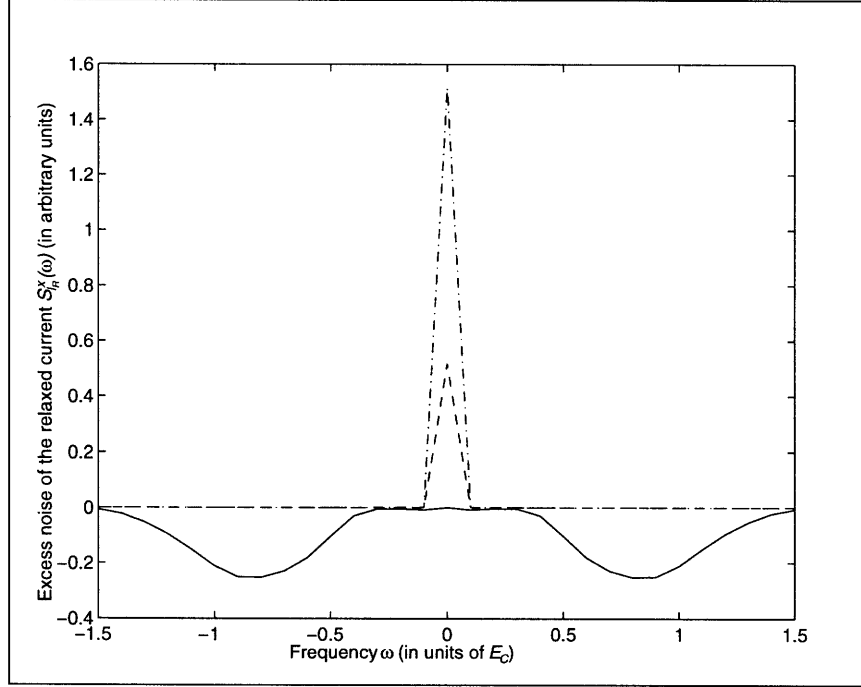


(b)

Figure 4-5: The excess noise spectrum of the relaxed current $S_{I_R}^x(\omega)$ (solid line) vs. the excess noise spectrum of the tunneling current $S_{I_T}^x(\omega)$ (dashed line) at zero temperature. The dash-dotted line shows $1/(1 + \omega^2 R^2 C^2) S_{I_T}^x(\omega)$ for comparison. (a) $Z(\omega) = 0.01 R_Q$, $eV = 200 E_C$. The dash-dotted line is not visible because it overlaps with the solid line. (b) $Z(\omega) = 100 R_Q$, $eV = 0.5 E_C$. The solid line and the dash-dotted line are scaled up by a factor of 10^4 to magnify their features. Note that $S_{I_R}^x(\omega)$ is negative around $\hbar\omega \approx \pm E_C$.



(c)



(d)

(c) $Z(\omega) = R_Q$, $eV = 0.5E_C$. $S_{I_R}^x(\omega)$ has a single peak at $\omega = 0$, while $S_{I_T}^x(\omega)$ has two peaks. $S_{I_R}^x(\omega)$ deviates from $1/(1 + \omega^2 R^2 C^2) S_{I_T}^x(\omega)$ due to nontrivial behavior of the zero point fluctuations. (d) Evolution of the zero temperature relaxed excess noise with voltage bias in the high impedance environment $Z(\omega) = 100R_Q$. $eV = 0.5E_C$ (solid line) (scaled up by a factor of 10^5), $eV = 1.5E_C$ (dashed line), and $eV = 2.5E_C$ (dash-dotted line).

problem can be solved by a conventional circuit analysis, and it is found that the relaxation of the additional charge takes finite time, so that the relaxed current is retarded:

$$I_R(t) = \int ds \mathcal{R}(t-s) I_T(s) + \delta I_R(t), \quad (4.42)$$

where $\mathcal{R}(t)$ is the retarded response function with $\mathcal{R}(t < 0) = 0$, $\mathcal{R}(\omega) = 1/(1 - i\omega CZ(\omega))$, and $\delta I_R(t)$ is the intrinsic fluctuation of the relaxed current which is not correlated with $I_T(t)$. Then Eq. (4.42) quickly leads to Eq. (4.41), and one finds that the extra factor in Eq. (4.41) originates from the finite relaxation time of the charge on the junction.

4.5.3 High impedance limit

Let us first study the noise in a low frequency regime, $\omega \ll (RC)^{-1}$. In this regime, $S_{I_R}^{(2A)}(\omega)$ is dominant over other second order terms, and one finds the noise $S_{I_R}(\omega) = S_{I_R}^{(0)}(\omega) + S_{I_T}(\omega)$. Notice that, since $S_{I_R}^{(0)}(\omega)$ is independent of the voltage, the linear superposition assumption is valid in this regime. However, it should also be noted that this regime lies far below the charging energy E_C since $\hbar/RC = (R_Q/\pi R)E_C$.

In a high frequency regime $\omega \gg (RC)^{-1}$, $S_{I_R}^{(2B)}(\omega)$ becomes of the same order as $S_{I_R}^{(2A)}(\omega)$, and for small voltage $|eV| < E_C$, simple calculation shows $S_{I_R}^{(2B)}(\omega) = -2S_{I_R}^{(2A)}(\omega)$. $S_{I_R}^{(2C)}(\omega)$ is smaller than the other second order terms by a factor of $(\omega RC)^{-2}$, and one finds the noise $S_{I_R}(\omega) = S_{I_R}^{(0)}(\omega) - (\omega RC)^{-2} S_{I_T}(\omega)$. Notice that the total second order correction is negative, and that the excess is now *negative*.

Figure 4.5.2(b) shows the zero temperature excess noise of the relaxed current in comparison with the tunneling excess noise. Here, it is assumed that $E_C > eV \gg \hbar/RC$. While the tunneling excess noise (dashed line) shows two peaks at $\hbar\omega = \pm E_C$, the relaxed excess noise (solid line) instead shows two *negative* dips at $\hbar\omega \approx \pm E_C$. The relaxed excess noise is scaled up by a factor of 10^4 to magnify the dips. At higher voltage bias $eV > E_C$ (see Fig. 4.5.2(d)), the relaxed excess noise shows a peak at $\hbar\omega = 0$ and shallow dips at $\hbar\omega \approx \pm E_C$.

It is clear from the above discussion that the noise in the high impedance limit

is so non-trivial that the finite relaxation time alone cannot explain its behavior. To gain an understanding, let us first study the noise in the no tunneling limit. Then, the Hamiltonian $H_{qp} + H_{env}$ is quadratic, and one can diagonalize H_{env} as a set of independent harmonic oscillators. Due to the uncertainty principle, a harmonic oscillator, even in the ground state, shows fluctuations. It can be verified that the fluctuations of a harmonic oscillator with a frequency ω_0 results in a finite spectral density of the relaxed noise at $\omega = \omega_0$, and that the zeroth order noise $S_{I_R}^{(0)}(\omega)$ is the sum of such contributions.

The situation becomes less simple if one turns on the tunneling. In the high impedance limit, each tunneling of a quasi-particle induces an infinite number of excitations in the environment with a total excitation energy E_C (for detailed discussion on this point, see [72]). Those excitations alter the state of the environment, and one finds that the fluctuation $\delta I_R(t)$ in Eq. (4.42) is correlated with $I_T(t)$. Note that this is in a clear contrast with the low impedance limit where the tunneling leaves the environment essentially unperturbed [72], and therefore $\delta I_R(t)$ is not correlated with $I_T(t)$. Then, the correlation in the high impedance limit results in additional contributions to the excess noise, and the classical argument in Sec. 4.5.2 is no longer valid. However, it is still surprising that the additional contributions lead to the negative excess noise.

4.5.4 Ohmic impedance environment

Figure 4.5.2(c) shows the two excess noises at zero temperature in the Ohmic environment $Z(\omega) = R$. It is assumed that $R = R_Q = h/e^2$ and $eV = 0.5E_C$. The tunneling excess noise (dashed line) shows two peaks, while the relaxed excess noise (solid line) shows a single peak at $\hbar\omega = 0$. The dash-dotted line shows $1/(1 + \omega^2 R^2 C^2) S_{I_T}^x(\omega)$ for comparison. The dash-dotted line exhibits qualitatively the same feature as $S_{I_R}(\omega)$, and its agreement with the solid line improves with the lower impedance.

4.5.5 Experimental implications

Recently, there was an experimental study of the excess noise in a quantum point contact in a low impedance environment [22]. The voltage bias V of the order of 1mV was applied, and the excess noise was measured at frequency $\omega \sim 10\text{GHz}$ which is much lower than the voltage, $\hbar\omega \ll eV$. The frequency was chosen to avoid complications due to other noise sources at even lower frequency such as the $1/f$ noise. The measured excess noise was compared to theoretical calculations of the noise power (for example, Ref. [11, 12, 13]), assuming that the measured excess noise is essentially the same as the noise power, since $\hbar\omega \ll eV$. This assumption is apparently supported by theoretical calculations of the tunneling noise (for example, see Ref. [30, 33] or $S_{I_T}^x(\omega)$ in this paper). It was found that the experiment agrees with the theory in the ballistic regime. However, in the pinched off regime which corresponds to the weak tunneling limit, it was found that the measured noise level for a relatively small current ($< 100\text{nA}$) is about 1/3 of the theoretical predictions¹.

The quantum point contact in Ref. [22] is induced electrostatically in the plane of a 2DEG embedded in GaAs-AlGaAs heterostructure. Due to its low carrier density, the behavior of a quantum point contact is in general different from that of a (metallic) tunnel junction. However, we believe that the two must have the same behavior in the weak tunneling limit (at least) and that the present noise calculation in a single tunnel junction is applicable. Then, by recalling the relation (4.41) between the relaxed excess noise and the tunneling excess noise, it is reasonable to expect that the observed suppression factor 1/3 corresponds to the ratio of the two excess noises, $(1+\omega^2 R^2 C^2)^{-1}$ in Eq. (4.41). From the estimations of R and C provided by the authors of Ref. [22], we find that ωRC is order of 1. This expectation is also supported by a more recent experiment [23], where a similar measurement was carried out. The experiment found that the noise suppression in the previous experiment vanishes

¹The experiment also finds stronger noise suppression for a relatively large current ($>100\text{nA}$). We believe that the large current result is beyond the scope of the present calculation since the model Hamiltonian (4.8) assumes instantaneous tunneling. In contrast, the tunneling time in the large current experiment can no longer be assumed to be instantaneous since the time interval between two consecutive tunneling events is estimated [22] to be comparable with the tunneling time.

for a quantum point contact with much smaller capacitance, which is in qualitative agreement with Eq. (4.41). At this point, however, we are unable to establish a more quantitative agreement of the experiments with our result Eq. (4.41) because the precise values of R and C are not available. More experiments, for example, on the frequency dependence of the suppression factor, are required to test the present calculation.

As another way of testing the present calculation, we propose to measure the excess noise in the high impedance Ohmic environment. According to the result (Fig. 4.5.2(b)) in Sec. 4.5.3, the excess noise $S_{I_R}^x(\omega)$ becomes negative at frequency $\hbar\omega \approx \pm E_C$. If observed, such unusual behavior of the excess noise would be a verification of our calculation.

4.5.6 Weak scattering limit

Our calculation is restricted to the weak tunneling limit $R_T \gg R_Q$. It will be interesting to extend the calculation to the opposite limit. In the weak scattering limit, we expect that the relation between the tunneling noise and the relaxed noise should be different from the relation in the weak tunneling limit since electron transport is more "continuous" in the weak scattering limit. This expectation is supported by recent theoretical works [73, 74] which find that the junction becomes purely Ohmic and the capacitive effect vanishes in the weak scattering limit. However, further study is required to gain the quantitative understanding in the weak scattering limit.

4.6 Conclusion

In this paper, we consider current fluctuations in a single tunnel junction connected to external leads. We define two kinds of current, the tunneling current and the relaxed current, corresponding to the current within the junction and in the leads, respectively. We calculate the fluctuations of the two currents, and find that, contrary to conventional expectation, they have different excess noises. In the low impedance environment, the difference is due to the finite relaxation time of the charge on the

junction, whereas in the high impedance environment, the difference is due to the combined effect of the relaxation time and the quantum dynamics of the environment. In the high impedance environment, it is found that the spectral density of the relaxed current at frequency $\hbar\omega \approx \pm E_C$ decreases below the equilibrium level when a small voltage bias is applied. In such a situation, the measured excess noise would be negative.

Acknowledgments

We are grateful to M. Reznikov for kindly sending us his manuscripts before publication.

Chapter 5

Excitations Induced by Switching in Quantum Wires

5.1 Introduction

The fabrication technology rapidly progresses, and it is now possible to create samples with desired structures in sub-micron scale. This leads to higher degree of circuit integration, and thereby reduced size of electric devices. By reducing the size, one can usually improve circuit quality. In small devices, electrons travel shorter distances, and so such devices are usually faster than larger devices. Also, because fewer electrons are required to carry out logical operations, less power is consumed.

In the past decade, many experiments (for a review, see Ref. [75]) demonstrated that it is possible to control electric properties of a device by a *single* electron. For example, it is now well established that conductance through a quantum dot can be altered by several orders of magnitude by adding (or removing) a single electron to (from) the dot [76]. To make a comparison with present technological level of electronics, let us note that the electric devices currently available are still quite large on the atomic scale and their operations involve macroscopic number of electrons. It is expected that the single electron devices will be smaller and faster by orders of magnitude than the presently existing electronics. Because of that, the single electronics has received great attention and simulated many theoretical and experimental works

(for a review, see Ref. [77]).

The operation of single electron devices raises several physical issues. One of the fluctuations and noise. Another is the role of the excitations generated during circuit operation. To control electrons on a microscopic level, one has to reduce the number of generated excitations, which may require low temperatures as well as shielding the circuit from external perturbations that may induce excitations. In fact, there is a possibility that the factor that limits performance of single electron devices is the effectiveness of the scheme to avoid excitations.

In this chapter, we consider perturbations such as an on-off switching, which are generic in device operation. While their effects are negligible in conventional devices, they have a potential of becoming a main mechanism of excitation generation in single electron devices.

Here we study two kinds of problems. In Sec. 5.2, we calculate excitations generated in a quantum wire by an on-off switching. Specifically we consider breaking a connection of a quantum wire and then restoring it after some time, that is, turning on the perturbation for a finite time interval. For low frequency modes whose inverse frequencies are much higher than the switching time interval, we find that the numbers of induced excitations vanish linearly in the mode frequencies. However for higher frequency modes, we find that the perturbation induces logarithmically divergent number of excitations.

In Sec. 5.3, we consider a situation when a connection in the middle of a wire is broken by an external perturbation and electron flow between the two separate parts is blocked. We calculate the excitations induced by such a switching-off perturbation. We compare them to thermal excitations and discuss similarities and differences.

5.2 Excitations generated by an on-off perturbation

A one-dimensional quantum wire can be described using the bosonization technique (for example, see Ref. [49, 78]) by the following Lagrangian:

$$\mathcal{L} = \int dx \left\{ \frac{1}{2} \rho (\partial_t \phi)^2 - \frac{1}{2} \rho c^2 (\partial_x \phi)^2 \right\}, \quad (5.1)$$

where $\phi(x, t)$ is a local displacement field of the electron liquid in the wire from its equilibrium position. Here the parameters ρ and c depend on details of the wire. For example, for free fermions the velocity is the Fermi velocity, $c = v_F$, and the density is related to the Fermi wave number, $\rho = 2\rho_F/\pi\hbar$. This action is identical to the action of a one-dimensional string, and for convenience, we will use terminology of string below.

Now, let us suppose that the displacement of the string at $x = 0$ is fixed suddenly at time $t = -\tau$ and it remains fixed until it is released to freely vibrate at time $t = \tau$:

$$\phi(x = 0, t) = \phi(x = 0, t = -\tau) \quad \text{for } |t| < \tau. \quad (5.2)$$

We assume that the field $\phi(x, t)$ is in thermal equilibrium at temperature T before the perturbation is applied. If the temperature is low enough, the perturbation will be the main source of vibration and we will calculate the vibration spectrum of the string at time $t > \tau$.

This problem turns out to be simpler in the Hamiltonian formulation. For $|t| > \tau$, the Hamiltonian is just the free string Hamiltonian, since the perturbation is localized in time, and one can expand the field in Fourier components:

$$\begin{aligned} \hat{\phi}(x, t) &= \int \frac{dk}{2\pi} \left\{ \hat{\phi}_i(k) e^{i(kx - \omega(k)t)} + \hat{\phi}_i^\dagger(k) e^{-i(kx - \omega(k)t)} \right\} \quad \text{for } t < -\tau, \\ &= \int \frac{dk}{2\pi} \left\{ \hat{\phi}_f(k) e^{i(kx - \omega(k)t)} + \hat{\phi}_f^\dagger(k) e^{-i(kx - \omega(k)t)} \right\} \quad \text{for } t > \tau, \end{aligned} \quad (5.3)$$

where $\omega(k) = c|k|$.

To calculate vibration spectrum at $t > \tau$, we need to study how the perturbation relates $\hat{\phi}_f(k)$ to $\hat{\phi}_i(k)$ (for example, in the absence of the perturbation, $\hat{\phi}_f(k) = \hat{\phi}_i(k)$). In the Hamiltonian formulation, one can introduce the perturbation by interpreting Eq. (5.2) as a constraint on the field operator $\hat{\phi}(x, t)$. Then the evolution of a traveling wave k between $-\tau < t < \tau$ is similar to the wave reflection at a hard wall. A portion of a traveling wave $\exp(i(kx - \omega(k)t))$ which reaches the perturbation is reflected and travels in the opposite direction (see Fig. 5-1):

$$- \exp(i(-kx - \omega(k)t)) + \exp(i\omega(k)\tau) . \quad (5.4)$$

Here the first term is the usual reflected wave and the second term comes from the difference between the constraint (5.2) and the hard wall reflection. If we had adopted the usual hard wall constraint, $\hat{\phi}(x = 0, |t| < \tau) = 0$, this term would be absent.

Using the analogy to the classical wave reflection problem, one can relate the field components $\hat{\phi}_f(k)$ and $\hat{\phi}_i(k)$. One can also generalize this analogy to relate destruction operators of vibrational modes before and after the perturbation:

$$\begin{aligned} a_f(k) &= a_i(k) + \int \frac{dq}{2\pi} \sqrt{\frac{\omega(k)}{\omega(q)}} a_i(q) \left\{ \frac{-2 \sin(\omega(k) - \omega(q))\tau}{(\omega(k) - \omega(q))/c} + \frac{2 \sin \omega(k)\tau}{\omega(k)/c} e^{i\omega(q)\tau} \right\} \\ &- \int \frac{dq}{2\pi} \sqrt{\frac{\omega(k)}{\omega(q)}} a_i^\dagger(q) \left\{ \frac{-2 \sin(\omega(k) + \omega(q))\tau}{(\omega(k) + \omega(q))/c} + \frac{2 \sin \omega(k)\tau}{\omega(k)/c} e^{-i\omega(q)\tau} \right\} . \quad (5.5) \end{aligned}$$

Before we move on to the calculation of the radiation generated by the string fixing, let us recall the vibration spectrum of the string in thermal equilibrium:

$$\begin{aligned} \langle a_i^\dagger(k) a_i(q) \rangle &= n(k) \delta(k - q) , \\ \langle a_i(k) a_i^\dagger(q) \rangle &= (n(k) + 1) \delta(k - q) , \\ \langle a_i(k) a_i(q) \rangle &= \langle a_i^\dagger(k) a_i^\dagger(q) \rangle = 0 , \end{aligned} \quad (5.6)$$

where $n(k) = (\exp(\beta \hbar \omega(k)) - 1)^{-1}$.

Now we have all ingredients and straightforward calculation produces a general

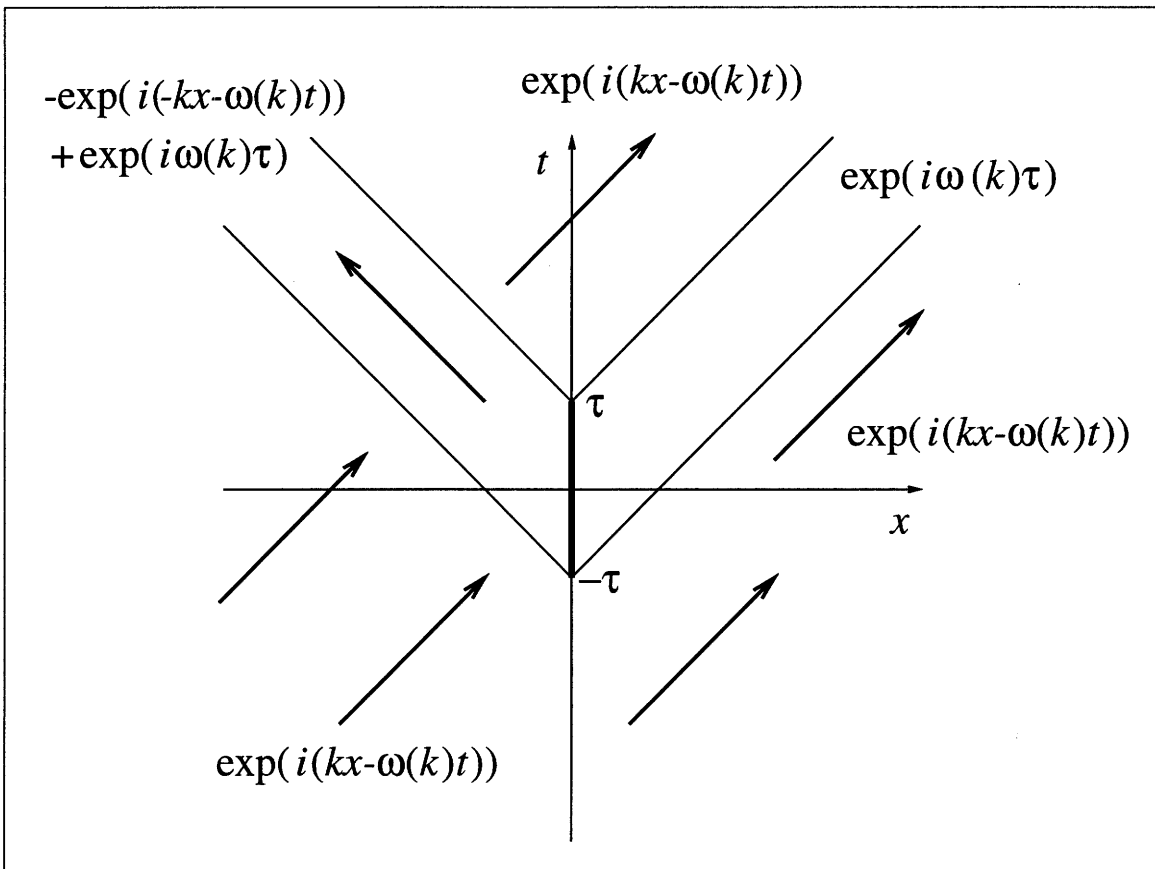


Figure 5-1: Wave reflection. The evolution of the field $\hat{\phi}(x, t)$ can be obtained from the analogy to the classical wave reflection problem.

expression of $\langle a_f^\dagger(k)a_f(q) \rangle$. However this expression is rather long and so the expression is presented in Appendix D. Here we instead focus on the zero temperature limit. At zero temperature, $n(k)$ vanishes for any finite k . One can remove the zero mode vibration as well by requiring that the center of mass of the string is fixed to zero. Then only the second expectation value in Eq. (5.6) survives and from the relation between $a_f^\dagger(k), a_f(k)$ and $a_i^\dagger(k), a_i(k)$, one finds

$$\begin{aligned} \langle a_f^\dagger(k)a_f(q) \rangle &= \frac{2}{\pi} \int_0^\infty \frac{ds}{\pi} \frac{\sqrt{\omega(k)\omega(q)}}{\omega(s)} \left\{ \frac{\sin(\omega(k) + \omega(s))\tau}{(\omega(k) + \omega(s))/c} - \frac{\sin \omega(k)\tau}{\omega(k)/c} e^{i\omega(s)\tau} \right\} \\ &\quad \times \left\{ \frac{\sin(\omega(q) + \omega(s))\tau}{(\omega(q) + \omega(s))/c} - \frac{\sin \omega(q)\tau}{\omega(q)/c} e^{-i\omega(s)\tau} \right\}, \end{aligned} \quad (5.7)$$

for non-vanishing wave vectors k and q .

Let us check whether Eq. (5.7) is well defined. For all finite s , the integrand is well defined. For very small s , the integrand is proportional to s since each of the expressions in curly brackets is proportional to s . For very large s , however, the integrand decays as s^{-1} and the large s gives logarithmically divergent contribution to $\langle a_f^\dagger(k)a_f(q) \rangle$. To regularize Eq. (5.7), we introduce an upper cutoff a^{-1} , where a corresponds, for example, to an atomic spacing. Let us comment that if we would have adopted the hard wall constraint, each second term in the curly brackets of Eq. (5.7) would be absent and Eq. (5.7) would have logarithmic infrared divergence instead.

For diagonal components ($k = q$), Eq. (5.7) simplifies further:

$$\langle a_f^\dagger(k)a_f(k) \rangle = \frac{2}{\pi} \int_0^\infty \frac{ds}{\pi} \frac{\omega(k)}{\omega(s)} \left| \frac{\sin(\omega(k) + \omega(s))\tau}{(\omega(k) + \omega(s))/c} - \frac{\sin \omega(k)\tau}{\omega(k)/c} e^{i\omega(s)\tau} \right|^2. \quad (5.8)$$

With a finite upper cutoff a^{-1} , this integration can be evaluated to

$$\begin{aligned} \langle a_f^\dagger(k)a_f(k) \rangle &= \frac{2}{\pi^2} c\tau \left\{ \frac{\sin^2 \omega(k)\tau}{\omega(k)\tau} \log \frac{c}{ea\omega(k)} + \text{si}(2\omega(k)\tau) \right. \\ &\quad \left. + \frac{1}{2\omega(k)\tau} (\log 2\omega(k)\tau + \gamma - \cos(2\omega(k)\tau)\text{ci}(2\omega(k)\tau) - \sin(2\omega(k)\tau)\text{si}(2\omega(k)\tau)) \right\}, \end{aligned} \quad (5.9)$$

where $\gamma = 0.577215\dots$ is the Euler constant. The functions $\text{si}(x)$ and $\text{ci}(x)$ are sine- and cosine-integral, respectively:

$$\begin{aligned}\text{si}(x) &= -\int_x^\infty \frac{\sin t}{t} dt = -\frac{\pi}{2} + x + \dots, \\ \text{ci}(x) &= -\int_x^\infty \frac{\cos t}{t} dt = \gamma + \log x - \frac{x^2}{4} + \dots.\end{aligned}\tag{5.10}$$

It is reasonable to expect that since the perturbation is applied only for a finite time interval 2τ , low energy modes with frequencies much lower than τ^{-1} are not affected significantly. For $\omega(k)\tau \ll 1$, one uses the series expansions of $\text{si}(x)$ and $\text{ci}(x)$ to obtain

$$\langle a_f^\dagger(k)a_f(k) \rangle \rightarrow c\tau \left\{ \frac{2}{\pi^2} \omega(k)\tau \left(\log \frac{2c\tau}{ae} + \frac{1}{2} + \gamma \right) + O(\omega(k)\tau)^2 \right\}.\tag{5.11}$$

Notice that for small k , the expectation value of the number of the excited quanta indeed vanishes linearly in k .

However, for higher frequency modes the number of excitations is large due to the logarithmically divergent factor. So we find that the perturbation excites higher frequency modes more significantly.

5.3 Excitations generated by a switching-off perturbation

In this section, we consider excitations induced by a switching-off perturbation in a quantum wire. Specifically we assume that the wire is cut at some time and remains disconnected at all later times.

We again use the bosonized description [49, 78] of a quantum wire and the terminology of the string. However, this time we perform an imaginary time calculation. Imaginary time dynamics of a free string is described by the following action:

$$S\{\phi(x, t)\} = \int dt dx \left\{ \frac{1}{2} \varrho (\partial_t \phi)^2 + \frac{1}{2} \varrho c^2 (\partial_x \phi)^2 \right\}.\tag{5.12}$$

Let us consider an external perturbation that breaks the string in the middle. Specifically, we assume that the two ends of the string are stretched by a small force f . This force introduces a perturbation to the action, $S_p = \int dt f \{\phi(x = L/2) - \phi(x = -L/2)\}$, and the value of the total action becomes unbounded from below. Therefore even an infinitesimal is sufficient to break the string and makes the connected string metastable.

In an imaginary time functional integral approach, the tunneling from a metastable state to a stable state can be described by the instanton method [79]. The most dominant contribution to the functional integral comes from the classical solution of the imaginary time equation of motion, the so called “bounce”.

This problem was studied previously in the context of quantum breaking of a polymer [80], where it was found that the bounce solution is collective in its nature: the displacement of the string is not localized, but rather it extends to large distance. Due to its collective nature, the bounce solution can be obtained in good approximation by introducing a branch cut $x = 0, |t| < \tau$, and imposing a boundary condition on the field $\phi(x, t)$:

$$\partial_x \phi(x = 0\pm, t) = 0 \text{ for } |t| < \tau. \quad (5.13)$$

This simplification generates a correct bounce solution if the value of τ is chosen properly and following Ref. [80], we set $\tau = 2\rho c E_0 / \pi f^2$ where E_0 is the energy of the broken connection.

Then one can obtain excitations induced by the string breaking perturbation by calculating the density matrix at the time $t = 0$. Here the excitations are the vibrations in the string, and for simplicity we assume that one is interested only in the vibration on the right side of the string, and the measurement is restricted to the semi-infinite region $x > 0$. For this purpose, we may just calculate a reduced density matrix,

$$\rho\{\phi_1(x), \phi_2(x)\} = \int \mathcal{D}\{\phi(x, t)\} \exp(-S\{\phi(x, t)\}), \quad (5.14)$$

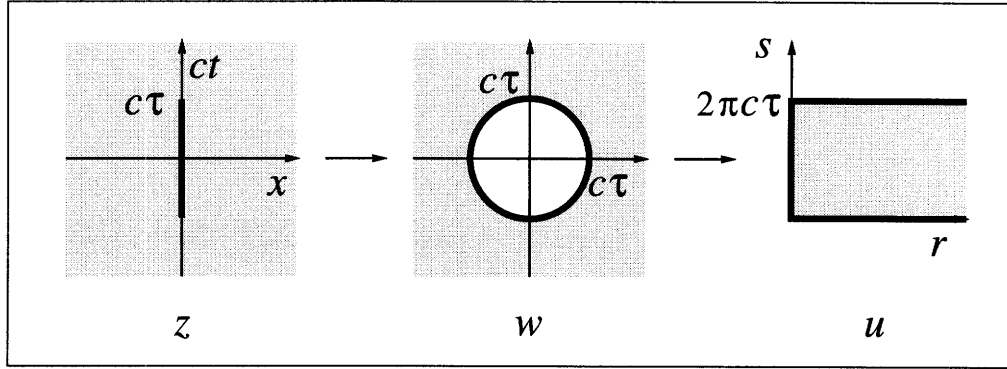


Figure 5-2: The conformal transformations used to simplify the boundary conditions.

where the field $\phi(x, t)$ is subject to additional boundary conditions,

$$(i) \quad \phi(x > 0, t = 0+) = \phi_1(x) , \quad (5.15)$$

$$(ii) \quad \phi(x > 0, t = 0-) = \phi_2(x) .$$

The action S is purely quadratic and therefore one finds

$$\rho\{\phi_1(x), \phi_2(x)\} \propto \exp(-S\{\phi_{cl}(x, t)\}), \quad (5.16)$$

where $\phi_{cl}(x, t)$ is the unique solution of a classical equation of motion satisfying the boundary conditions. However, evaluation of $S\{\phi_{cl}(x, t)\}$ is rather tedious due to the complex boundary conditions. Here, instead of dealing with the boundary conditions, we exploit the invariance of the action under conformal transformations and perform the following sequence of conformal transformations:

$$z = x + ict \rightarrow w = z + (z^2 + c^2\tau^2)^{1/2} , \quad (5.17)$$

$$w \rightarrow u = r + is = c\tau \log \frac{w}{c\tau} . \quad (5.18)$$

The action of these transformations is illustrated in Figure 5-2.

Let us call the displacement in u -space, $\psi(u)$, which is related to $\phi(z)$ by $\psi(u) =$

$\phi(z(u))$. The boundary conditions on the new field $\psi(u)$ are

$$\begin{aligned}
\text{(i)} \quad & \partial_r \psi(r=0) = 0, \\
\text{(ii)} \quad & \psi(r > 0, s=0) = \psi_1(r) = \phi_1(x(r)), \\
\text{(iii)} \quad & \psi(r > 0, s=2\pi c\tau) = \psi_2(r) = \phi_2(x(r)).
\end{aligned} \tag{5.19}$$

Now the boundary conditions are easier to treat and from a straightforward calculation one finds

$$\rho\{\psi_1(r), \psi_2(r)\} \propto \exp(-S\{\psi_{cl}(u)\}), \tag{5.20}$$

$$S\{\psi_{cl}(u)\} = \frac{\rho c}{\pi} \int_0^\infty dk k \frac{(\psi_1^2(k) + \psi_2^2(k)) \cosh 2\pi k c\tau - 2\psi_1(k)\psi_2(k)}{\sinh 2\pi k c\tau}, \tag{5.21}$$

where $\psi_{1(2)}(k) = \int_0^\infty dr \psi_{1(2)}(r) \cos kr$. Notice that this density matrix corresponds to the density matrix of an semi-infinite string that is at thermal equilibrium with temperature $k_B T = \hbar/(2\pi\tau)$.

Calculation of the vibration spectrum in the transformed space u is simple and one finds

$$\langle a^\dagger(k)a(q) \rangle = \delta(k-q) \frac{1}{\exp(2\pi k c\tau) - 1}, \tag{5.22}$$

where $a(k)$ is a destruction operator of a normal mode k in the u -space:

$$a(k) = \sqrt{\frac{\pi}{4\rho\hbar ck}} \left(\frac{\hbar}{i} \frac{\delta}{\delta\psi(k)} - i \frac{2\rho ck}{\pi} \psi(k) \right). \tag{5.23}$$

Notice that the spectrum (5.22) is a Bose-Einstein distribution.

To obtain the vibration spectrum in the original space z , one may write down Eq. (5.21) in terms of the original fields $\phi_1(x)$ and $\phi_2(x)$, and calculate the expectation value of $\langle b^\dagger(p)b(q) \rangle$ directly, where $b(p)$ is the annihilation operator of the mode p at time $t=0$ in the original space,

$$b(p) = \sqrt{\frac{\pi}{4\rho\hbar cp}} \left(\frac{\hbar}{i} \frac{\delta}{\delta\phi(p)} - i \frac{2\rho cp}{\pi} \phi(p) \right), \tag{5.24}$$

and $\phi(p) = \int_0^\infty dx \phi(x, t=0) \cos px$.

Instead of that, we take a rather indirect approach. Specifically, we first find a linear transformation relating $b(p)$ and $b^\dagger(p)$ to $a(k)$ and $a^\dagger(k)$, and extract the vibration spectrum in the original space z from the spectrum in the u -space, using the linear transformation.

For this purpose, let us first find a relation between the fields:

$$\phi(p) = \int_0^\infty dk \lambda(p, k) \psi(k), \quad (5.25)$$

where

$$\lambda(p, k) = \frac{2}{\pi} \int_0^\infty dx \cos \left(kc\tau \sinh^{-1} \frac{x}{c\tau} \right) \cos px. \quad (5.26)$$

One can also relate the field momenta:

$$\frac{\hbar}{i} \frac{\delta}{\delta \phi(p)} = \int_0^\infty dk \frac{\hbar}{i} \frac{\delta}{\delta \psi(k)} \chi(k, p), \quad (5.27)$$

where

$$\chi(k, p) = \frac{2}{\pi} \int_0^\infty dr \cos \left(pc\tau \sinh \frac{r}{c\tau} \right) \cos kr. \quad (5.28)$$

These relations allow one to relate the two creation and destruction operators and one finds

$$\langle b^\dagger(p)b(q) \rangle = \frac{1}{\pi^2} \frac{1}{\sqrt{pq}} \int_0^\infty d\nu \frac{\nu}{\sinh \pi\nu} K_{i\nu}(pc\tau) K_{i\nu}(qc\tau), \quad (5.29)$$

where $K_\nu(z)$ is a modified Bessel function of order ν . Notice that the expectation value is no longer proportional to the delta function $\delta(p - q)$. This result is natural since in the original space the excitation created by $b^\dagger(p)$ is not a normal mode.

For diagonal components of the expectation value, Eq. (5.29) reduces to

$$\langle b^\dagger(p)b(p) \rangle = \frac{1}{2\pi^2 p} \int_0^\infty dx \operatorname{sech}^2 x K_0(2pc\tau \cosh x). \quad (5.30)$$

Using the series expansion and the asymptotics of the Bessel function, one obtains

the following limiting behaviors:

$$\begin{aligned}\langle b^\dagger(p)b(p) \rangle &\rightarrow \frac{1}{4\sqrt{2}\pi p} \frac{e^{-pc\tau}}{pc\tau} \quad \text{for } pc\tau \gg 1 \\ &\rightarrow \frac{1}{2\pi^2 p} \log \frac{2}{epc\tau} \quad \text{for } pc\tau \ll 1.\end{aligned}\tag{5.31}$$

Notice that the spectrum shares the same features as the Bose-Einstein distribution at finite temperature: exponential decay for large p and p^{-1} divergence for small p . Therefore, in some loose sense, one may say that the breaking injects vibrations with a finite temperature spectrum into the string, which originally is at zero temperature.

One notes, however, the difference between the calculated spectrum (5.31) and the Bose-Einstein distribution, which is the logarithm factor in (5.31), as well as the presence of off-diagonal components in the density matrix. For the expectation value of off-diagonal components, one can write down an estimate by expanding the expectation value around the diagonal components:

$$\langle b^\dagger(p + \delta p/2)b(p - \delta p/2) \rangle = \langle b^\dagger(p)b(p) \rangle + \frac{1}{2}C_2(p)(\delta p)^2 + \dots\tag{5.32}$$

Naive physical intuition suggests that a peak would appear at $\delta p = 0$ and $C_2(p)$ be negative. However, from the general expression (5.29), one finds that $C_2(p)$ is *positive*, and that the off-diagonal correlation does not vanish. The increase of the off-diagonal terms indicates that the excitations are coherent and thus they are somewhat different from thermal excitations.

Appendix A

Larmor Clock Measurement of Tunneling Time

How long does it take a particle to tunnel under a barrier? More precisely, suppose a particle of energy E is moving in one dimension, and is scattered on a potential barrier:

$$i\frac{\partial}{\partial t}\psi(x,t) = \left[-\frac{1}{2}\frac{\partial^2}{\partial x^2} + U(x) \right] \psi(x,t) . \quad (\text{A.1})$$

What is the probability that during the scattering the particle spends time τ within the region $a < x < b$ under the barrier? Questions of that kind arise naturally in discussion of any quantum-mechanical process that takes finite time, like nuclear or chemical reactions, resonance scattering, or tunneling.

There have been several attempts to treat such problems [17, 18, 19] that resulted in formulation of a very interesting concept of Larmor clock. It has various analogies with the spin galvanometer discussed above, and it seems useful to review the Larmor clock here using the same language. The Larmor clock uses an auxiliary spin $1/2$ attached to the scattering particle, and an auxiliary constant magnetic field ω localized within the region of interest, $a < x < b$,

$$\hat{\mathcal{H}}_{int} = -\frac{1}{2}\omega\sigma_z \int_a^b \psi^\dagger(x)\psi(x)dx . \quad (\text{A.2})$$

The choice of coupling is such that the spin precession angle is proportional to the time spent in the region $a < x < b$. The difference from our spin-galvanometer is that the spin is not stationary, but travels with the particle, and also that the spin is coupled to the particle density, rather than to the current.

To find the distribution of times one has to write down the system density matrix evolved in time, and take partial trace over the particle outgoing states. (We assume that one does not have to distinguish between different results of scattering, and is interested in the tunneling time only, regardless of whether the particle went through the barrier, or has been reflected.) Then, by following the argument of Sec. 2.3 one obtains the spin density matrix:

$$\hat{\rho}_s(t) = \begin{bmatrix} \hat{\rho}_{\uparrow\uparrow}(0) & \chi(\omega)\hat{\rho}_{\uparrow\downarrow}(0) \\ \chi(-\omega)\hat{\rho}_{\downarrow\uparrow}(0) & \hat{\rho}_{\downarrow\downarrow}(0) \end{bmatrix}. \quad (\text{A.3})$$

Here

$$\chi(\omega) = \text{tr}_e(e^{-i\hat{\mathcal{H}}_\omega t} \hat{\rho}_e e^{i\hat{\mathcal{H}}_{-\omega} t}), \quad (\text{A.4})$$

where $e^{-i\hat{\mathcal{H}}_\omega t}$ is the evolution operator for the one-particle problem with no spin:

$$i\frac{\partial}{\partial t}\psi(x, t) = \left[-\frac{1}{2}\frac{\partial^2}{\partial x^2} + U(x) - \frac{1}{2}\omega\theta_{ab}(x) \right] \psi(x, t), \quad (\text{A.5})$$

where $\theta_{ab} = \theta(x-a)\theta(b-x)$. The auxiliary magnetic field ω now turns into a constant potential within the region $a < x < b$. Here again, with the spin degrees of freedom taken care of by (A.3), we are left with a single particle problem. By using cyclic property of the trace one finds

$$\chi(\omega) = \langle e^{i\hat{\mathcal{H}}_{-\omega} t} e^{-i\hat{\mathcal{H}}_\omega t} \rangle. \quad (\text{A.6})$$

Here the brackets $\langle \dots \rangle$ mean averaging over the particle initial state. Note that $\chi(\omega)$ is written in terms of a purely single particle problem, not involving spin variables.

The quantity $\chi(\omega)$ obtained by measuring precession of the spin is a generating

function for the distribution of times, which is clear from the Fourier transform

$$\chi(\omega) = \int P(\tau) e^{i\omega\tau} d\tau . \quad (\text{A.7})$$

The probabilities $P(\tau)$ of different precession angles of the spin should be interpreted as the scattering time distribution.

The probabilities $P(\tau)$ defined by (A.5), (A.6), and (A.7) have several interesting properties:

- a) $\int P(\tau) d\tau = 1$.
- b) $P(\tau)$ are real numbers.
- c) $P(\tau)$ vanish at negative times $\tau < 0$.

The normalization property *a)* is derived from (A.6) by setting $\omega = 0$. Property *b)* (real valuedness) is derived from $\chi(-\omega) = \bar{\chi}(\omega)$ which follows from (A.6). The causality property *c)* follows from considering the evolution in the problem (A.5) with ω continued to complex values. One notes that both the solution $\psi(x, t)$ of Eq. (A.5) and the evolution operator $e^{-i\hat{\mathcal{H}}_\omega t}$ are regular in the upper half-plane $\text{Im } \omega > 0$, which means that the same is true for $\chi(\omega)$. From that, the causality property *c)* follows by the usual argument using Cauchy theorem in the integral

$$P(\tau) = \int_{-\infty}^{\infty} \chi(\omega) e^{-i\omega\tau} \frac{d\omega}{2\pi} \quad (\text{A.8})$$

by closing the integration contour in the upper half-plane.

The properties *a)*, *b)*, *c)*, suggest that $P(\tau)$, so far defined formally as Fourier spectrum of $\chi(\omega)$, can have a meaning of probability. However, generally the sign of $P(\tau)$ can be either positive or negative, which makes the probabilistic interpretation problematic.

For the one particle problem one can write the generating function $\chi(\omega)$ in terms of the scattering amplitudes A and B . For that, it is convenient to use the expressions (2.22), (2.23) for the evolution operator in terms of the scattering matrix $\hat{\mathcal{S}}$,

written using the wave-packet scattering states (2.18). Specializing to one particle and taking partial trace, one finds

$$\chi(\omega) = \bar{A}_{-\omega}(E)A_{\omega}(E) + \bar{B}_{-\omega}(E)B_{\omega}(E) , \quad (\text{A.9})$$

where $A(\omega)$ and $B(\omega)$ are the transmission and reflection amplitudes of the problem (A.5) taken at the energy E of incident particle.

To see the Larmor clock working, let us consider an example of resonance scattering, where a particle is scattered on a potential forming a quasibound state of life-time Γ . Using the method described above one can find the distribution of times it takes the particle to scatter. For simplicity, suppose that the particle can be only reflected, but not transmitted ($A = 0$). Then the reflection amplitude as function of energy is given by the Breit-Wigner formula:

$$B(E) = \frac{E - E_0 - i\Gamma/2}{E - E_0 + i\Gamma/2} . \quad (\text{A.10})$$

Turning on the field ω in the quasibound state region is equivalent to shifting the resonance energy: $E_0 \rightarrow E_0 - \omega/2$. Thus, the generating function of the time distribution is

$$\chi(\omega) = \frac{\varepsilon - \omega + i\Gamma}{\varepsilon - \omega - i\Gamma} \frac{\varepsilon + \omega - i\Gamma}{\varepsilon + \omega + i\Gamma} , \quad (\text{A.11})$$

where $\varepsilon = 2(E - E_0)$. The distribution $P(\tau)$ is found by Fourier transform:

$$\begin{aligned} P(\tau) &= \int \chi(\omega) e^{-i\omega\tau} \frac{d\omega}{2\pi} \\ &= \delta(\tau) - \frac{4\Gamma}{\varepsilon} (\Gamma \sin \varepsilon\tau - \varepsilon \cos \varepsilon\tau) e^{-\Gamma\tau} \\ &= \frac{\partial}{\partial\tau} \left(\theta(\tau) - \frac{4\Gamma}{\varepsilon} \sin \varepsilon\tau e^{-\Gamma\tau} \right) . \end{aligned} \quad (\text{A.12})$$

The δ -function term corresponds to the non-resonance scattering channel. Other terms describe dwelling in the quasibound state. In this example $P(\tau)$ is changing sign, which makes the probabilistic interpretation ambiguous.

The paradox arising due to negative $P(\tau)$ is only an apparent one. Really, the mea-

surement of time performed by the Larmor clock is not the usual quantum-mechanical measurement, since the time is not an operator, and thus it cannot be measured in the same sense as other quantum-mechanical observables. This should be contrasted with the measurement of charge described above. Although the measurement scheme we use looks quite similar to Larmor clock, there is a difference: Electric charge is an observable in the usual quantum-mechanical sense, it takes quantized values, and the probabilities of those values, as we verified by calculation, are non-negative.

Appendix B

Asymptotic Expression for $\langle\langle Q^k \rangle\rangle$

For the evaluation of q integration, we note that due to its symmetry (or antisymmetry), it is enough to integrate over q from 0 to ∞ . For example for odd k ,

$$\int_{-\infty}^{\infty} dq e^{-iqx} \frac{q^{k-1}}{\sinh(\pi q - i0+)} = 2 \operatorname{Re} I \quad (\text{B.1})$$

where

$$I = \int_0^{\infty} dq e^{-iqx} q^{k-1} \frac{2e^{-\pi q}}{1 - e^{-2\pi q}}. \quad (\text{B.2})$$

Similar relation holds for even k with Re replaced by $i\operatorname{Im}$. Then we change the variable from q to $p = sq$ with $s = k - 1$

$$I = s \int_0^{\infty} dp e^{-ispx} (sp)^s \frac{2e^{-s\pi p}}{1 - e^{-2s\pi p}} \quad (\text{B.3})$$

$$= 2s^{s+1} \int_0^{\infty} dp \exp[sf_s(p)], \quad (\text{B.4})$$

$$f_s(p) \equiv \log p - ipx - \pi p - \frac{\log(1 - e^{-2s\pi p})}{s}. \quad (\text{B.5})$$

Above expression is the standard form for which the steepest descent method gives asymptotic expression for large s , except that $f_s(p)$ depends on s . However its dependence is exponentially weak and therefore it is safe to ignore the dependence just by dropping the last term of $f_s(p)$. Then following the standard procedure of the

steepest descent method, we find

$$I \sim \frac{2(k-1)!}{(\pi+ix)^k} \quad \text{for large } k. \quad (\text{B.6})$$

To perform the next integration in Eq. (2.53) over x , we introduce a new variable ν by $e^x = \sinh^2 \nu$,

$$J \equiv \int_{-\infty}^{\infty} dx \frac{1}{\sqrt{1+e^{-x}}} \frac{1}{(\pi+ix)^k} \quad (\text{B.7})$$

$$= 2 \int_0^{\infty} d\nu \exp[kg(\nu)], \quad (\text{B.8})$$

$$g(\nu) = -\log(\pi + i \log \sinh^2 \nu). \quad (\text{B.9})$$

Even though its analytic structure is quite complicated because it requires many branch cuts, still the above expression is the standard form of the steepest descent methods. Then following the standard procedure of the steepest descent method, we obtain

$$J \sim \frac{1}{\sqrt{k}} \frac{1-i}{(2\pi)^{k-1}} \quad \text{for large } k, \quad (\text{B.10})$$

and putting everything together, we finally get

$$\overline{\langle\langle Q^k(t) \rangle\rangle} \sim \frac{Q_0}{(2\pi)^{k-1}} \frac{(k-1)!}{\sqrt{k}} \begin{cases} (-1)^{\frac{k+2}{2}} & \text{for even } k, \\ (-1)^{\frac{k+1}{2}} & \text{for odd } k. \end{cases} \quad (\text{B.11})$$

Appendix C

Variance of $\langle\langle Q^k \rangle\rangle$

Beenakker derived a general formula for the variance of linear statistic $A = \sum_j a(T_j)$ assuming the interaction between eigenvalues is exactly logarithmic [56],

$$\text{var}(A) = \frac{1}{\beta\pi^2} \int_0^\infty dq \tilde{a}(q) \tilde{a}(-q) q \tanh \pi q, \quad (\text{C.1})$$

$$\tilde{a}(q) = \int_{-\infty}^\infty dx e^{iqx} a\left(\frac{1}{1+e^x}\right). \quad (\text{C.2})$$

Instead of Fourier transforming each $\langle\langle Q^k(t) \rangle\rangle$, we first take Fourier transform of $\log \chi(\lambda)$,

$$\tilde{a}(q) = \int_{-\infty}^\infty dx e^{ikx} \log \left(\frac{e^{i\lambda}}{1+e^x} + \frac{e^x}{1+e^x} \right) \quad (\text{C.3})$$

$$= \frac{\pi}{k \sinh \pi k} (1 - e^{-k\lambda}) \quad \text{for } -\pi < \lambda < \pi, \quad (\text{C.4})$$

and expand it in λ to get Fourier transform $\tilde{a}_k(q)$ of the k -th order cumulant,

$$\tilde{a}(q) = \sum_{k=1}^{\infty} \frac{(i\lambda)^k}{k!} \tilde{a}_k(q) \quad (\text{C.5})$$

$$\tilde{a}_k(q) = -M \frac{\pi}{q \sinh \pi q} (iq)^k. \quad (\text{C.6})$$

Then we use Eq. (C.1, C.2) to obtain

$$\text{var} \left(\langle\langle Q^k(t) \rangle\rangle \right) = \frac{1}{\beta\pi^2} \int_0^\infty dq \frac{M^2\pi^2}{\sinh^2 \pi q} q^{2k-1} \tanh \pi q \quad (\text{C.7})$$

$$= \frac{2M^2}{\beta} \int_0^\infty dq \frac{q^{2k-1}}{\sinh 2\pi q} \quad (\text{C.8})$$

$$= \frac{M^2}{\beta} \frac{2^{2k} - 1}{2^{2k}} \frac{|B_{2k}|}{k}, \quad (\text{C.9})$$

where B_{2k} is the $2k$ -th Bernoulli number. And by using an asymptotic expression for Bernoulli number, we finally get

$$\text{var} \left(\langle\langle Q^k(t) \rangle\rangle \right) \sim \frac{4(2k-1)!}{(2\pi)^{2k}\beta} M^2. \quad (\text{C.10})$$

Appendix D

Correlation Function at Finite Temperature

At non-zero temperature,

$$\begin{aligned}
\langle a_f^\dagger(k) a_f(q) \rangle &= n(k) \delta(k - q) \\
&+ \frac{1}{2\pi} \sqrt{\frac{\omega(q)}{\omega(k)}} n(k) \left\{ \frac{-2 \sin(\omega(q) - \omega(k))\tau}{(\omega(q) - \omega(k))/c} + \frac{2 \sin \omega(q)\tau}{\omega(q)/c} e^{i\omega(k)\tau} \right\} \\
&+ \frac{1}{2\pi} \sqrt{\frac{\omega(k)}{\omega(q)}} n(q) \left\{ \frac{-2 \sin(\omega(k) - \omega(q))\tau}{(\omega(k) - \omega(q))/c} + \frac{2 \sin \omega(k)\tau}{\omega(k)/c} e^{-i\omega(q)\tau} \right\} \\
&+ \int \frac{ds}{(2\pi)^2} \frac{\sqrt{\omega(k)\omega(q)}}{\omega(s)} n(s) \left\{ \frac{-2 \sin(\omega(k) - \omega(s))\tau}{(\omega(k) - \omega(s))/c} + \frac{2 \sin \omega(k)\tau}{\omega(k)/c} e^{-i\omega(s)\tau} \right\} \\
&\quad \times \left\{ \frac{-2 \sin(\omega(q) - \omega(s))\tau}{(\omega(q) - \omega(s))/c} + \frac{2 \sin \omega(q)\tau}{\omega(q)/c} e^{i\omega(s)\tau} \right\} \\
&+ \int \frac{ds}{(2\pi)^2} \frac{\sqrt{\omega(k)\omega(q)}}{\omega(s)} (n(s) + 1) \left\{ \frac{-2 \sin(\omega(k) + \omega(s))\tau}{(\omega(k) + \omega(s))/c} + \frac{2 \sin \omega(k)\tau}{\omega(k)/c} e^{i\omega(s)\tau} \right\} \\
&\quad \times \left\{ \frac{-2 \sin(\omega(q) + \omega(s))\tau}{(\omega(q) + \omega(s))/c} + \frac{2 \sin \omega(q)\tau}{\omega(q)/c} e^{-i\omega(s)\tau} \right\}.
\end{aligned} \tag{D.1}$$

Bibliography

- [1] H. Lee and L. S. Levitov, Orthogonality Catastrophe in a Mesoscopic Conductor due to a Time-dependent Flux, unpublished (cond-mat/9312013).
- [2] H. Lee and L. S. Levitov, Estimate of Minimal Noise in a Quantum Conductor, unpublished (cond-mat/9507011).
- [3] H. Lee, L. S. Levitov, and A. Yu. Yakovets, Phys. Rev. B **51**, 4079 (1995).
- [4] H. Lee and L. S. Levitov, Phys. Rev. B **53**, 7383 (1996).
- [5] D. A. Ivanov, H.-W. Lee, and L. S. Levitov, Coherent States of Alternating Current, preprint, to appear in Phys. Rev. B.
- [6] L. S. Levitov, H. Lee, and G. B. Lesovik, Electron Counting Statistics and Coherent States of Electric Current, preprint, submitted to J. Math. Phys.
- [7] H. Lee, L. S. Levitov, and A. V. Shytov, Excitations Induced by Switching Perturbations in Quantum Wires, in preparation.
- [8] R. Landauer, in *Localization, Interaction, and Transport Phenomena*, edited by B. Kramer, G. Bergmann, and Y. Bruynsraede (Springer-Verlag, Heidelberg, 1985).
- [9] Y. Imry, in *Directions in Condensed Matter Physics*, edited by G. Grinstein and G. Mazenko (World Scientific, Singapore, 1986).
- [10] R. Landauer, in *Analogies in Optics and Micro Electronics*, edited by W. van Haeringen and D. Lenstra (Kluwer Academic Publishers, Dordrecht, 1990).
- [11] G. B. Lesovik, Pis'ma Zh. Eksp. Teor. Fiz. **49**, 513 (1989) [JETP Lett. **49**, 592 (1989)].
- [12] B. Yurke and G. P. Kochanski, Phys. Rev. B **41**, 8184 (1990).
- [13] M. Büttiker, Phys. Rev. Lett. **65**, 2901 (1990).
- [14] K. E. Nagaev, Phys. Lett. A **169**, 103 (1992).

- [15] G. D. Mahan, in *Many Particle Physics*, 2nd ed. (Plenum, New York, 1990), sec. 8.3.
- [16] A. N. Cleland, J. M. Schmidt, and J. Clarke, *Phys. Rev. Lett.* **64**, 1565 (1990).
- [17] M. Büttiker, *Phys. Rev. B* **27**, 6178 (1983).
- [18] A. I. Baz', *Zh. Eksp. Teor. Fiz.* **47**, 1874 (1964) [*Sov. Phys. JETP* **20**, 1261 (1965)].
- [19] A. I. Baz', Y. B. Zeldovich, and A. M. Perelomov, *Scattering, Reactions and Decay in Nonrelativistic Quantum Mechanics* (Israel Program for Scientific Translations, Jerusalem, 1969).
- [20] M. H. Devoret *et al.*, *Phys. Rev. Lett.* **64**, 1824 (1990).
- [21] S. M. Girvin *et al.*, *Phys. Rev. Lett.* **64**, 3183 (1990).
- [22] M. Reznikov, M. Heiblum, H. Shtrikman, and D. Mahalu, *Phys. Rev. Lett.* **75**, 3340 (1995).
- [23] M. Reznikov *et al.*, Temporal Correlation of Electrons: Suppression of Shot Noise in a Ballistic Quantum Point Contact, Weizmann institute preprint.
- [24] F. Reif, in *Fundamentals of Statistical and Thermal Physics* (McGraw-Hill, New York, 1986), sec. 15.8.
- [25] H. Nyquist, *Phys. Rev.* **32**, 110 (1928).
- [26] R. Kubo, M. Toda, and N. Hashitsume, in *Statistical Mechanics II: Nonequilibrium Statistical Mechanics, Springer Series in Solid-State Sciences 31* (Springer-Verlag, Berlin, 1978), sec. 4.4.1.
- [27] H. B. Callen and T. A. Welton, *Phys. Rev.* **83**, 34 (1951).
- [28] A. O. Caldeira and A. J. Leggett, *Phys. Rev. Lett.* **46**, 211 (1981).
- [29] A. O. Caldeira and A. J. Leggett, *Ann. Phys. (N.Y.)* **149**, 374 (1983); (**153**, 445(E) (1984)).
- [30] A. J. Dahm *et al.*, *Phys. Rev. Lett.* **22**, 1416 (1969).
- [31] *Mesoscopic Phenomena in Solids*, edited by B. L. Al'tshuler, P. A. Lee, and R. A. Webb (North Holland, Amsterdam, 1991).
- [32] M. Büttiker, *Phys. Rev. B* **46**, 12485 (1992).
- [33] S.-R. E. Yang, *Solid State Commun.* **81**, 375 (1992).
- [34] C. W. J. Beenakker and M. Büttiker, *Phys. Rev. B* **46**, 1889 (1992).

- [35] T. Martin and R. Landauer, Phys. Rev. B **45**, 1742 (1992).
- [36] M. J. M. de Jong and C. W. J. Beenakker, Phys. Rev. B **46**, 13400 (1992).
- [37] L. S. Levitov and G. B. Lesovik, Pis'ma Zh. Eksp. Teor. Fiz. **58**, 225 (1993) [JETP Lett. **58**, 230 (1993)].
- [38] L. S. Levitov and G. B. Lesovik, Quantum Measurement in Electric Circuit, unpublished (cond-mat/9401004).
- [39] D. A. Ivanov and L. S. Levitov, Pis'ma Zh. Eksp. Teor. Fiz. **58**, 450 (1993) [JETP Lett. **58**, 461 (1993)].
- [40] R. J. Glauber, Phys. Rev. Lett. **10**, 84 (1963).
- [41] R. J. Glauber, Phys. Rev. **130**, 2529 (1963).
- [42] L. Mandel and E. Wolf, Rev. Mod. Phys. **37**, 231 (1965).
- [43] C. W. Gardiner, in *Quantum Noise* (Springer-Verlag, Heidelberg, 1991), chap. 8.
- [44] J. R. Klauder and E. C. G. Sudarshan, in *Fundamentals of Quantum Optics* (W. A. Benjamin, Inc., New York, 1968), chap. 8.
- [45] R. H. Koch, D. van Harlingen, and J. Clarke, Phys. Rev. B **26**, 74 (1982).
- [46] S. Saito *et al.*, Phys. Lett. A **162**, 442 (1992).
- [47] A. J. Leggett, Prog. Theor. Phys. Suppl. **69**, 80 (1980).
- [48] K. D. Schotte and U. Schotte, Phys. Rev. **182**, 479 (1969).
- [49] F. D. M. Haldane, J. Phys. C **14**, 2585 (1981).
- [50] J. B. Johnson, Phys. Rev. **29**, 367 (1927).
- [51] O. N. Dorokhov, Zh. Eksp. Teor. Fiz. **85**, 1040 (1983) [Sov. Phys. JETP **58**, 606 (1983)].
- [52] A. D. Stone, P. A. Mello, K. A. Muttalib, and J.-L. Pichard, in *Mesoscopic Phenomena in Solids*, edited by B. L. Al'tshuler, P. A. Lee, and R. A. Webb (North Holland, Amsterdam, 1991). See Ref. [31].
- [53] P. A. Mello, P. Pereyra, and N. Kumar, Ann. Phys. **181**, 290 (1993).
- [54] C. W. J. Beenakker and B. Rejaei, Phys. Rev. Lett. **71**, 3689 (1993).
- [55] J. T. Chalker and A. M. S. Macêdo, Phys. Rev. Lett. **71**, 3693 (1993).
- [56] C. W. J. Beenakker, Phys. Rev. Lett. **70**, 1155 (1993).

- [57] K. A. Muttalib and Y. Chen, Distribution Function for Shot Noise in Disordered Multi-channel Quantum Conductors, unpublished (cond-mat/9405068).
- [58] B. L. Al'tshuler, L. S. Levitov, and A. Yu. Yakovets, Pis'ma Zh. Eksp. Teor. Fiz. **59**, 821 (1994) [JETP Lett. **59**, 857 (1994)].
- [59] L. S. Levitov and G. B. Lesovik, Phys. Rev. Lett. **72**, 538 (1994).
- [60] P. W. Anderson, Phys. Rev. Lett. **18**, 1049 (1967).
- [61] P. Nozières and C. T. deDominicis, Phys. Rev. **178**, 1084 (1969).
- [62] A. A. Belavin and A. M. Polyakov, Pis'ma Zh. Eksp. Teor. Fiz. **22**, 503 (1975) [JETP Lett. **22**, 245 (1975)].
- [63] A. M. Polyakov, in *Gauge Fields and Strings* (Harwood Academic Publishers, Switzerland, 1987), chap. 6, sec. 1.
- [64] C. de C. Chamon, D. E. Freed, and X. G. Wen, Phys. Rev. B **51**, 2363 (1995).
- [65] P. Fendley, A. W. W. Ludwig, and H. Saleur, Phys. Rev. Lett. **75**, 2196 (1995).
- [66] Y. P. Li, D. C. Tsui, J. J. Heremans, and J. A. Simmons, Appl. Phys. Lett. **57**, 774 (1990).
- [67] C. Dekker *et al.*, Phys. Rev. Lett. **66**, 2148 (1991).
- [68] F. Liefrink *et al.*, Phys. Rev. B **49**, 14066 (1994).
- [69] R. Landauer and T. Martin, Physica B **175**, 167 (1991).
- [70] G.-L. Ingold and Y. V. Nazarov, in *Single Charge Tunneling*, edited by H. Grabert and M. H. Devoret (Plenum, New York, 1992), chap. 2. See Ref. [77].
- [71] E. Ben-Jacob, E. Mottola, and G. Schön, Phys. Rev. Lett. **51**, 2064 (1983).
- [72] K. Flensberg *et al.*, Phys. Scrip. T **42**, 189 (1992).
- [73] W. Zwerger and M. Scharpf, Z. Phys. B **85**, 421 (1991).
- [74] V. Scalia, G. Falci, R. Fazio, and G. Giaquinta, Z. Phys. B **85**, 427 (1991).
- [75] D. Esteve, in *Single Charge Tunneling*, edited by H. Grabert and M. H. Devoret (Plenum, New York, 1992), chap. 2. See Ref. [77].
- [76] M. A. Kastner, Physics Today **46**, 24 (1993).
- [77] *Single Charge Tunneling*, edited by H. Grabert and M. H. Devoret (Plenum, New York, 1992).

- [78] F. D. M. Haldane, in *Proceedings of the International School of Physics 121, Varenna, 1992*, edited by R. Schrieffer and R. A. Broglia (North-Holland, New York, 1994).
- [79] S. Coleman, in *Aspects of Symmetry* (Cambridge University, Cambridge, 1985), chap. 7.
- [80] L. S. Levitov, A. V. Shytov, and A. Yu. Yakovets, *Phys. Rev. Lett.* **75**, 370 (1995).